

# The Institute of Paper Chemistry

Appleton, Wisconsin

## Doctor's Dissertation

**The Effect of  
Liquor Composition on the Rate of Reaction of a  
Lignin Model Compound (Acetovanillone) Under  
Oxygen-Alkali Conditions**

**Jer-Fei Mih**

**June, 1982**

THE EFFECT OF  
LIQUOR COMPOSITION ON THE RATE OF REACTION OF A LIGNIN MODEL  
COMPOUND (ACETOVANILLONE) UNDER OXYGEN-ALKALI CONDITIONS

A thesis submitted by

Jer-Fei Mih

B.S. 1972, National Chung-Hsing University

M.S. 1976, Illinois Institute of Technology

M.S. 1978, Lawrence University

in partial fulfillment of the requirements  
of The Institute of Paper Chemistry  
for the degree of Doctor of Philosophy  
from Lawrence University,  
Appleton, Wisconsin

Publication Rights Reserved by  
The Institute of Paper Chemistry

June, 1982

# TABLE OF CONTENTS

	Page
SUMMARY	1
INTRODUCTION	3
Perspective	3
Background	4
Oxygen-Alkali Delignification	4
Oxygen-Alkali Pulping	4
Oxygen-Alkali Bleaching	5
Reaction Mechanism	7
Radical Pathways	7
Side-Chain Elimination	9
Demethoxylation	10
The Recombination of Phenolic Nuclei	10
Ionic Pathways	10
Summary	12
Effect of Alkaline Media	12
THESIS OBJECTIVE	14
RESULTS AND DISCUSSION	16
Reaction Rate of Acetovanillone (AV)	16
AV-NaOH/Na <sub>2</sub> CO <sub>3</sub> /NaHCO <sub>3</sub> -Oxygen Reactions	16
Disappearance of AV	16
Kinetics	21
Summary	29
AV-Borax-Oxygen Reactions	29
AV-Phosphate-Oxygen Reactions	33
Effect of pH	35
Effect of DMSO	35

Introduction	35
Reactions in Presence of DMSO	39
Product Formation	40
Hydrogen Peroxide	41
Methanol	41
Acetic Acid	44
Carboxylic Acids	45
Black Precipitate	51
Mechanism	58
Effect of pH	59
Carbonate Radical Anion	60
CONCLUSIONS	64
EXPERIMENTAL	65
General Analytical Procedures	65
Solutions and Reagents	66
Water	66
Oxygen and Reagents	66
Ultrapure Chemicals	66
Titanium Sulfate Reagent	66
Sodium Thiosulfate Solution	66
Model Compound	67
Acetovanillone (AV)	67
Gas-Liquid Chromatography Internal Standards	67
Acetosyringone (AS)	67
Ethanol	67
Butyric Acid	68

Reaction Procedure	68
Reaction System	68
Reaction Vessel	68
Magnetic Stirrer	68
Oil Bath and Temperature Apparatus	70
Sampling System	70
Conditioning of Reactor and Labware	70
Preparation of Reaction Solutions and Loading the Reactor	71
Reaction Sampling	71
Analysis of Reaction Solution	71
Starting Material Analysis	71
Methanol Analysis	72
Acetic Acid Analysis	72
Acidic Products Analysis	72
Hydrogen Peroxide Analysis	73
Black Precipitate	75
UV Samples Preparation	75
ACKNOWLEDGMENTS	76
LITERATURE CITED	77
APPENDIX I. GAS-LIQUID CHROMATOGRAPHY	82
APPENDIX II. EXPERIMENTAL DATA	85
APPENDIX III. DATA ANALYSIS BY MULTIPLE REGRESSION ANALYSIS PROGRAM	90
APPENDIX IV. GAS CHROMATOGRAPHIC-MASS SPECTRAL ANALYSIS	94
APPENDIX V. METALS IN ALKALINE SOLUTIONS	100

## SUMMARY

Acetovanillone (AV; 4-hydroxy-3-methoxyacetophenone) was reacted with molecular oxygen (150 psig) in a Teflon-line reactor at 80°C and in different alkaline solutions. This study was undertaken to gain more information on the effects of different alkaline media on the reaction of lignin with oxygen. The rates of the reactions were followed by quantitative gas-liquid chromatography. Some of the reaction products, such as methanol, hydrogen peroxide, and carboxylic acids were determined by various analytical methods.

Based on the results of kinetic studies, all the reactions exhibited a first-order dependence on the initial AV concentration, and AV showed a faster reaction in oxygen-sodium carbonate/bicarbonate systems compared with other systems. The reactions of AV in oxygen/noncarbonate systems all had the same reaction rate, regardless of their initial pH. Once the pH of the solution dropped below 7.5 (pKa of AV), the reaction rate slowed. These results imply that it is important to keep the pH of the cooking liquor above the pKa of lignin in order to obtain reasonable reaction rates.

The presence of carbonate radical anions ( $\text{CO}_3^{\cdot-}$ ) may account for the faster reaction rates in the oxygen-sodium carbonate/bicarbonate systems. Carbonate radical anions are known to be generated in carbonate/bicarbonate systems when hydroxyl radicals are present. Also, DMSO is known to scavenge hydroxyl radicals. The addition of DMSO to both AV-oxygen-sodium hydroxide and AV-oxygen-sodium bicarbonate led to slower reaction rates, with the latter showing the greatest rate reduction. These results suggest that both hydroxyl radicals and carbonate radical anions play important roles during the oxygen-alkali reactions of AV.

Hydrogen peroxide was produced as an intermediate. It showed similar trends of formation and disappearance in different oxygen-alkali systems. Based on methanol

and acetic acid analyses, more demethoxylation and side-chain elimination occurred in the higher pH systems than in the lower pH. During reactions in which the pH was low (AV-NaHCO<sub>3</sub>-O<sub>2</sub>; AV-borax/HCl-O<sub>2</sub>), a black precipitate was observed. Spectral analyses indicate that the black precipitate was a higher molecular condensation product of AV. This implies that higher pH favors degradation reactions and lower pH favors polymerization. Carboxylic acids detected in the reaction solutions were common to all reactions, but there were exceptions. These acids accounted for ca. 20-40 percent of consumed AV during the reactions.

## INTRODUCTION

### PERSPECTIVE

The oxygen-alkali delignification of wood and pulps has received considerable attention in recent years due to increasingly stringent environmental regulations. Its major advantage is that it can reduce air pollution by eliminating sulfur compounds produced during the kraft pulping process. It can also reduce water pollution by minimizing the amount of chlorinated compounds that result from conventional bleaching. However, the oxygen-alkali process has its drawbacks. The major disadvantage is that it produces low strength pulp as a result of extensive degradation of the wood polysaccharides.

One approach to improving the pulp strength during the oxygen-alkali stage is to lower the pH of the cooking liquor. Most of the results in the literature show that polysaccharides are degraded less with sodium carbonate/bicarbonate as the added alkali (pH 8-10) compared to delignification at higher pH (12-13) with sodium hydroxide as active alkali. This is demonstrated by the higher yield. However, the rate of delignification is faster at higher pH. To date, few investigators have studied the lignin reaction in different alkaline media during oxygen-alkali treatment. This investigation was directed to obtaining more information about the effect of alkaline media on lignin reactions under oxygen-alkali delignification conditions.



## BACKGROUND

### OXYGEN-ALKALI DELIGNIFICATION

Oxygen-alkali delignification is a process which, through the use of oxygen and alkaline solution, removes the lignin in the wood chips or pulp. Oxygen-alkali delignification is a broad terminology. More precisely, it can be divided into two categories: oxygen-alkali pulping, if the process removes lignin from wood chips or wood meal, or oxygen-alkali bleaching, if the process removes lignin from pulp.

#### Oxygen-Alkali Pulping

The delignifying action of oxygen has been known for a long time. As early as 1928, Kleinert, et al. found that oxygen removes lignin from lignin-containing plant materials in an alkaline system (1). A patent granted to Harris (2) in 1954 states the reaction conditions in oxygen pulping, such as a temperature between 125 and 175°C, under a pressure of oxygen of at least 800 psi. The high pressure specified in his patent has discouraged application in this area.

Since 1970, many paper companies and research institutes have devoted their efforts to the oxygen-alkali pulping area. The incentive to study oxygen-alkali pulping is to eliminate sulfur malodors by replacing the conventional kraft process with a sulfur-free process. Results reported in the literature indicate that pulps of high brightness and low lignin contents can be prepared by digestion of wood chips or wood meal with sodium hydroxide solution under much lower oxygen pressure (100-200 psi) than that prepared by earlier researchers (3,4). Two barriers have inhibited commercialization. One is the nonuniform pulping due to the oxygen diffusion problems, the other is the lower pulp strength, due to cellulose degradation in the high pH liquors. These problems could be lessened somewhat by using lower pH liquors such as carbonate, bicarbonate, and borax instead of sodium hydroxide

(5-11). Most data show that oxygen-alkali pulping at lower pH (8-10) gives better results. For instance, higher yield and better physical strength are obtained than when sodium hydroxide is employed. The rate of delignification is generally much slower in the lower pH, however. Using sodium carbonate or sodium bicarbonate in the pulping liquor provides another advantage over kraft: a recovery system may be based on wet combustion, which does not require the causticizing sequence (8,11).

The other approach to solving the nonuniform pulping problem is to develop a two-stage sulfur-free pulping process (12-16). Basically, this two-stage treatment consists of precooking of chips in an alkaline medium to a high yield followed by the oxygen-alkali delignification. Researchers have used caustic soda (soda-oxygen process) (12,13), sodium carbonate (HOPES process) (14), and sodium bicarbonate (15,16) as the pulping agent in both precooking and oxygen stages. In general, the two-stage pulp gives equal or higher pulp yield than reference kraft pulp depending on the pH of the alkaline medium. The strength properties are lower than or comparable to kraft hardwood pulps. Cox and Worster (17) pointed out in their report that oxygen-alkali pulping, especially the two-stage process, appears to be the most promising approach to a sulfur-free pulping process.

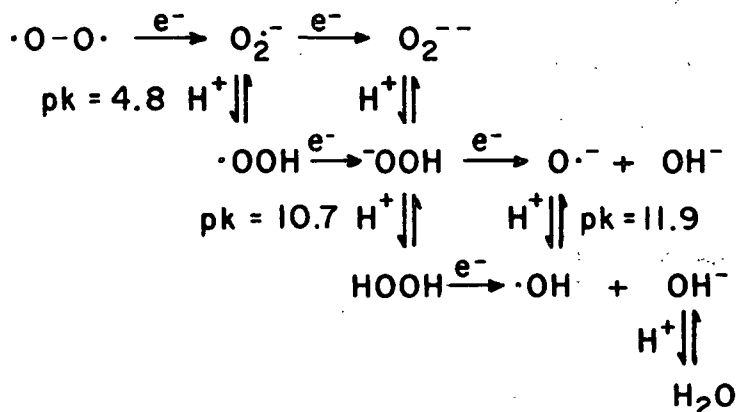
#### Oxygen-Alkali Bleaching

The investigation of the brightening action of oxygen on cellulose pulp in an alkaline medium was initiated by the Soviet researchers Nikitin and Akim in the middle 1950's (18,19). The low viscosity and strength properties of these pulps inhibited commercialization at that time. Robert, et al. (20,21) discovered that the presence of a small amount of magnesium salt, such as magnesium carbonate, permits much of the strength property of the pulp to be maintained during oxygen-alkali bleaching. This discovery spurred further investigations and led to the development of commercial bleaching processes.

Generally, oxygen bleaching is a one stage operation located between the digester and the conventional bleaching sequence. This stage can remove about 50% of the residual lignin from the pulp. Its effluent can be introduced into the chemical recovery system of the kraft pulp mill. The main advantage of oxygen bleaching is: it can reduce the pollutant load and the chemical cost of subsequent bleaching stages (22). At least 16 mills in the world are using oxygen bleaching in their daily operations (23). So far, oxygen bleaching is the only commercially applied proven alternative process that can significantly reduce the water pollution problem within the bleach plant itself. In practice, oxygen-alkali bleaching is carried out with sodium hydroxide as the active alkali. Several investigators have studied the oxygen bleaching of kraft and sulfite pulp with carbonate or bicarbonate as the added alkali (24-26). The results show that the yield from oxygen-sodium bicarbonate bleaching is significantly higher than that obtained with sodium hydroxide (26).

## REACTION MECHANISM

The reactions between oxygen and lignin are extremely complex due to the large variety of competing reactions occurring during the oxidation. Oxygen itself has two unpaired electrons and has a tendency to react with many organic substances. Several different species can be formed during the reduction of oxygen; these are shown below (27).



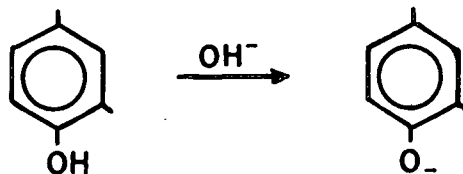
Among these species, the molecular or ionic compounds are the mild oxidants, whereas radical species are generally the strong oxidants.

Model compound studies have proven useful in understanding the reactions of different lignin structures. A substantial amount of literature is available on the oxidative reaction of lignin model compounds during oxygen-alkali treatment (28-34). On the basis of these studies, we may distinguish between radical and ionic pathways in these overall oxidation reactions.

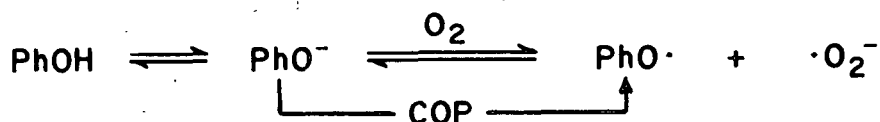
### Radical Pathways

Much research in this area has been carried out by Kratzl and co-workers (28-30) using phenolic models. Numerous studies have revealed that the phenolic structure is the most important site for oxidative attack in alkaline media

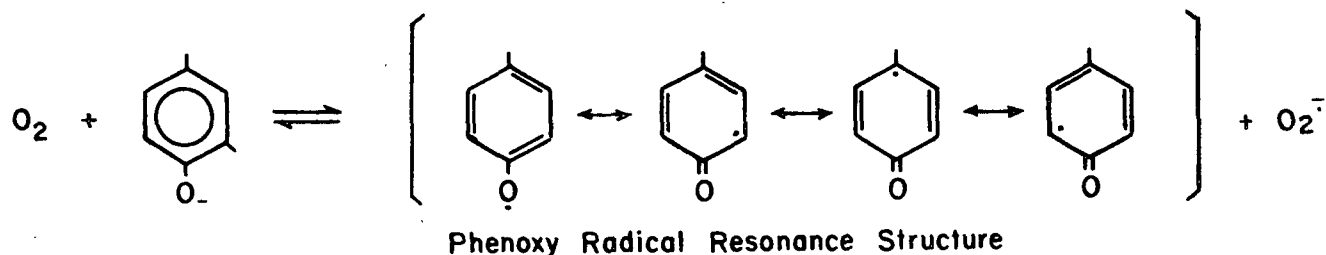
(29,35,36). The first step involves the ionization of a free phenolic hydroxyl group to form a phenolate anion:



In the next step, oxygen abstracts a single electron from a phenolate anion to yield a resonance stabilized phenoxy radical and hydroperoxy radical (superoxide radical anion if in alkaline solution) (30).



This step is probably the rate-determining step (30,37). One useful concept advanced by Kratzl, *et al.* (30) is that of relating critical oxidation potential (COP) to lignin systems. The COP values represent a useful measure for the ease



of electron release from lignin related phenolate models and is an indication of the reactivity of the models. The lower the COP value for a compound, the greater is its reactivity. The phenoxy radicals can react in different ways which are summarized as shown below and in Fig. 1.

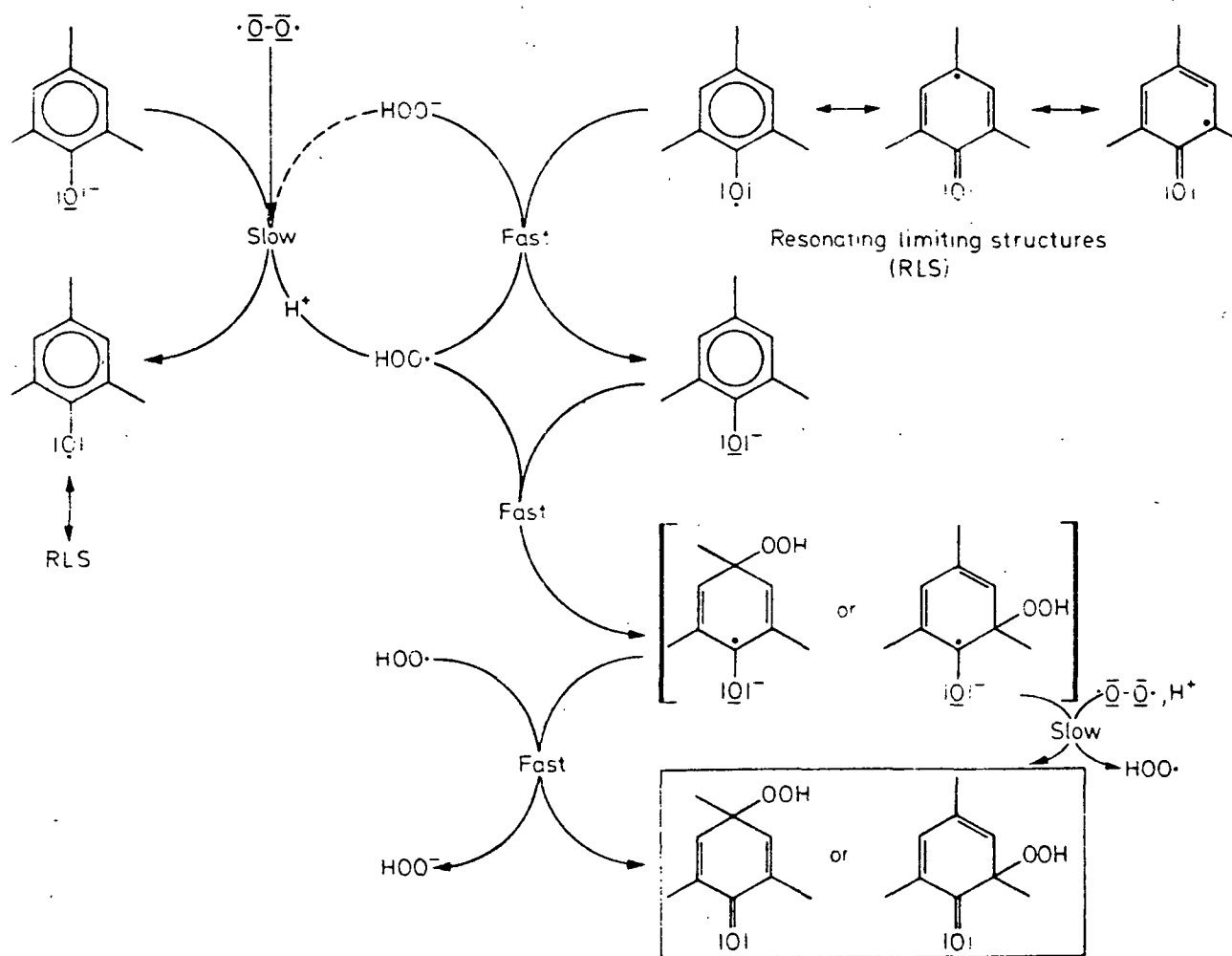


Figure 1. Primary radical reactions in the oxygenation of phenolic structures (30).

The hydroperoxyl radical is a stronger oxidant than molecular oxygen. It reacts with phenoxyl radicals forming cyclohexadienone hydroperoxides which are believed to be the "key intermediates" in the oxidative scheme (30,31). Several possibilities of evolution exist for these unstable hydroperoxides.

#### Side Chain Elimination

Model compound studies show that aromatic side chains are degraded under oxygen-alkali conditions, especially when they contain alpha-carbonyl and

alpha-carbinol structures (28-30). Side chains containing alpha-carbonyls are eliminated as acids by a reaction which resembles the Dakin reaction (29,40).

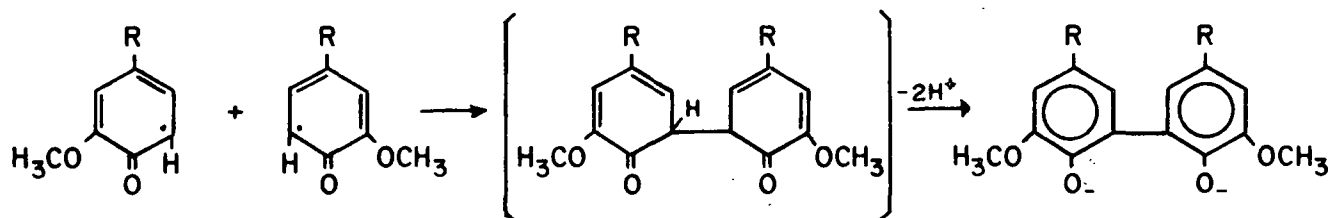
These reactions split the lignin macromolecule and the resulting compounds pass into solution if they are small enough. The quinones formed can be further degraded to the carboxylic acids (41).

#### Demethoxylation

Demethoxylation is one of the most important degradation reactions during oxidation. It increases the hydrophilic character of the lignin. The true mechanism has not been clarified. Formation of ortho-quinones represents the most acceptable routes (28), and ultimately leads to acids of low molecular weight (41).

#### The Recombination of Phenolic Nuclei

Recombination of phenoxy radicals may occur through a C-O, or a C-C coupling. However, the C-C coupling of the two phenoxy radicals seems to be the dominant coupling mode (28). The corresponding o,o-dihydroxybiphenyls are further oxidized resulting in rupture of one of these two aromatic nuclei (28).



#### Ionic Pathways

By means of lignin model compound studies, Nakano, *et al.* showed that alpha-carbonyl groups are also reactive as shown in Fig. 2 (33,42). The first step involves the base-catalyzed ionization of the beta hydrogens. The alpha-carbonyl increases the acidity of the beta-methine proton and facilitates ionization. Molecular oxygen attacks the carbanion of the side chain forming a hydroperoxide anion, which rearranges to many kinds of products (33).

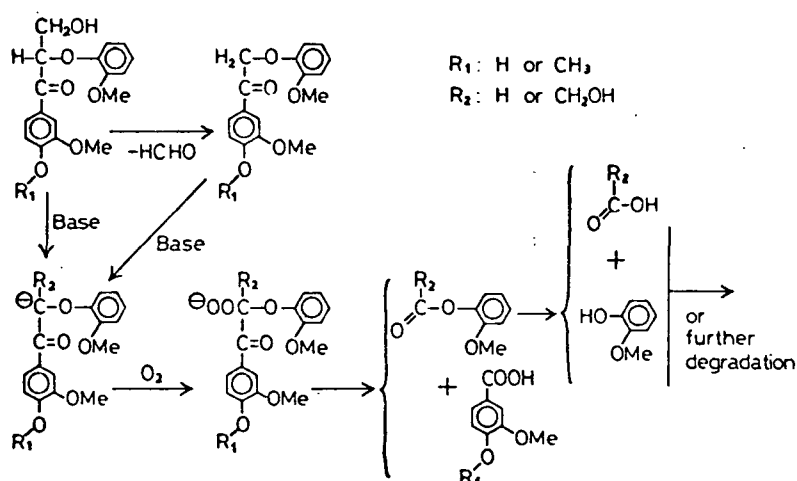


Figure 2. Reaction of lignin etherified model compound with oxygen-alkali (33).

In a related study of lignin model compounds containing a phenolic hydroxyl or an alpha-carbonyl, Gierer, *et al.* (34) proposed that lignin degradations are preceded by the alkali promoted reactions, followed by formation of carbanions, which constitute the substrates for the subsequent attack by oxygen. The hydroperoxide then degrades through dioxetane or epoxide intermediates. Some examples are depicted in Fig. 3.

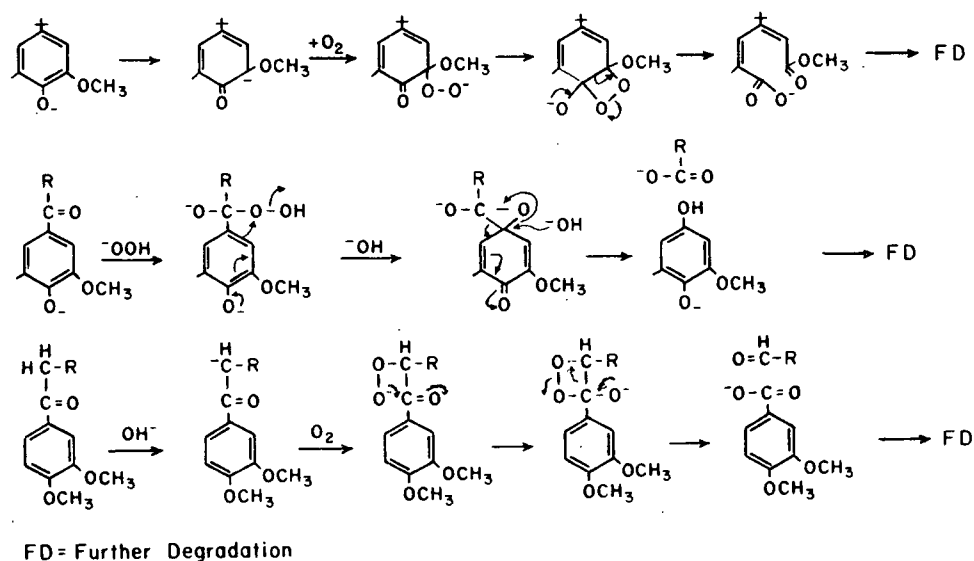


Figure 3. Proposed mechanism for the base-catalyzed, ionic degradation of lignin model compounds with oxygen in alkaline media (34).



### Summary

According to the radical pathway sequences, a key step in the oxidation process involves ionization of the free phenolic hydroxyl group. This leads to the formation of stabilized phenoxy and hydroperoxyl radicals. Phenolic hydroxyl and alpha-carbonyl structures are important groups in the ionic pathway, which constitute the substrates for the attack by oxygen and hydroperoxide anions. Both ionic and radical pathways are composed of a number of different reactions and may play an important role during oxygen-alkali delignification.

### EFFECT OF ALKALINE MEDIA

As mentioned in the previous section, the delignification of wood or pulps can be achieved by the combination of oxygen and alkaline media (i.e., sodium hydroxide, carbonate, bicarbonate, phosphate or borax). Generally, the higher the pH in the system, the faster the delignification rate will be. Many researchers (36,43) noticed that the rate of delignification shifts to a slower rate as soon as the pH drops below 10. The accepted value for the pKa of phenolic groups in lignin is 10 (44).

Some researchers claimed that it is important to keep the pH of the cooking liquor above 10 in order to obtain a reasonable delignification rate (43). Others (46,50) claimed that the main role of alkali in the oxygen-alkali stage is to neutralize the acids formed during the oxidation process, thus preventing any additional degradation of the polysaccharides through acid-catalyzed hydrolysis.

Oxidation at higher pH generally causes the lignin to degrade into a greater number of low molecular weight fragments than at lower pH (45,47-49). However, after the first hour of pulping, Bolker and his co-workers (50) found there is little difference in the rate of delignification and selectivity between the hydroxide,

carbonate, bicarbonate, and borate anions. Bolker, et al. concluded that the nature of the base does not affect the course of delignification. The main difference occurring at the beginning of the cook is due to an increased dissolution of carbohydrates with increasing initial pH of the liquor. Markham (10) on the other hand reported that pulping with borax-oxygen results in a faster delignification rate and superior selectivity as opposed to other alkalis such as sodium carbonate at a similar pH. He suggested that borax may have another effect than just simply neutralizing the acidic products.

Most of the studies were performed using either wood chips or wood meal to investigate the effect of alkaline media during oxygen-alkali treatment. By using the lignin model compounds, apocynol ( $\alpha$ -methylvanillyl alcohol) and acetovanillone (4-hydroxy-3-methoxyacetophenone), Nakano, et al. (45) found that both compounds were consumed more rapidly in the oxygen-sodium carbonate system (lower pH) than in the oxygen-sodium hydroxide system (higher pH). This is contradictory to the results obtained by other researchers using wood chips or wood meal as the raw material. Therefore, it would be interesting to further investigate the role of alkali toward lignin under oxygen-alkali conditions.

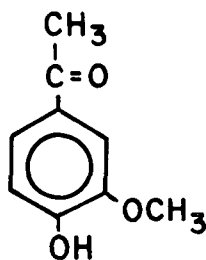
## THESIS OBJECTIVE

It has been established that the degree of wood polysaccharide degradation is proportional to the pH of the alkaline media during oxygen-alkali delignification (12,14,89). The role of the alkali in lignin reactions is not yet fully understood. Only the importance of the phenolate anion as the starting point for oxygen attack has been confirmed. Some researchers claim it is important to keep the pH of the reaction above the pKa value of the phenolic units if acceptable reaction rates are to be achieved (36,43). Others claim that the role of alkali is just to neutralize the organic acids formed by the oxidation reaction.

Most of the results in the literature show that the rate of delignification is faster at higher pH (12-13) with sodium hydroxide as the active alkali compared to delignification at lower pH (8-10) with sodium carbonate or bicarbonate as the active alkali (5-11). Surprisingly, the result of a lignin model compound study shows that apocynol and acetovanillone are consumed more rapidly in the lower pH system (oxygen-sodium carbonate) than in the higher pH system (oxygen-sodium hydroxide) (45).

The rate of delignification in oxygen-alkali may be affected by oxygen mass transfer, wood morphology, temperature, pH of the cooking liquor, etc. The purpose of this study is to gain a better understanding of the role of the alkaline media on the reaction of lignin with oxygen. A lignin model compound (acetovanillone) was used in order to avoid the complications introduced by other factors, such as oxygen diffusion and wood structure. In addition to being commercially available, AV is a simple model of a repeating unit of softwood lignin and has a free phenolic hydroxyl group, which is believed to be the most reactive site of lignin toward oxidation (29,35,36). It also has a carbonyl group in the alpha-position of the side chain, which has been suggested to be important during the oxygen-alkali treatment (33,42).

There are not many alpha-carbonyl groups present in lignin (61), but most of the alpha-hydroxyl groups could be oxidized to alpha-carbonyl groups under the oxidation conditions (41). For this study, AV has a special advantage. It has a low pKa (7.5) which provides a wider pH range for studying the correlation between the pH of the cooking liquor and the reaction rate. Furthermore, AV has been used as a lignin model in other oxygen-alkali studies (29,45,51), allowing the results of this work to be compared with the findings of previous investigations.



**Acetovanillone  
(AV)**

## RESULTS AND DISCUSSION

### REACTION RATE OF ACETOVANILLONE

Reaction conditions for all AV reactions were 80°C and 150 psig oxygen pressure. Reactions were conducted in a magnetically-stirred, Teflon-lined reactor designed such that samples could be collected while hot and under pressure. Reaction samples were periodically collected and were analyzed for unreacted starting material (AV) and for selected AV reaction products. All of the alkaline solutions were prepared from ultrapure grade chemicals to minimize trace metal contamination. Experimental procedures are described in the Experimental section, and tabulated results of reactions appear in Appendix II. Appendix III describes the statistical approach used to determine the significant differences between sets of AV results.

#### AV-NaOH/Na<sub>2</sub>CO<sub>3</sub>/NaHCO<sub>3</sub>-OXYGEN REACTIONS

##### Disappearance of AV

Acetovanillone (33.6 mM) was reacted with oxygen in three different alkaline solutions - sodium hydroxide (initial pH = 12.8), sodium carbonate (initial pH = 10.8), and sodium bicarbonate (initial pH = 8.9). All the reactions were carried out for 24 hours in duplicate runs. Samples were collected at intervals for determination of unreacted AV using quantitative gas-liquid chromatography (GLC) of their trimethylsilyl (TMS) derivatives.

The results of the reaction of AV with oxygen in sodium hydroxide solution (1.25N) are shown in Fig. 4. The concentration of AV declined steadily during the 24-hour reaction. In this case, the two sets of data are not statistically

distinguishable at the 95% confidence level on the basis of the student's  $t$ -test ( $t = 0.36 < 2.15$ ) (54).

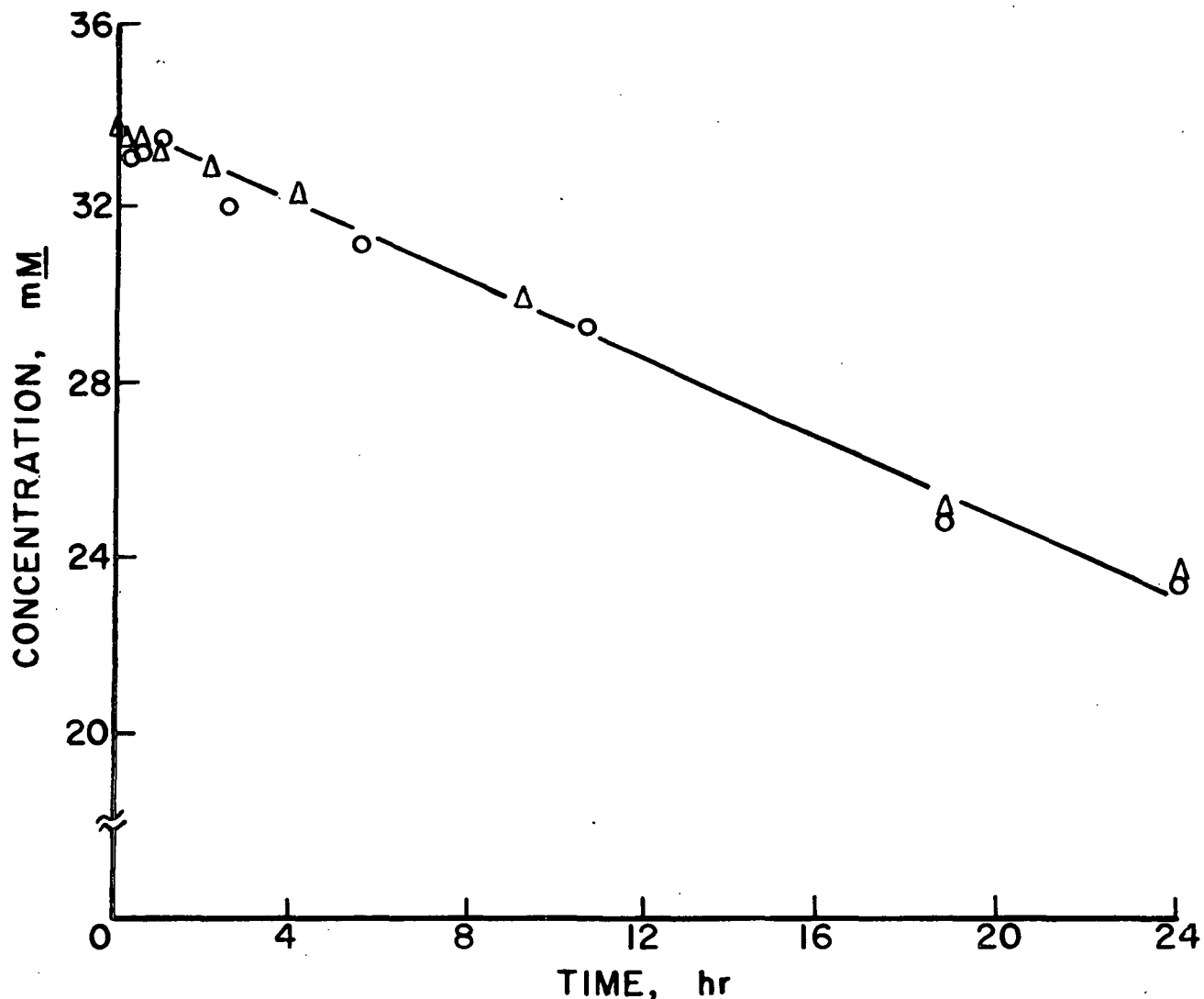


Figure 4. Disappearance of AV (33.6 mM) in 1.25N NaOH at 80°C and 150 psig O<sub>2</sub> (O AV-NaOH-O<sub>2</sub>-2; Δ AV-NaOH-O<sub>2</sub>-3).

Results of two AV-O<sub>2</sub>-Na<sub>2</sub>CO<sub>3</sub> (1.25N) runs are shown in Fig. 5, while Fig. 6 shows the disappearance curve of AV in oxygen-sodium bicarbonate (1.25N). Fig. 7 shows the disappearance curves of AV in all three different oxygen-alkali systems. The three

curves in Fig. 7 are statistically distinguishable from each other (see Appendix III). The results show that AV was consumed more rapidly in the oxygen-sodium bicarbonate system (initial pH = 8.9) than in the oxygen-sodium hydroxide (initial pH = 12.8). The AV-oxygen sodium carbonate (initial pH = 10.8) was intermediate in behavior. This observation parallels that of Nakano, et al. (45) for model compound studies, but contradicts the results obtained by other researchers using wood chips or meal as a raw material.

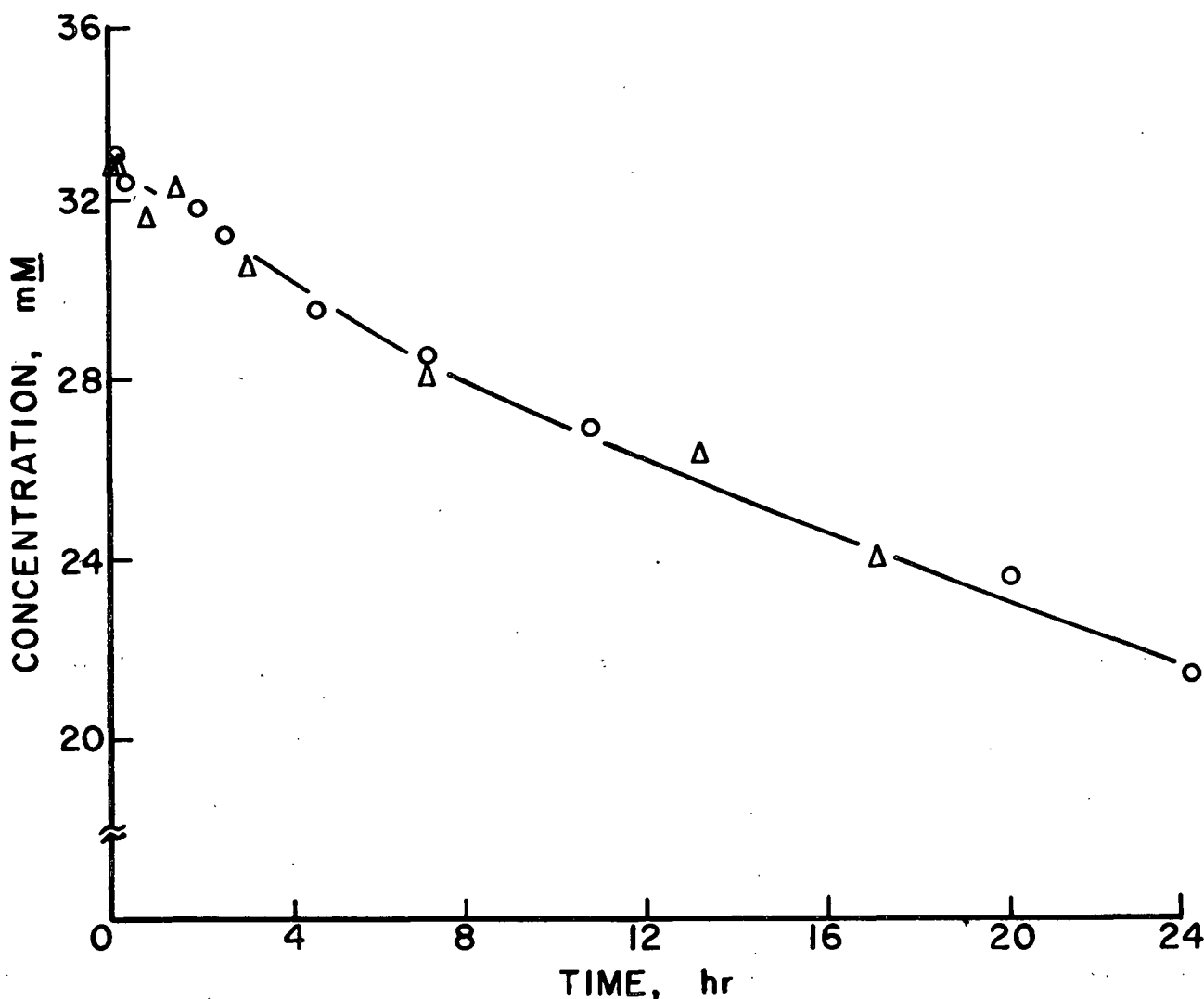


Figure 5. Disappearance of AV (33.6 mM) in 1.25N  $\text{Na}_2\text{CO}_3$  at 80°C and 150 psig  $\text{O}_2$  (O AV- $\text{Na}_2\text{CO}_3$ - $\text{O}_2$ -1; Δ AV- $\text{Na}_2\text{CO}_3$ - $\text{O}_2$ -2).

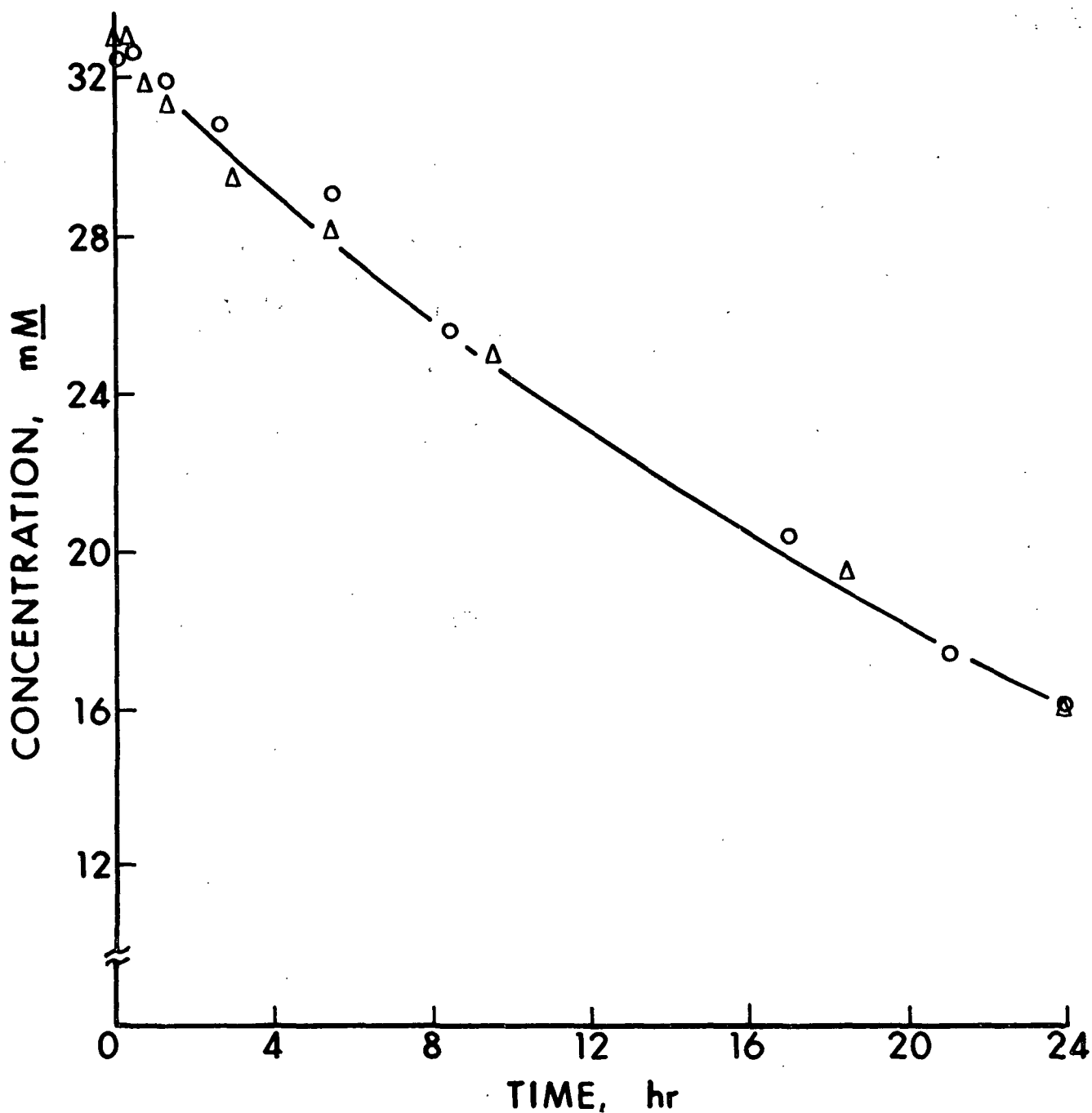


Figure 6. Disappearance of AV (33.6 mM) in 1.25N NaHCO<sub>3</sub> at 80°C and 150 psig O<sub>2</sub> (O AV-NaHO<sub>3</sub>-O<sub>2</sub>-2; Δ AV-NaHCO<sub>3</sub>-O<sub>2</sub>-3).

Changing the ionic strength of the reaction of AV with oxygen in NaOH from 1.25 to 0.8 to 0.4 but maintaining the pH approximately constant, had no detectable effect upon the initial rate of reaction (Table I) although different product distributions were attained. (Table II).



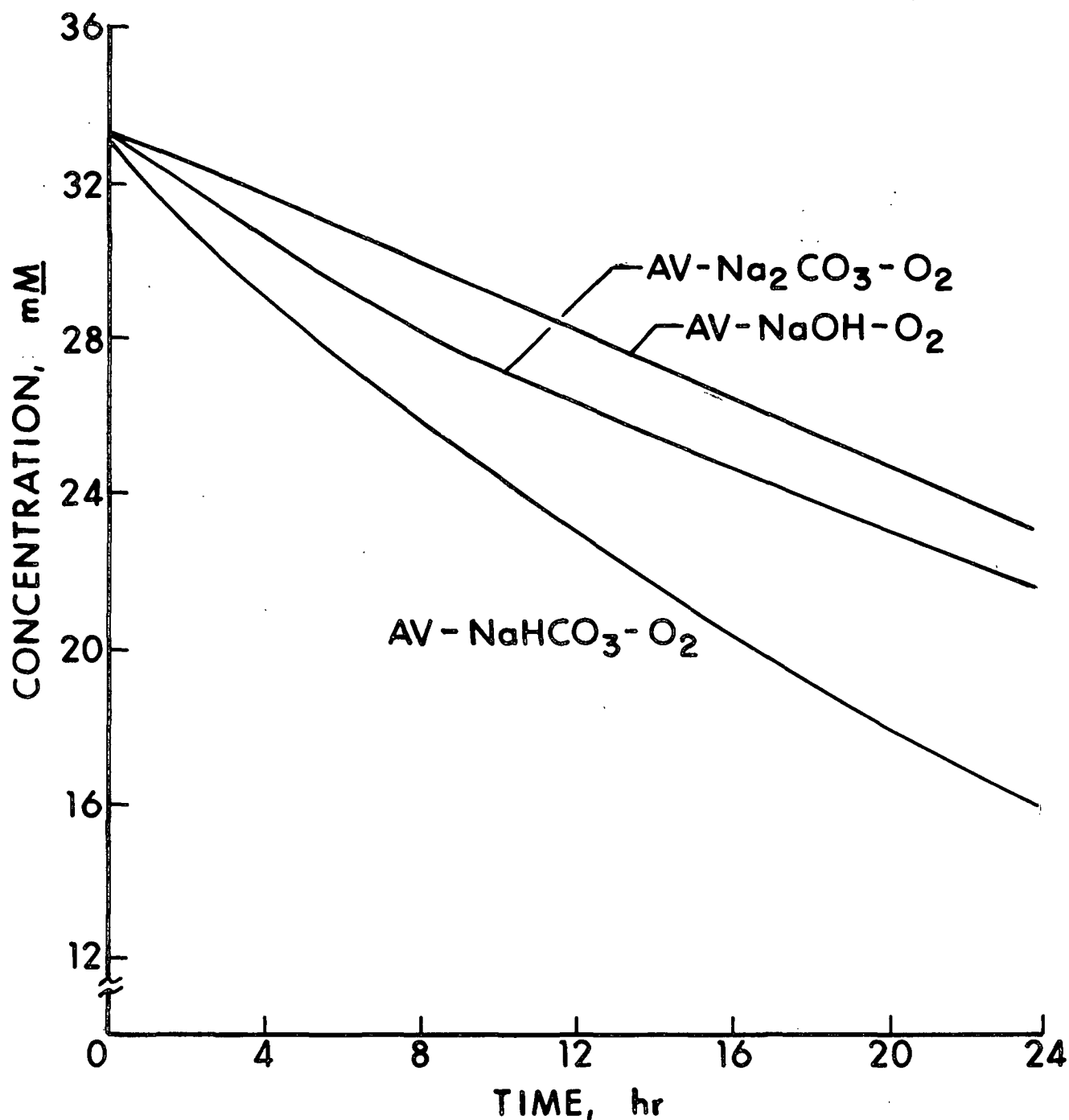


Figure 7. Disappearance of AV (33.6 mM) at 80°C and 150 psig O<sub>2</sub> in three different alkaline solutions: NaOH (initial pH = 12.8), Na<sub>2</sub>CO<sub>3</sub> (initial pH = 10.8), and NaHCO<sub>3</sub> (initial pH = 8.9).

Two reactions (AV-Na<sub>2</sub>CO<sub>3</sub>-O<sub>2</sub>) were also carried out at different ionic strength in reaction media ( $I = 1.25$  vs.  $I = 1.875$ ), but they showed an almost identical disappearance rate (Table XIII, Appendix II and Table I).

## Kinetics

It is improper to conclude that AV has a faster reaction rate in the oxygen-sodium bicarbonate unless it can be shown that AV has the same reaction order in all three systems. Therefore, the kinetics of the AV disappearance were studied in order to obtain the reaction order of AV in three different oxygen-alkali systems.

There are two main methods of treating kinetic data. These are the integral method and the differential method (55). The integral method is the most widely used. This employs the integrated form of the rate equation for an assumed reaction order. Using a trial and error method, one must first guess the reaction order, and then determine whether the guess fits the experimental results. The method of integration is not reliable when complicated reactions are involved. When complications exist, or are suspected, it is better to employ the differential method.

The differential method may be applied in two different ways. One way involves a single run. A plot of the logarithm of the rate against the logarithm of the concentration at various reaction times gives the order with respect to time. The reaction intermediates may interfere with the order determined in this way. The other way is to measure the initial rates of reactions at various initial concentrations. In this study, AV, oxygen, and alkali were present. The initial rates in our system can be expressed by rate Eq. (1) written in terms of the initial conditions.

$$-d[AV]_i/dt = k [AV]_i^a [O_2]_i^b [Alkali]_i^c \quad (1)$$

where  $-d[AV]_i/dt$  = initial rate of disappearance of AV

$k$  = rate coefficient

$[AV]_i$  = initial concentration of AV

$[O_2]_i$  = initial concentration of oxygen

$[Alkali]_i$  = initial concentration of alkaline solutions

$a, b, c$ , = orders with respect to the corresponding reactants

The order in AV,  $a$ , can be obtained by varying the initial AV concentration while maintaining constant oxygen and alkaline concentrations. Under these conditions, Eq. (1) can be simplified to Eq. (2).

$$-d[AV]_i/dt = r_i = k' [AV]_i^a \quad (2)$$

where

$$k' = k [O_2]_i^b [Alkali]_i^c$$

Taking the logarithm of Eq. (2) will give Eq. (3).

$$\log r_i = \log k' + a \log [AV]_i \quad (3)$$

The logarithm of the initial rate can be plotted against the logarithm of the initial concentration. The slope of the plot then gives the order in AV. One of the advantages of this method is that it relates to initial conditions where intermediates or products cannot interfere.

In the case of AV-oxygen-sodium hydroxide, the disappearance curves of AV at initial concentrations of 11.2 mM and 100.8 mM are shown in Fig. 8. Based on Eq. (3), a log-log plot of the initial rate versus the initial concentration (11.2 mM, 33.6 mM, and 100.8 mM) was obtained (Fig. 9). The best straight-line fit of the data has a slope of 1.05, which suggests a first-order dependence on AV.

The same kinetic treatment was applied to oxygen-sodium carbonate and oxygen-sodium bicarbonate systems. Figures 10 and 12 show the disappearance curves of AV in two systems at two different initial AV concentrations (11.2 mM, 100.8 mM). The slopes obtained from the log-log plots were 1.16 (AV-Na<sub>2</sub>CO<sub>3</sub>-O<sub>2</sub>; Fig. 11) and 1.07 (AV-NaHCO<sub>3</sub>-O<sub>2</sub>; Fig. 13), respectively.

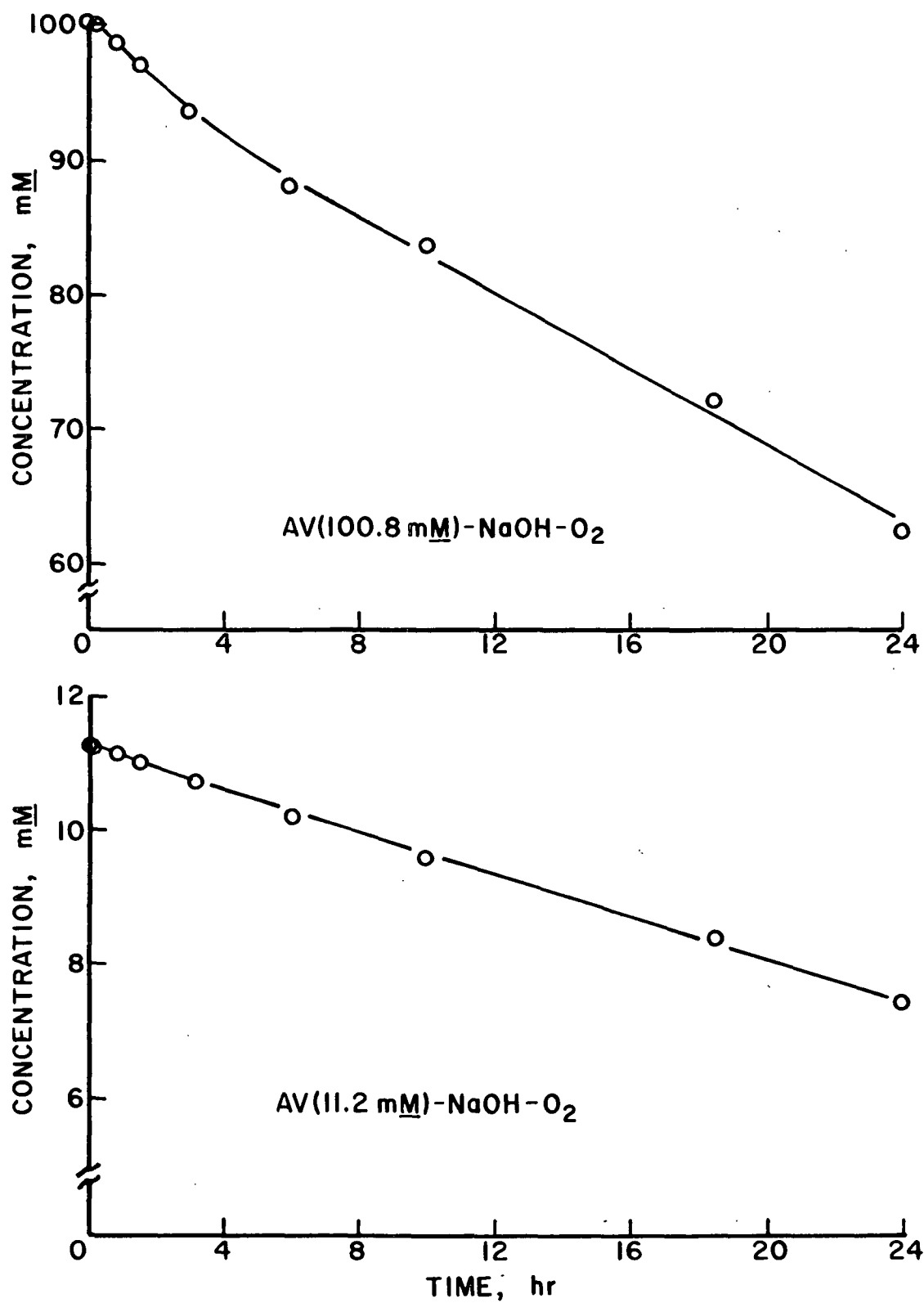


Figure 8. Disappearance of AV (100.8 mM - top; 11.2 mM - bottom) in 1.25N NaOH at 80°C and 150 psig O<sub>2</sub>.

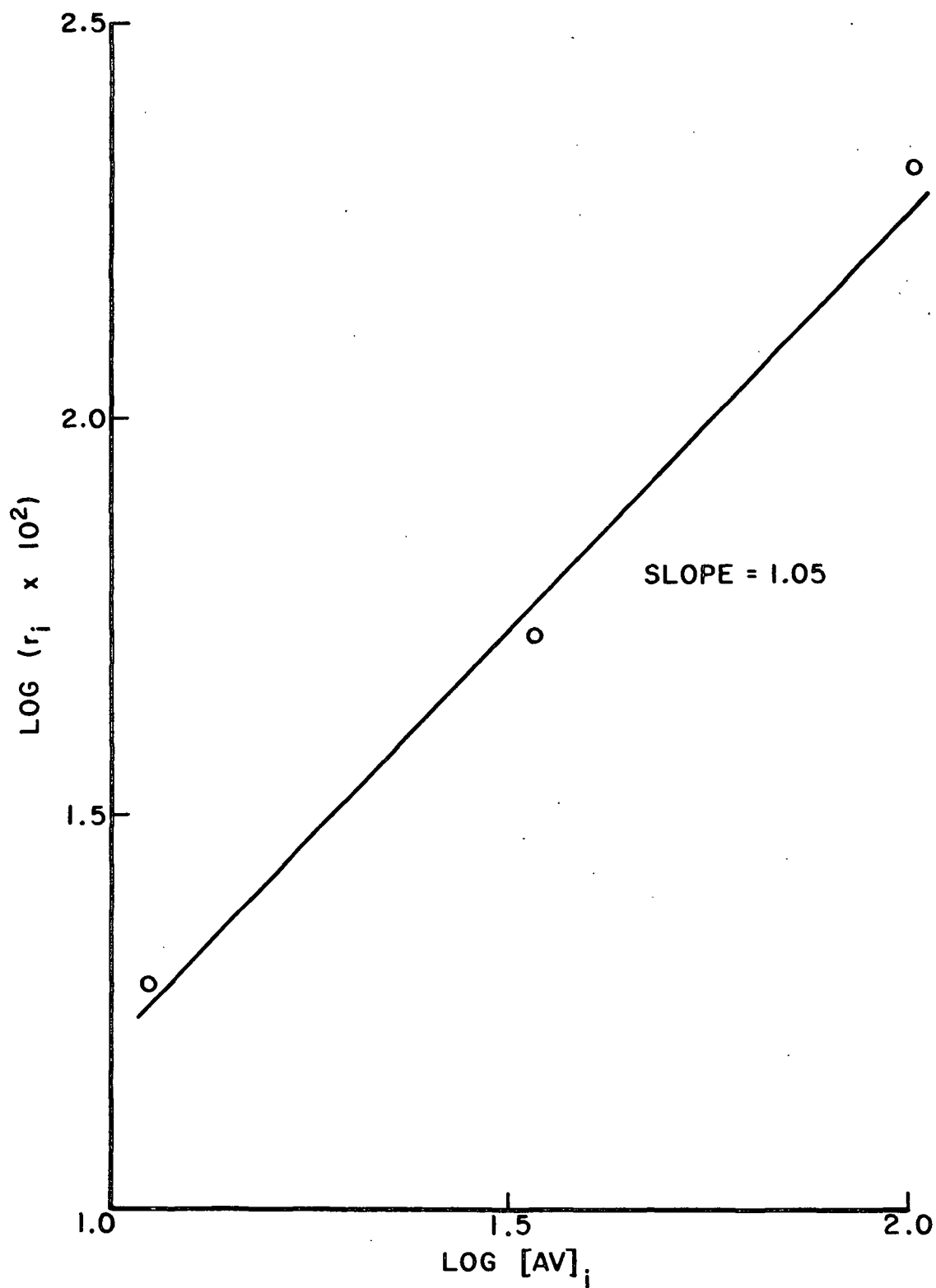


Figure 9. Kinetic plot of reactions of AV-NaOH-O<sub>2</sub> according to the differential method by changing the initial AV concentration (11.2 mM, 33.6 mM, and 100.8 mM).

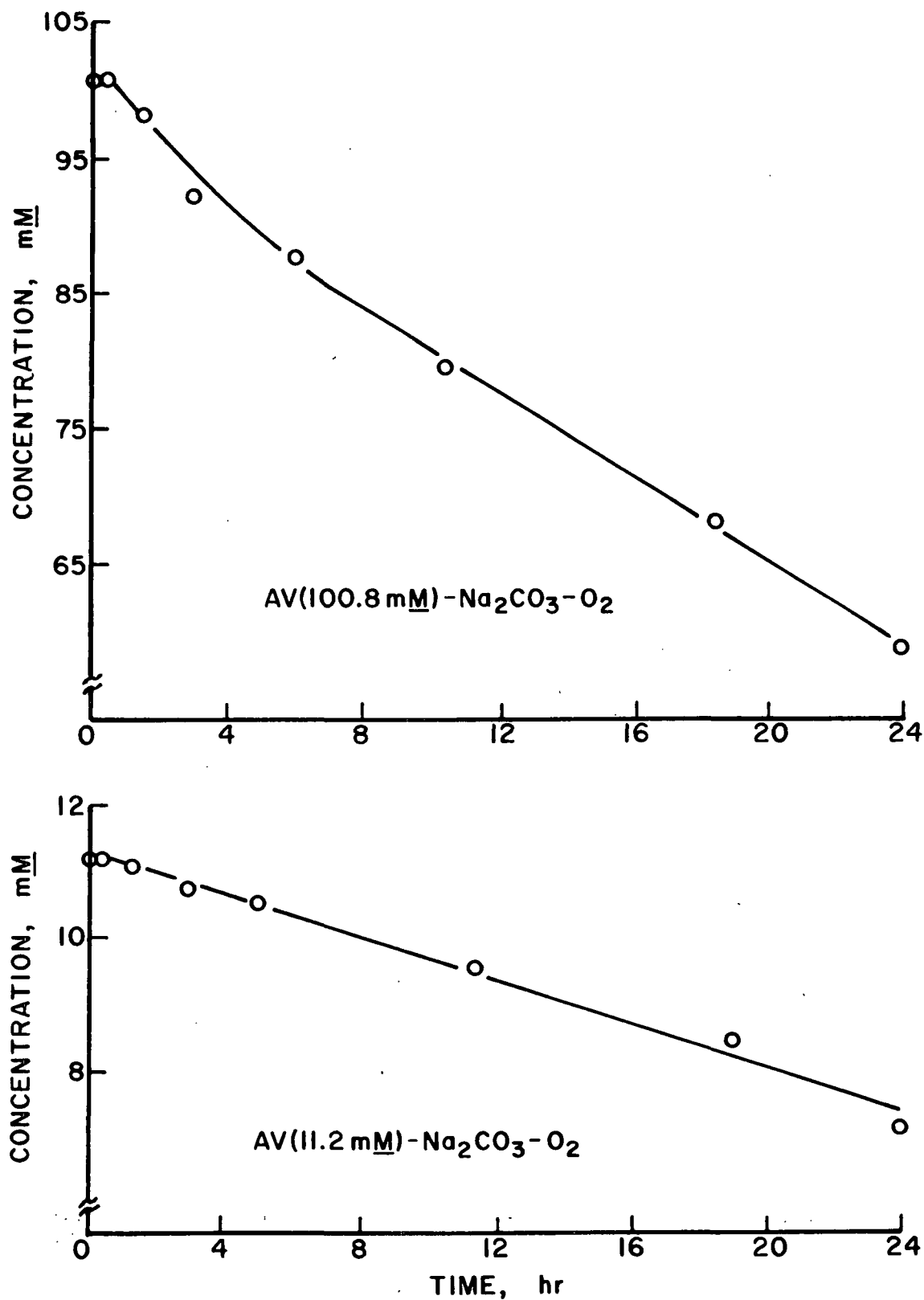


Figure 10. Disappearance of AV (100.8 mM - top, 11.2 mM - bottom) in Na<sub>2</sub>CO<sub>3</sub> at 80°C and 150 psig O<sub>2</sub>.

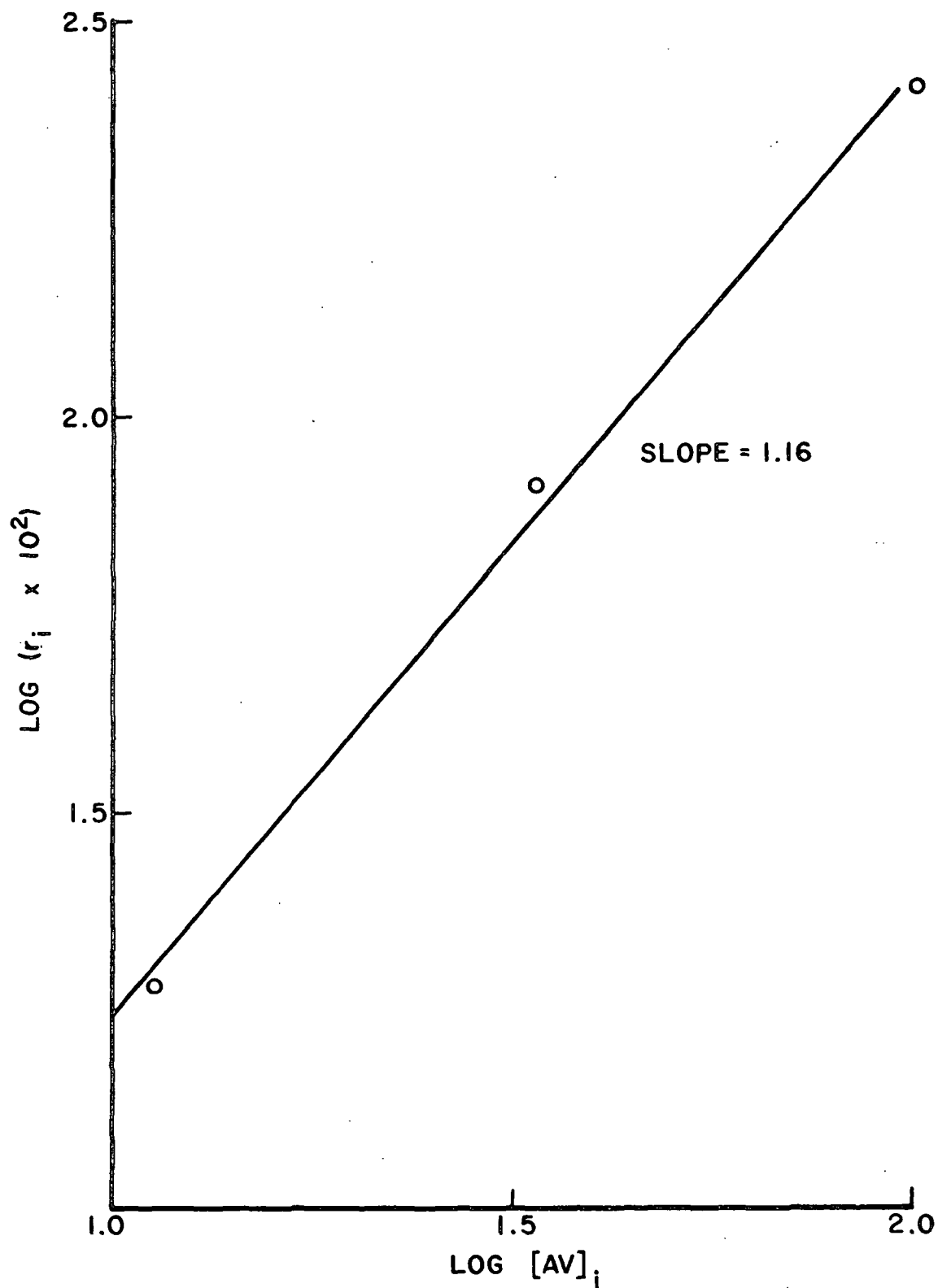


Figure 11. Kinetic plot of reactions of AV- $\text{Na}_2\text{CO}_3\text{-O}_2$  according to the differential method by changing the initial AV concentration (11.2 mM, 33.6 mM, and 100.8 mM).

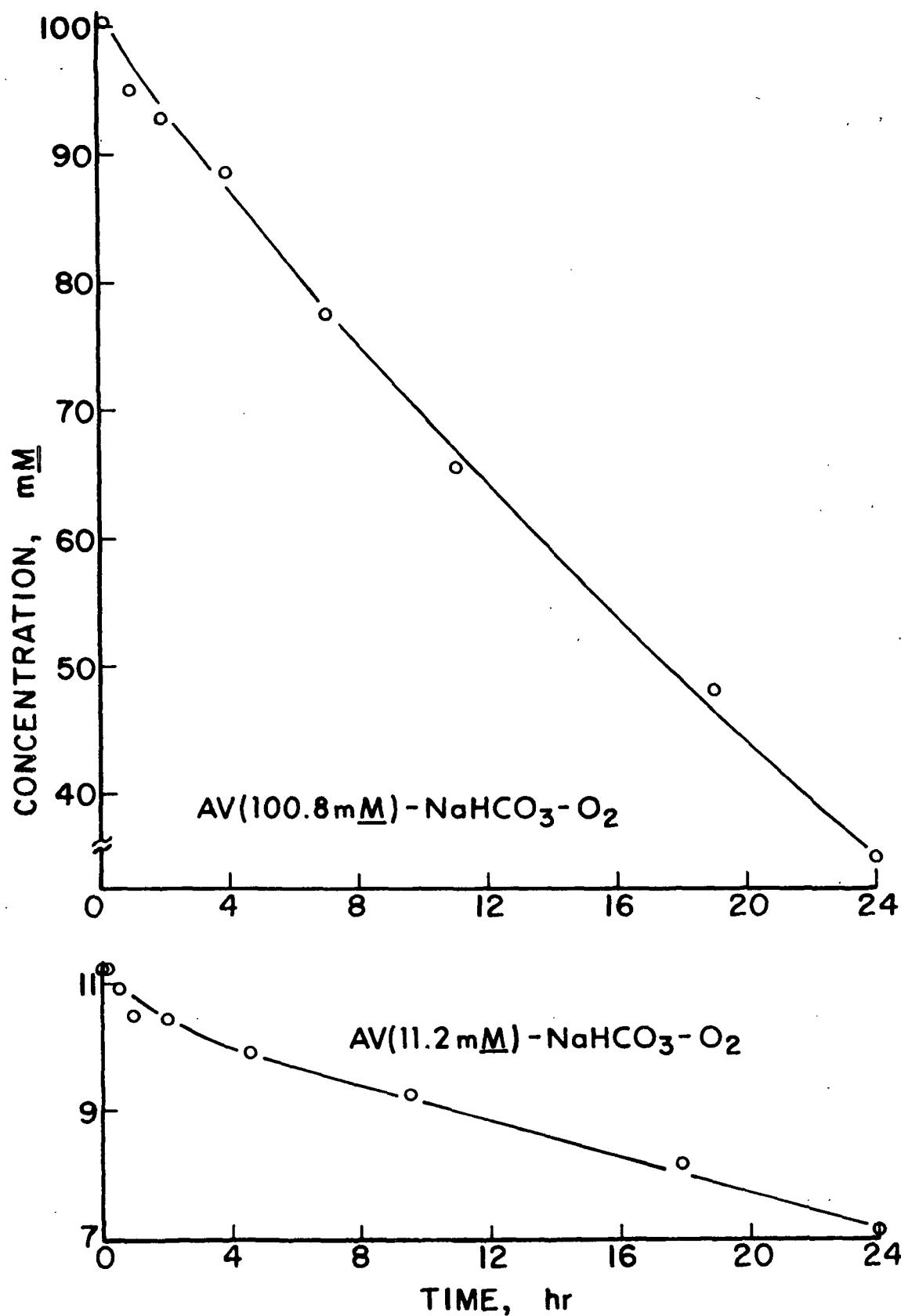


Figure 12.. Disappearance of AV (100.8 mM - top, 11.2 mM - bottom) in NaHCO<sub>3</sub> at 80°C and 150 psig O<sub>2</sub>.



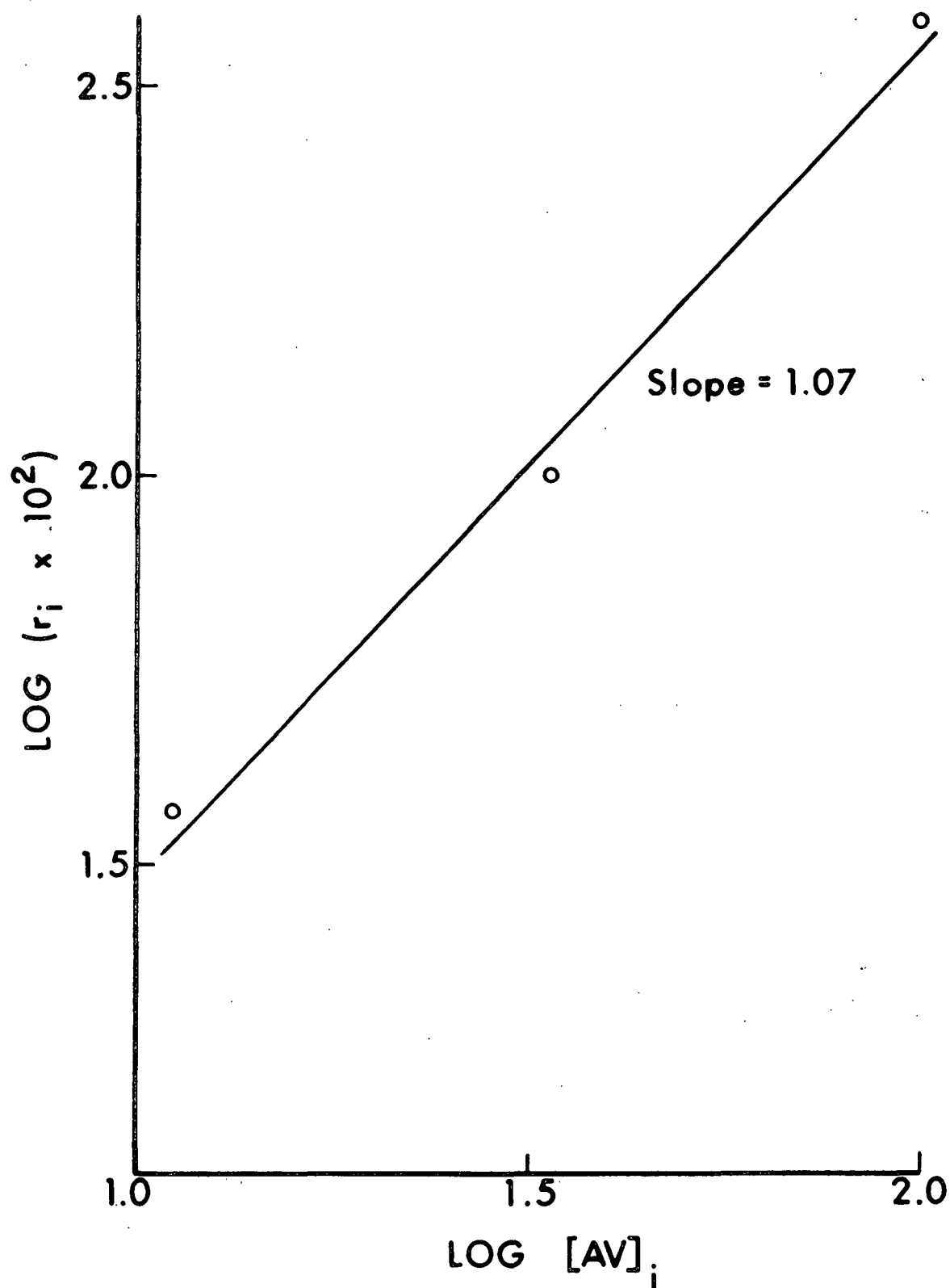


Figure 13. Kinetic plot of reactions of AV- $\text{NaHCO}_3\text{-O}_2$  according to the differential method by changing the initial AV concentration (11.2  $\text{mM}$ , 33.6  $\text{mM}$ , and 100.8  $\text{mM}$ ).

### Summary

All three systems thus appear to exhibit first-order dependence on AV concentration. The rate constants evaluated from the intercepts of the log-log plots (Fig. 9, 11, and 13) were as follows: AV-NaHCO<sub>3</sub>-O<sub>2</sub> ( $0.030 \pm 0.003 \text{ hour}^{-1}$ ) > AV-Na<sub>2</sub>CO<sub>3</sub>-O<sub>2</sub> ( $0.019 \pm 0.002 \text{ hour}^{-1}$ ) > AV-NaOH-O<sub>2</sub> ( $0.016 \pm 0.002 \text{ hour}^{-1}$ ). These results show that the lignin model compound AV has a faster reaction rate in the oxygen-sodium bicarbonate system (pH = 8.9) than in the oxygen-sodium carbonate (pH = 10.8) and oxygen-sodium hydroxide systems (pH = 12.8).

### AV-BORAX-OXYGEN REACTIONS

In order to determine if the pH of the solution is the major factor affecting the reaction rate, we reacted AV with oxygen in two borax buffer solutions - borax/NaOH (initial pH = 10.8), and borax/HCl (initial pH = 8.9). The initial pH of each buffer solution paralleled the initial pH of 1.25N sodium carbonate and sodium bicarbonate solutions.

As can be seen from Fig. 14, the disappearance curves of AV in two oxygen-borax buffer systems (borax/NaOH, borax/HCl) show great similarities not only qualitatively, but quantitatively, regardless of different initial pH (10.8 vs. 8.9) in their solutions. Similarity was also noticed between these two systems and AV-NaOH-O<sub>2</sub> (initial pH = 12.8) (Fig. 18).

A differential method of kinetic analysis, accomplished by changing the initial AV concentration, was employed here again to determine the reaction order with respect to AV in the oxygen-borax system.

Two reactions were carried out in the oxygen-borax/NaOH system with different initial AV concentrations (11.2 mM and 100.8 mM). Figure 15 shows the disappearance of AV during the two reactions. Based on Eq. (3), three sets of data ( $[AV]_1 = 11.2$

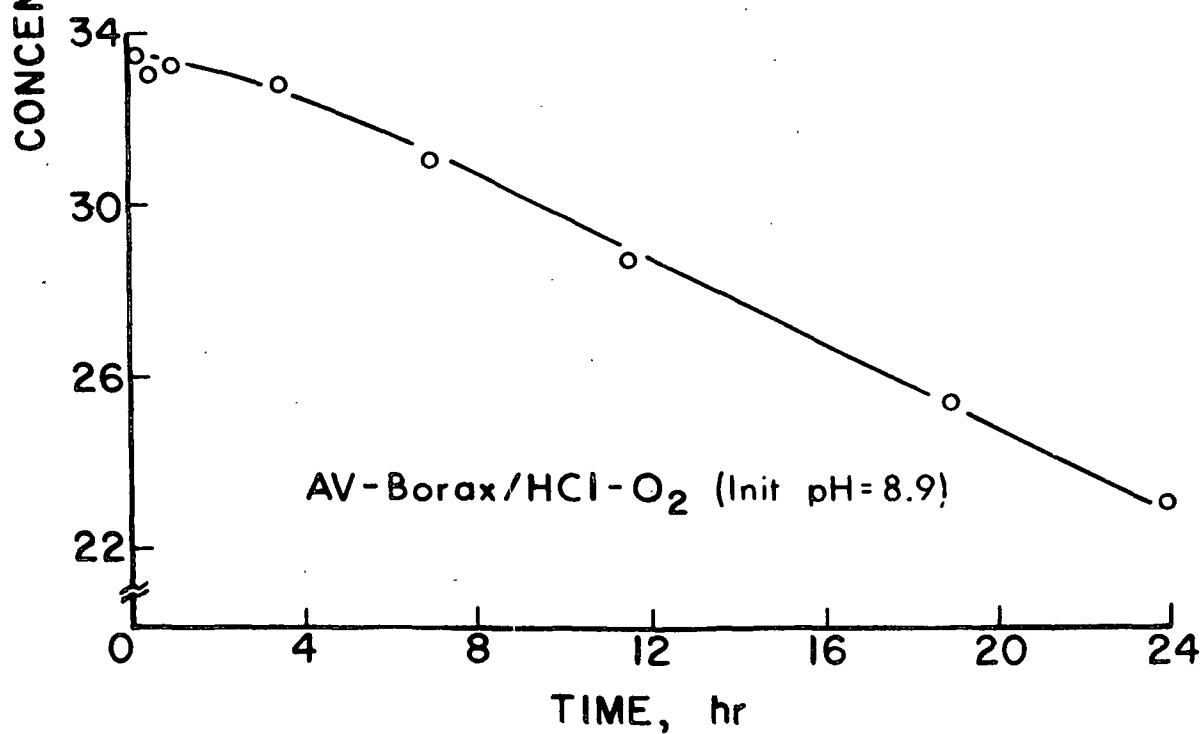
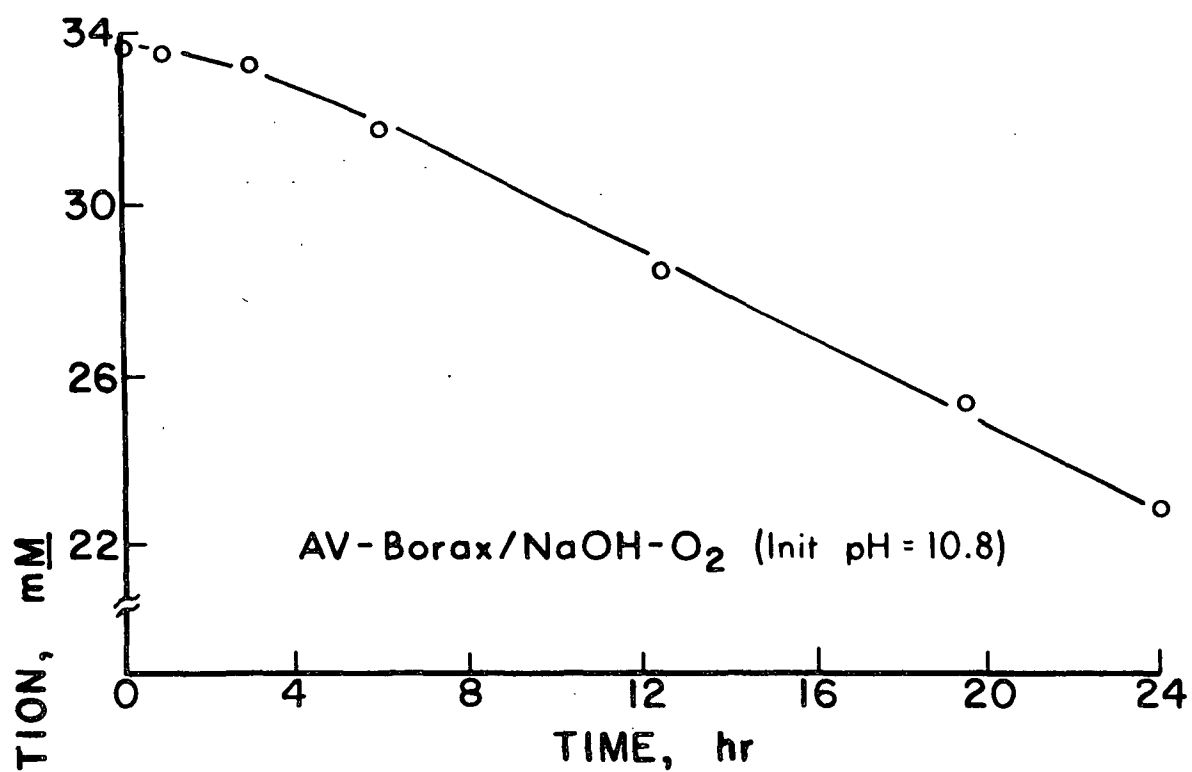


Figure 14. Disappearance of AV (33.6 mM) at 80°C and 150 psig O<sub>2</sub> in two borax buffer solutions.

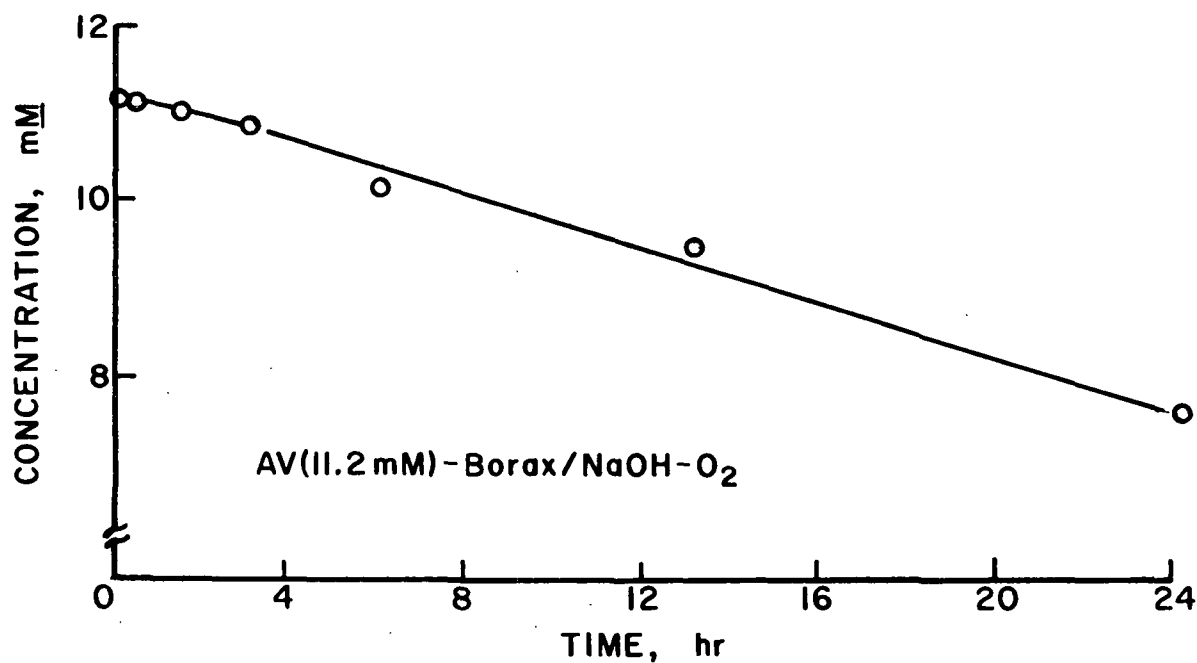
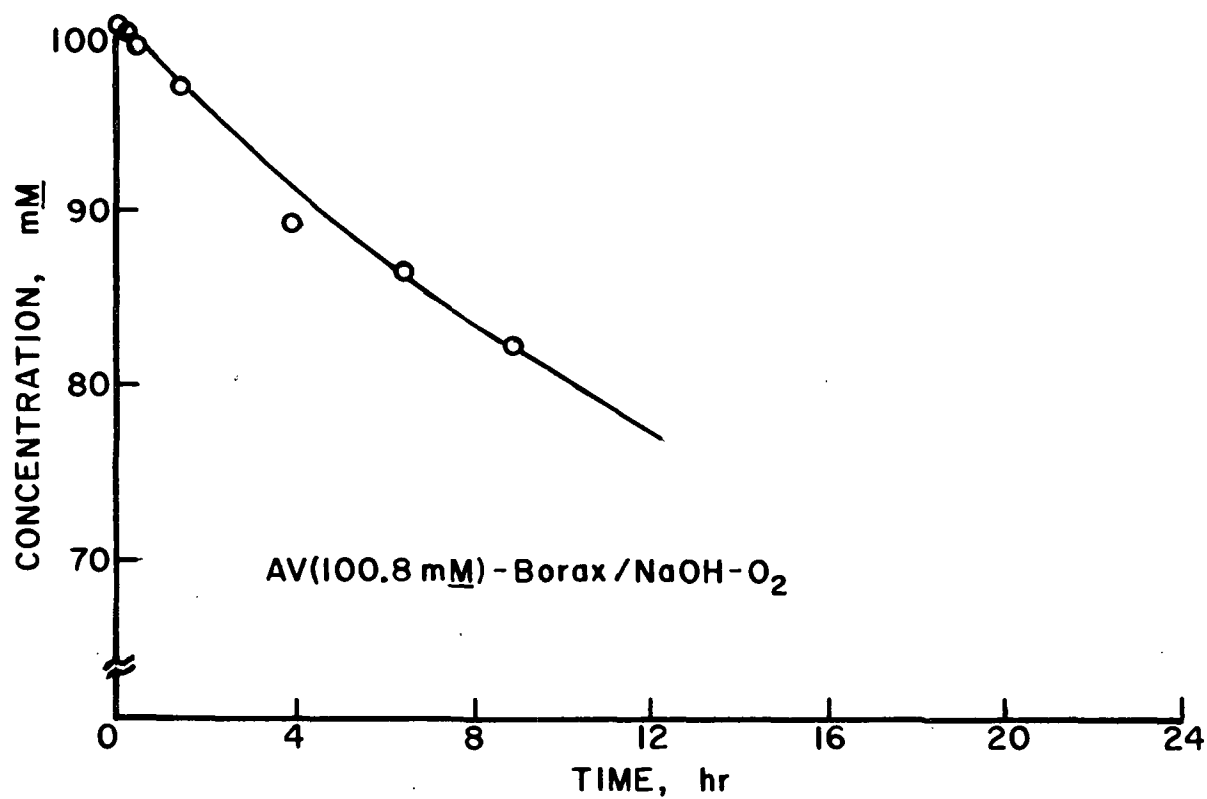


Figure 15. Disappearance of AV (100.8 mM - top, 11.2 mM - bottom) in borax/NaOH buffer solution at 80°C and 150 psig O<sub>2</sub>.

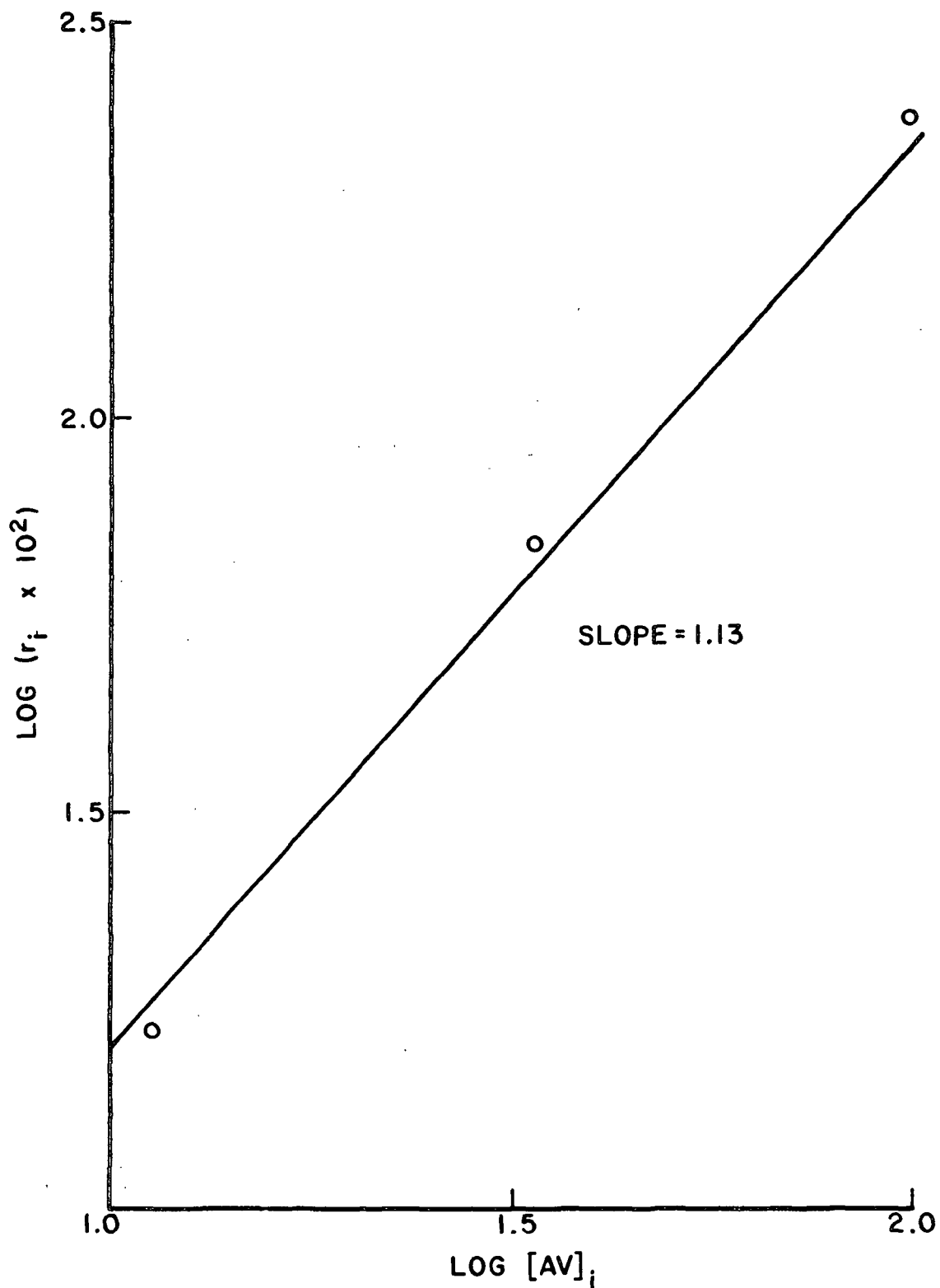


Figure 16. Kinetic plot of reactions of AV-borax/NaOH-O<sub>2</sub> according to the differential method by changing the initial AV concentration (11.2 mM, 33.6 mM, and 100.8 mM).

mM, 33.6 mM, and 100.8 mM) were plotted as the logarithm of the initial rates versus the logarithm of the initial concentrations. The best straight-line fit of the data has a slope of 1.13 (Fig. 16), which suggests the reaction has a first-order dependence on the AV concentration. Since the disappearance curves of two AV-borax-oxygen systems are almost identical (Fig. 14), the reaction of AV-borax/HCl-O<sub>2</sub> may be assumed also to be first-order in AV.

#### AV-PHOSPHATE-OXYGEN REACTIONS

On the basis of the borax reactions, it may be concluded that the pH of the reaction solutions is not a factor affecting the reaction rate. The faster reaction rate in Na<sub>2</sub>CO<sub>3</sub>/NaHCO<sub>3</sub>-O<sub>2</sub> systems is probably due to some peculiar species generated in the Na<sub>2</sub>CO<sub>3</sub>/NaHCO<sub>3</sub>-O<sub>2</sub> systems. In order to confirm our suspicions, we reacted AV with oxygen in phosphate buffer systems.

As can be seen in Fig. 17 (top, solid line), the disappearance rate after a ten-hour reaction time for AV-KH<sub>2</sub>PO<sub>4</sub>/NaOH-O<sub>2</sub> was slower than for the borax system (dotted line). However, the pH of the solution had dropped below 7.5 after several hours of reaction time (pK<sub>a</sub> of AV = 7.5).

Acetovanillone was then reacted in the O<sub>2</sub>-Na<sub>2</sub>HPO<sub>4</sub>/NaOH system (initial pH = 11). In this reaction, the pH of the solution was maintained above 7.5 during the entire reaction time. Figure 17 (bottom) shows the disappearance curves of two buffer systems (borax and phosphate) are almost identical.

Once again, the results indicate that the "abnormal" behavior of AV in Na<sub>2</sub>CO<sub>3</sub>/NaHCO<sub>3</sub>-O<sub>2</sub> is probably due to the particular species existing in those systems, and not to the pH of the solutions.

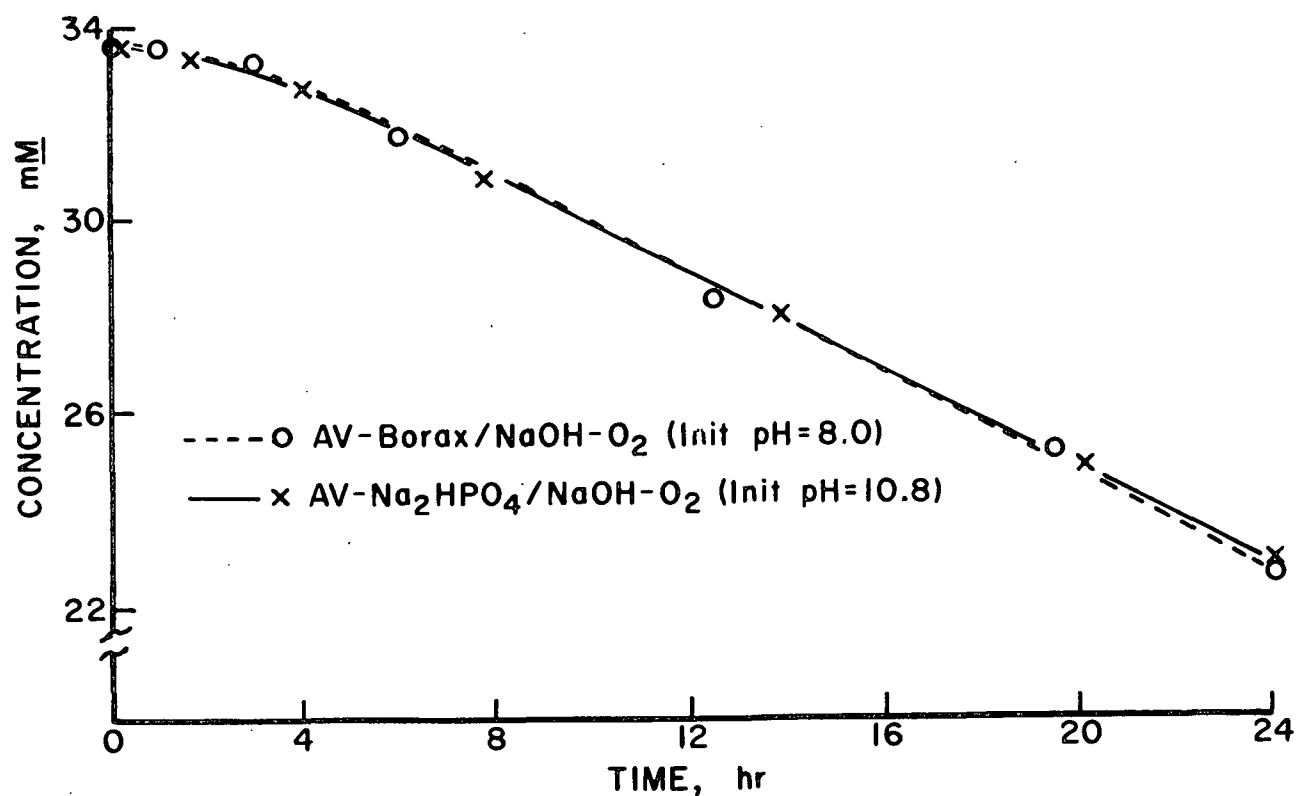
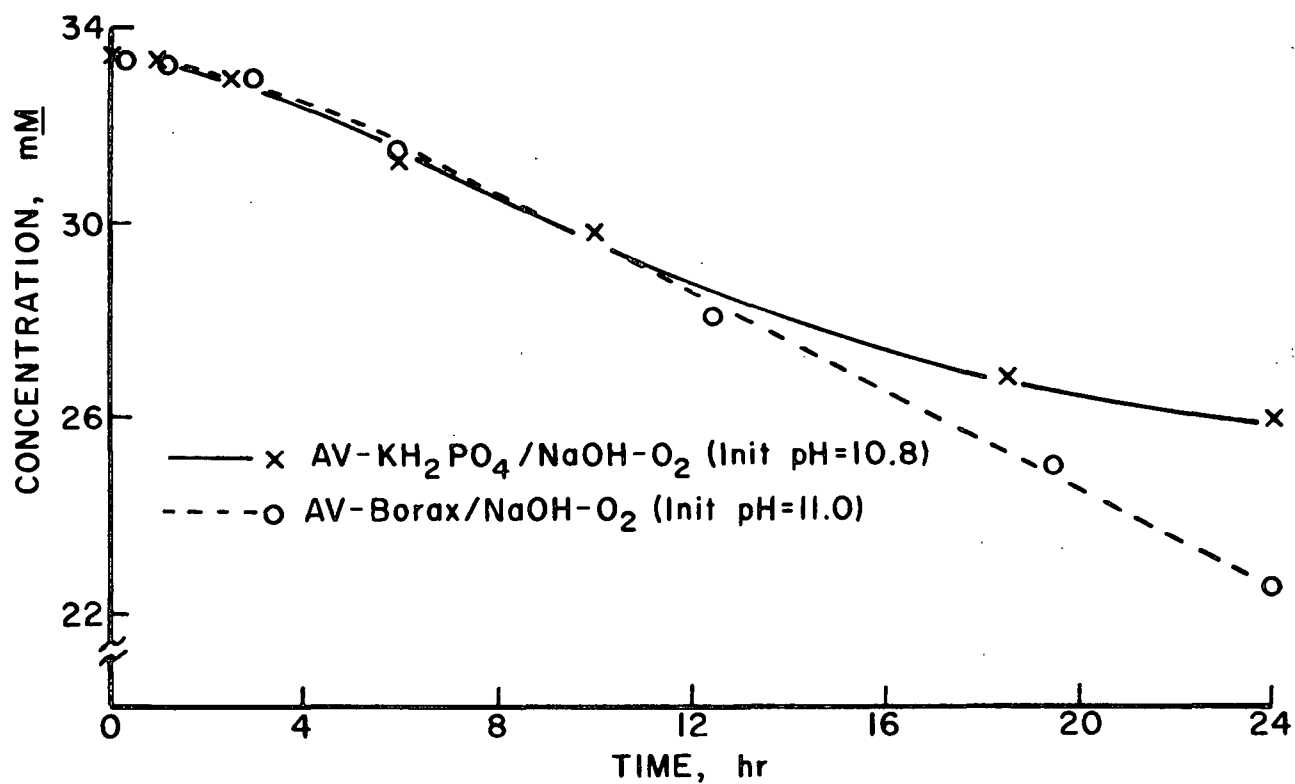


Figure 17. Disappearance of AV (33.6 mM) at 80°C and 150 psig O<sub>2</sub> in various buffer solutions.

## EFFECT OF pH

The AV disappearance curves for reactions with oxygen in different non-carbonate alkaline media are collected in Fig. 18. The solid line shows that if the pH of the solution was maintained above the pKa of AV, the reactions all had the same reaction rate, regardless of their initial pH. In the case where the pH dropped below 7.5 (the pKa of AV), the reaction rate slowed down (dotted line).

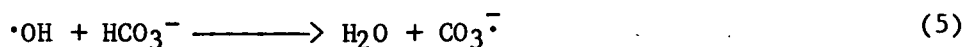
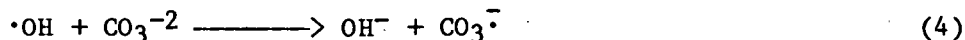
One more reaction (AV-borax/HCl-O<sub>2</sub>) was carried out, which started at a pH of 7.35. It showed a decrease in rate (upper curve in Fig. 19) compared with other reactions. The results suggest that it is important to keep the pH of the cooking liquor above the pKa of lignin in order to obtain a reasonable reaction rate. This is consistent with the findings by other researchers using wood pulp as a raw material (43).

## EFFECT OF DMSO

### Introduction

Based on the results of kinetic studies, AV showed a faster reaction rate in the oxygen-sodium carbonate and oxygen-sodium bicarbonate systems than in oxygen-sodium hydroxide and other buffer systems (Fig. 20). What could be causing the abnormally fast reactions in the two carbonate/bicarbonate systems?

Reports in the literature (63-68) indicate that carbonate radical anions can be generated in carbonate/bicarbonate solutions containing hydroxyl radicals, as shown in Eq. (4) and (5).





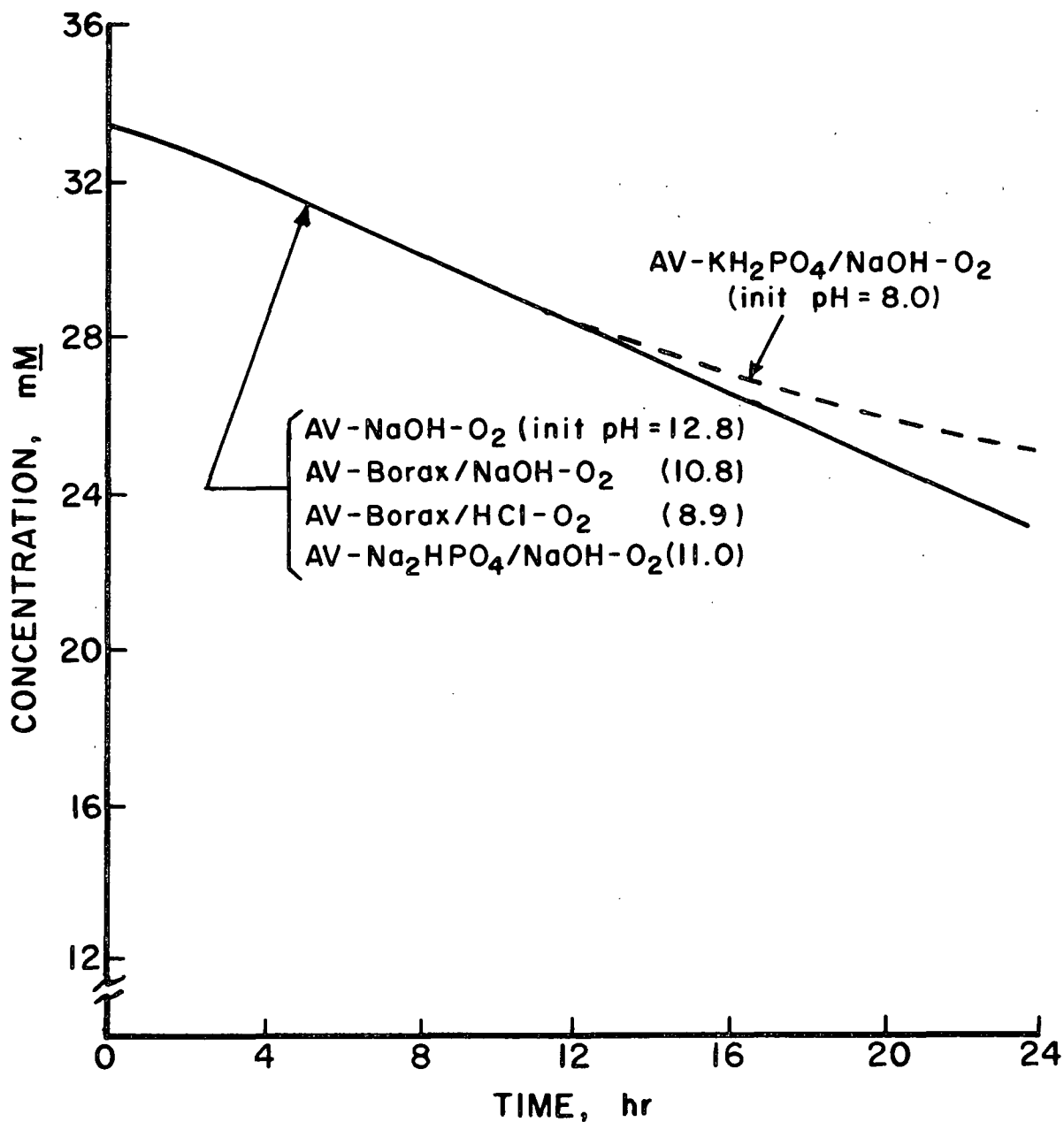


Figure 18. Disappearance of AV (33.6 mM) at 80°C and 150 psig O<sub>2</sub> in various alkaline solutions.

The presence of the carbonate radical anion was established using absorption spectroscopy (63,65,68). As a result, we speculate that the unusual behavior of AV in oxygen-sodium carbonate/bicarbonate system is due to the carbonate radical anion ( $\text{CO}_3^{\cdot-}$ ) generated in the O<sub>2</sub>-Na<sub>2</sub>CO<sub>3</sub> and O<sub>2</sub>-NaHCO<sub>3</sub> systems.

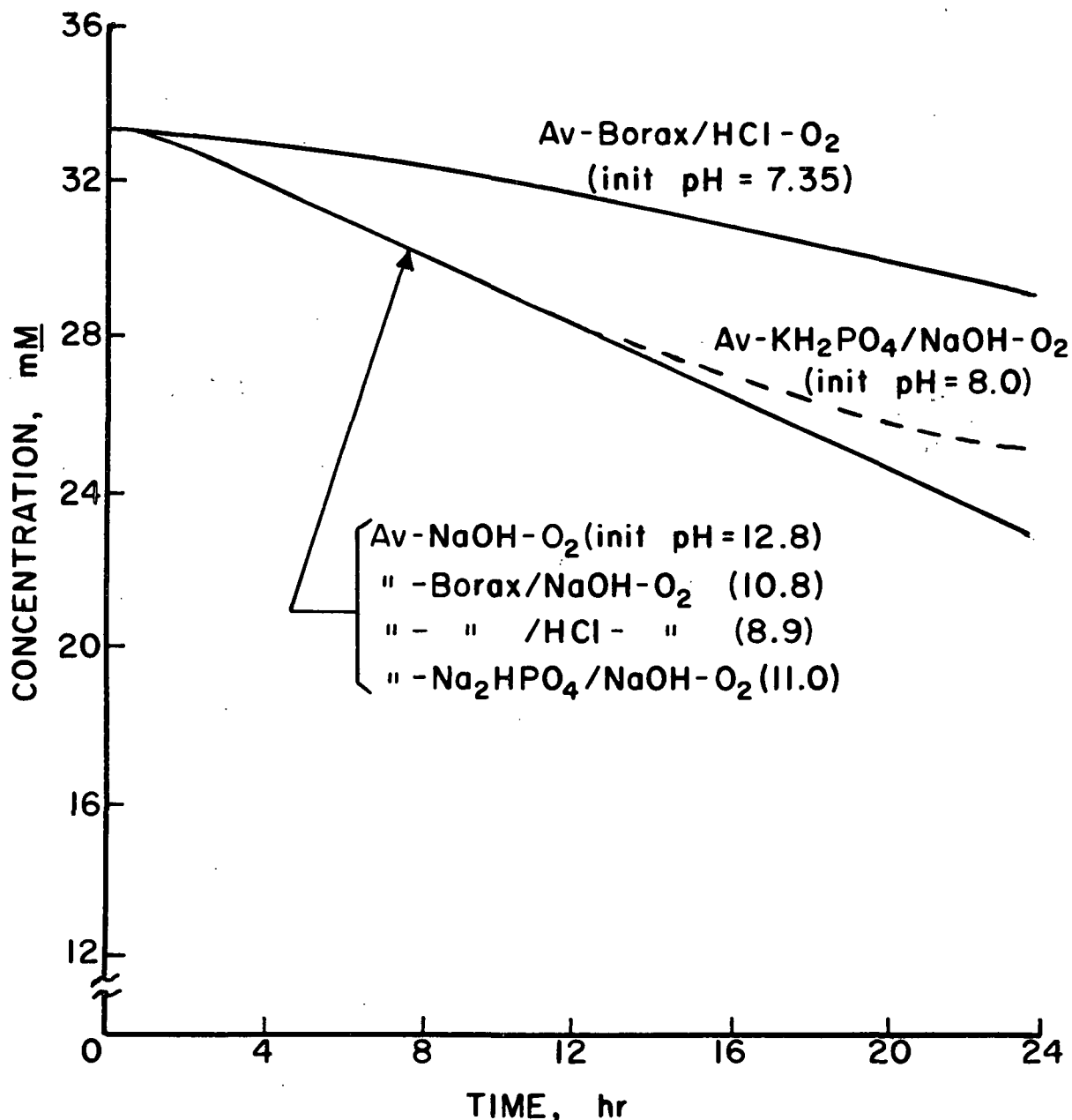
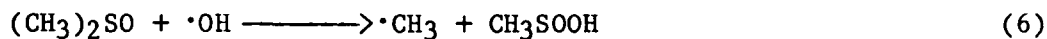


Figure 19. Disappearance of AV (33.6 mM) at 80°C and 150 psig O<sub>2</sub> in various alkaline solutions.

Other research workers have demonstrated a rapid reaction ( $k = 7 \times 10^9 \text{ M}^{-1} \text{ sec}^{-1}$ ) between hydroxyl radicals and dimethyl sulfoxide (DMSO) by using ESR/rapid mixing techniques [Eq. (6), (69-71)]. The presence of DMSO in the oxygen-alkali



solutions should diminish the concentration of hydroxyl radicals and secondary reaction products derived from the hydroxyl radical.

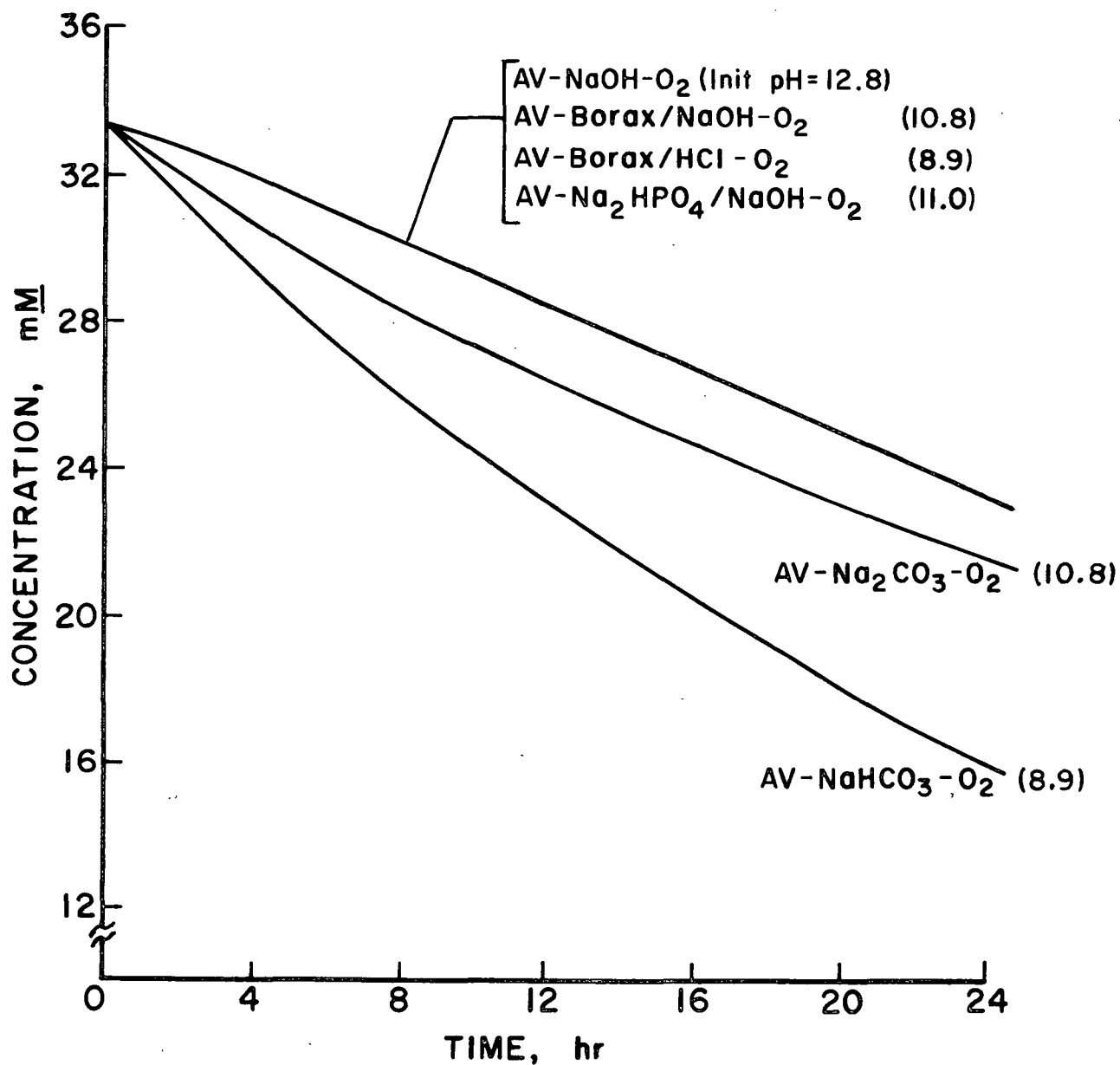


Figure 20. Disappearance of AV (33.6 mM) at 80°C and 150 psig O<sub>2</sub> in various alkaline solutions.

# Reactions in Presence of DMSO

Acetovanillone (33.6 mM) was reacted with oxygen in  $\text{NaHCO}_3$ , borax, and  $\text{NaOH}$  solutions with the addition of DMSO (66.7 mM) as a scavenging reagent to reduce the amount of hydroxyl radicals in these systems.

The slopes of the disappearance curves (Fig. 21) show a pronounced decrease of reaction rate of AV- $\text{NaHCO}_3$ - $\text{O}_2$ -DMSO compared with the reaction without DMSO. Similar, but less pronounced effects were observed for the borax and  $\text{NaOH}$  systems (Fig. 21). The observed reductions in reaction rates are not dependent on pH since the magnitudes of the rate reductions were the same for the reactions of AV- $\text{NaOH}$ - $\text{O}_2$ -DMSO (initial pH = 12.8) and AV-borax/ $\text{HCl}$ - $\text{O}_2$ -DMSO (initial pH = 8.9) regardless of their pH difference.

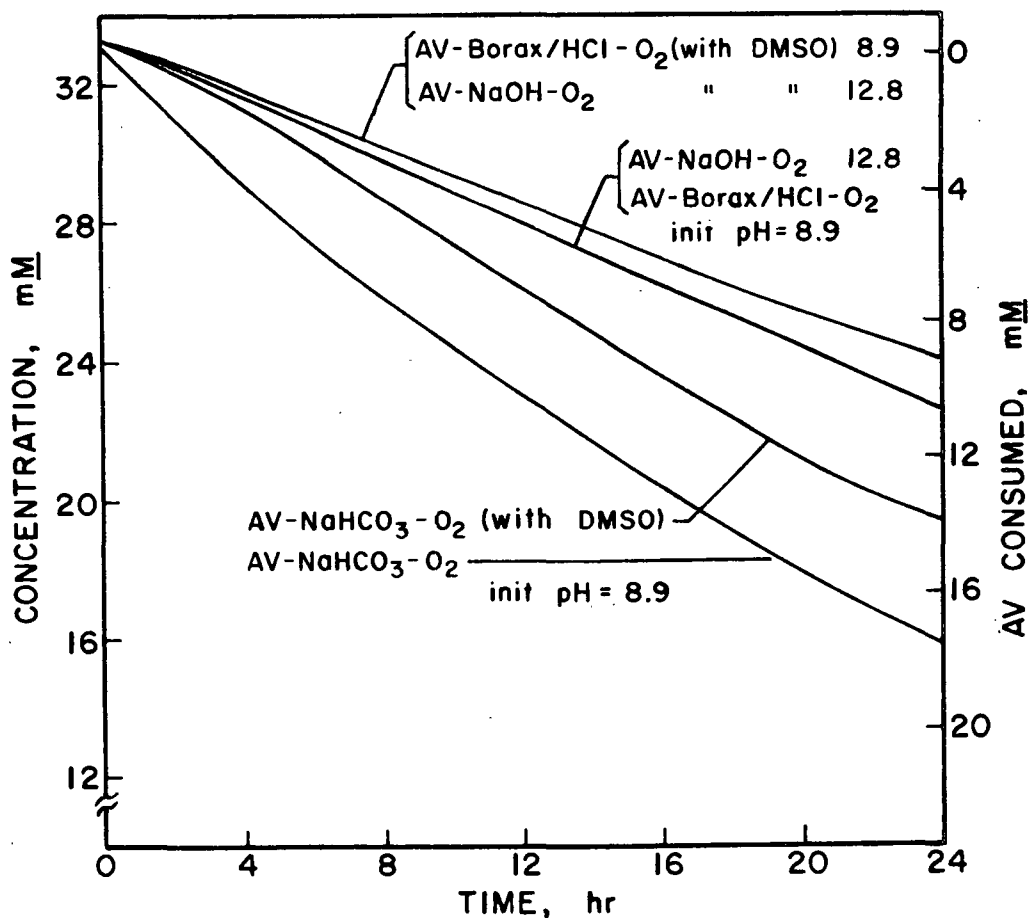


Figure 21. Disappearance of AV (33.6 mM) at 80°C and 150 psig  $\text{O}_2$  in various alkaline solutions.

Another way to examine the results is to compare the initial rates. As can be seen from Table I, the initial rate reduction was more prominent in the case of AV-NaHCO<sub>3</sub>-O<sub>2</sub>(1.1 → 0.6) as compared with the AV-NaOH-O<sub>2</sub> or AV-borax/HCl-O<sub>2</sub> (0.4 → 0.3).

TABLE I

THE INITIAL RATE OF AV IN DIFFERENT ALKALINE MEDIA AT 80°C AND 150 psig O<sub>2</sub>

Reaction	Initial pH	Ionic Strength	Initial Rate, $\frac{mM}{hr^a}$
AV-NaOH-O <sub>2</sub>	12.8	1.25	0.4 ± 0.06
AV-NaOH/KCl-O <sub>2</sub>	12.7	0.8	0.4 ± 0.06
AV-NaOH/KCl-O <sub>2</sub>	12.6	0.4	0.4 ± 0.06
AV-NaOH-O <sub>2</sub> -DMSO	12.8	1.25	0.3 ± 0.05
AV-Na <sub>2</sub> CO <sub>3</sub> -O <sub>2</sub>	10.8	1.25	0.8 ± 0.10
AV-Na <sub>2</sub> CO <sub>3</sub> -O <sub>2</sub>	10.8	1.875	0.8 ± 0.10
AV-NaHCO <sub>3</sub> -O <sub>2</sub>	8.9	1.25	1.1 ± 0.15
AV-NaHCO <sub>3</sub> -O <sub>2</sub> -DMSO	8.9	1.25	0.6 ± 0.09
AV-Borax-NaOH-O <sub>2</sub>	10.8	--	0.4 ± 0.06
AV-Borax-HCl-O <sub>2</sub>	8.9	--	0.4 ± 0.06
AV-Borax/HCl-O <sub>2</sub> -DMSO	8.9	--	0.3 ± 0.05
AV-Na <sub>2</sub> HPO <sub>4</sub> /NaOH-O <sub>2</sub>	11.0	--	0.4 ± 0.06
AV-KH <sub>2</sub> PO <sub>4</sub> /NaOH-O <sub>2</sub>	8.0	--	0.4 ± 0.06
AV-Borax/HCl-O <sub>2</sub>	7.35	--	0.1 ± 0.04

<sup>a</sup>Due to the difficulty in determining the initial slopes accurately, the numbers might vary within ± 15% range.

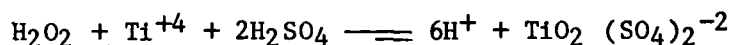
These results suggest that the hydroxyl radical and/or similar powerful radicals are an active participant during the AV-oxygen-alkali reactions and, as far as the reaction rate is concerned, the carbonate radical anion plays a more important role during the AV-oxygen-alkali reactions. More details will be presented in the Mechanism section.

#### PRODUCT FORMATION

Some of the products formed during the AV reactions were examined to determine if the different alkaline media caused a change in reaction pattern or product distribution.

## HYDROGEN PEROXIDE

Hydrogen peroxide has been postulated as an important intermediate during oxygen-alkali delignification reactions (29,39). The concentration of hydrogen peroxide was measured in the AV-oxygen-alkali reaction samples by employing the acid titanium sulfate method. In this method, hydrogen peroxide forms an immediate yellow complex with titanium under acidic conditions (pH 0 to 2) (52,53):



The amounts of hydrogen peroxide formed in solutions of the three different oxygen-alkali media are plotted against reaction time in Fig. 22. A comparison of the three plots shows similar trends of hydrogen peroxide formation and disappearance. The two AV-oxygen-borax systems behaved similarly. The level of hydrogen peroxide began to build up at the beginning of the reaction, reached a maximum, then decreased to a low level. Hydrogen peroxide thus appears to be an intermediate. The early peak (within two hours) in hydrogen peroxide concentration relative to total reaction time is consistent with the data of a previous investigator (51). The peak hydrogen peroxide concentration (ca. 0.2 mM) was less than one percent of the initial AV concentration (33.6 mM).

## METHANOL

During the oxygen-alkali reaction of AV, methanol is liberated as a result of oxidative demethoxylation (28,51). Freiberg (51) found an 85 percent yield of methanol during the degradation of AV at 120°C, with 1.79N NaOH and 150 psig O<sub>2</sub>. He also reported that the yield of methanol produced is constant during the entire reaction. Therefore, he concluded that the majority of the methanol is produced by primary reactions (51). Bailey and Dence (41) reported that 35 to 40 percent

methanol is liberated in the alkaline hydrogen peroxide reaction of AV (45°C, initial pH = 10.5). In our study, methanol formation was analyzed by quantitative GLC employing ethanol as an internal standard (57). According to the previous investigators, methanol is stable under the conditions of temperature and oxygen pressure used in this work (58,59).

Our results show that 48 to 65 percent methanol was liberated from AV by the end of a 24-hour reaction period in the different oxygen-alkali systems (Table II). The data also show that the yield of methanol was the highest (ca. 65%) when the pH was also higher (12.8). This is consistent with the findings by other researchers (34,36,45) using either model compounds or wood pulp. Tests have shown that the yields of methanol were increased with decreasing ionic strength at constant pH.

TABLE II

METHANOL PRODUCTION FROM AV AT THE END OF 24-HOUR REACTION PERIOD DURING THE OXIDATION IN DIFFERENT ALKALINE MEDIA AT 80°C, 150 psig O<sub>2</sub>

Reaction	Initial pH	Final pH	Ionic Strength	MeOH, mole % <sup>a</sup>
AV-NaOH-O <sub>2</sub>	12.8	12.6	1.25	65
AV-NaOH/KCl-O <sub>2</sub>	12.7	12.6	0.8	70
AV-NaOH/KCl-O <sub>2</sub>	12.6	12.5	0.4	74
AV-Na <sub>2</sub> CO <sub>3</sub> -O <sub>2</sub>	10.8	10.2	1.25	56
AV-NaHCO <sub>3</sub> -O <sub>2</sub>	8.9	8.7	1.25	53
AV-Borax-NaOH-O <sub>2</sub>	10.8	10.4	--	59
AV-Borax/HCl-O <sub>2</sub>	8.9	8.5	--	51
AV-Na <sub>2</sub> HPO <sub>4</sub> /NaOH-O <sub>2</sub>	11.0	10.0	--	53
AV-KH <sub>2</sub> PO <sub>4</sub> /NaOH-O <sub>2</sub>	8.0	7.1	--	48

<sup>a</sup>% of theoretical available for consumed AV.

A number of mechanisms can be visualized. The most plausible route which fits our results is depicted below.

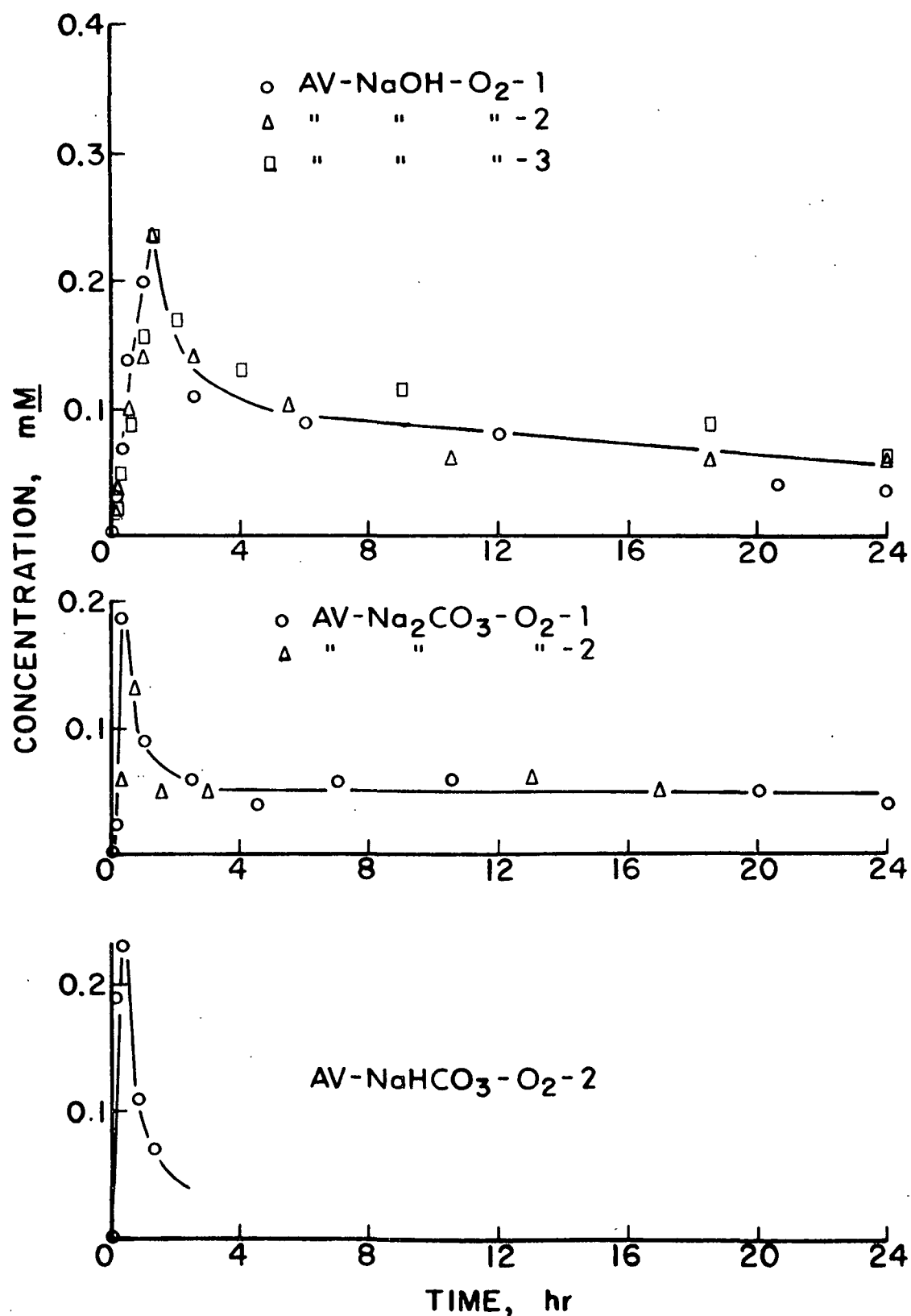
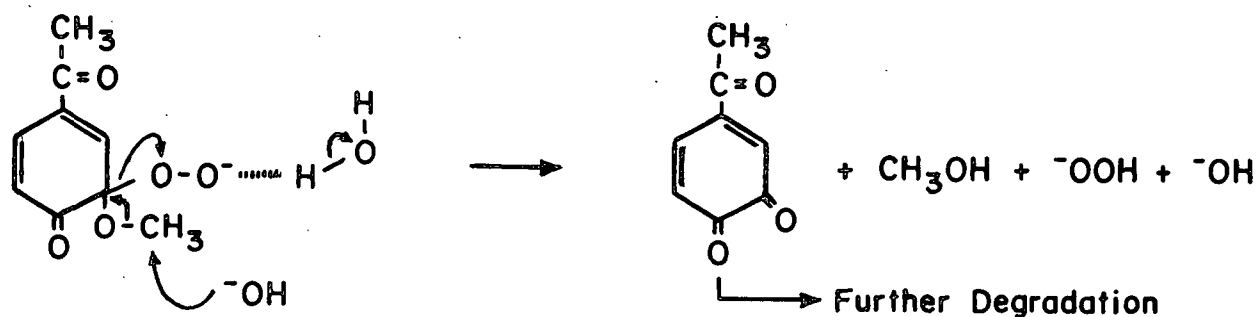


Figure 22. Hydrogen peroxide produced during the reactions of AV-oxygen-alkali.





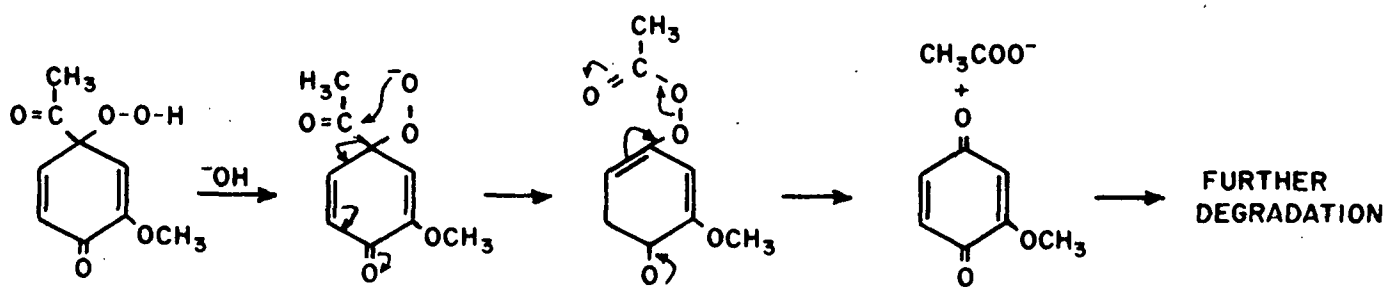
The cyclohexadienone hydroperoxide of AV might be converted into the corresponding ortho-quinone and methanol by attack of a hydroxyl anion at a methoxyl group. Higher alkalinity should favor this process. The quinone can be further degraded into muconic acid and carboxylic acids under oxygen-alkali conditions (34,39,41).

#### ACETIC ACID

Kratzl, et al. demonstrated that lignin units containing an alpha-carbonyl group in the side-chain may undergo a Dakin-like reaction to form acids (29,30). They also proved that the acetic acid originates solely from the side-chain by oxidation of the alpha-<sup>14</sup>C-labelled AV, and that acetic acid is very stable under oxygen-alkali conditions (29). In our study, acetic acid was analyzed by GLC employing butyric acid as an internal standard. The data show that 50 to 55 percent of acetic acid, based on the consumed AV, was produced at the end of a 24-hour reaction period in most of the oxygen-alkali systems. The exception was the reaction of AV in oxygen-sodium hydroxide, in which 90 percent of the theoretically available acetic acid was liberated (Table III).

The mechanism of the Dakin-like reaction (40) has not been clarified in its details. One proposal (29) is shown below, which involves an intramolecular

peroxide attack on the carbonyl carbon to form a perester. The perester then splits into o-methoxyquinone and acetic acid. This mechanism would be facilitated by ionization of the hydroperoxide, which should have a pKa value of 11.5 (49). In the case of AV-oxygen-sodium hydroxide (pH 12.8), most hydroperoxides would be ionized. This might be the reason for the extremely high acetic acid production (90%) in oxygen-sodium hydroxide in comparison to the other reaction conditions (50-55%).



(ROOH)

TABLE III

ACETIC ACID PRODUCTION FROM AV AT THE END OF 24-HOUR REACTION PERIOD DURING THE OXIDATION IN DIFFERENT ALKALINE MEDIA AT 80°C, 150 psig O<sub>2</sub>

Reaction	Initial pH	Final pH	CH <sub>3</sub> COOH, mole % <sup>a</sup>
AV-NaOH-O <sub>2</sub>	12.8	12.6	90
AV-Na <sub>2</sub> CO <sub>3</sub> -O <sub>2</sub>	10.8	10.2	50
AV-NaHCO <sub>3</sub> -O <sub>2</sub>	8.9	8.7	50
AV-Borax-NaOH-O <sub>2</sub>	10.8	10.4	55
AV-Borax/HCl-O <sub>2</sub>	8.9	8.5	50
AV-Na <sub>2</sub> HPO <sub>4</sub> /NaOH-O <sub>2</sub>	11.0	10.0	50
AV-KH <sub>2</sub> PO <sub>4</sub> /NaOH-O <sub>2</sub>	8.0	7.1	50

<sup>a</sup>% of theoretical available for consumed AV; due to the variation in response factor determination, the data might vary within ± 10% range.

## CARBOXYLIC ACIDS

Carboxylic acid products from the reaction solutions were analyzed as their trimethylsilyl (TMS) derivatives by gas chromatography-mass spectrometry (GC-MS).

The identification of the acidic products was made by interpretation of the spectra and in some cases by the comparison of the relative GC retention times and mass spectra with the silylated authentic samples (Table IV). Figures 22-26 show the chromatograms of the acidic reaction products in different oxygen-alkali systems after 24-hour reactions. These products include: 2-hydroxyisobutyric, lactic, glycolic, oxalic, malonic, succinic, maleic, hydroxymalonic, and malic acids. Semiquantitative estimates of their concentrations were made by estimating response factors on a molecular weight basis, or determining them by injecting a single sample together with AV. The sample workup procedure is described in the Experimental section. Appendices I and IV present GC-MS conditions and results.

TABLE IV  
MAJOR ACIDIC PRODUCTS

Product	Product Identification	Identification Method
1	Hydroxyisobutyric acid	MS <sup>a</sup>
2	Lactic acid	MS
3	Glycolic acid	GC <sup>b</sup> , MS
4	Oxalic acid	GC, MS
5	Malonic acid	GC, MS
6	Succinic acid	GC, MS
7	Maleic acid	GC, MS
8	Hydroxymalonic acid	MS
9	Malic acid	GC, MS

<sup>a</sup>Identified by gas chromatography-mass spectrometry. Mass spectra of all acids have been published. Mass spectral data for acids analyzed in this work are tabulated in Appendix IV.

<sup>b</sup>Identified by comparison to the GC retention time of reaction sample and authentic sample. GC conditions and retention times are given in Appendix I.

By comparing Fig. 23, 24, 25, and 26, one can see that most products were common to all reactions but that there were exceptions. Maleic acid (peak 7) was missing in the reactions of AV-NaOH-O<sub>2</sub> and AV-borax/NaOH<sub>2</sub>; hydroxyisobutyric acid (peak 1) was only found in AV-NaOH-O<sub>2</sub>; and more products (peaks 10 and 11, Fig. 25) were

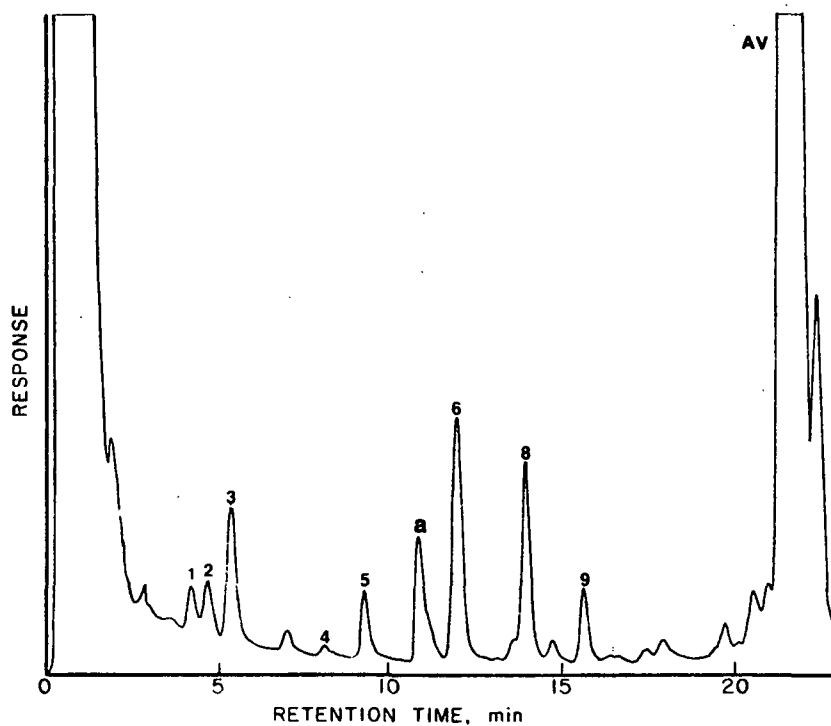


Figure 23. Sample GLC chromatogram of the acidic products of AV in oxygen (150 psig) and sodium hydroxide (1.25N) at 80°C (initial pH = 12.8).

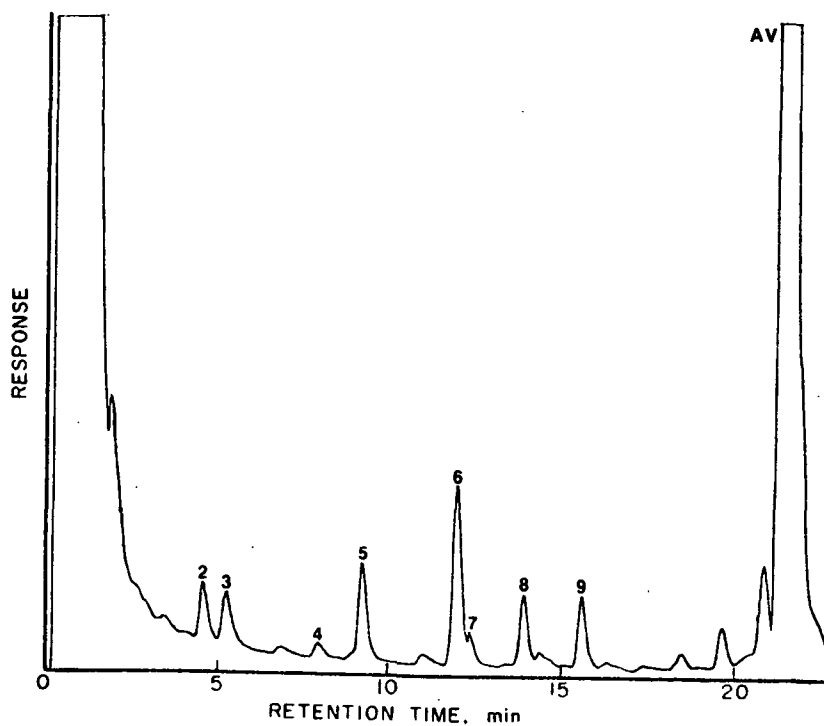


Figure 24. Sample GLC chromatogram of the acidic products of AV in oxygen (150 psig) and sodium carbonate at 50°C (initial pH = 10.8).

<sup>a</sup>Decamethyl tetrasilane.

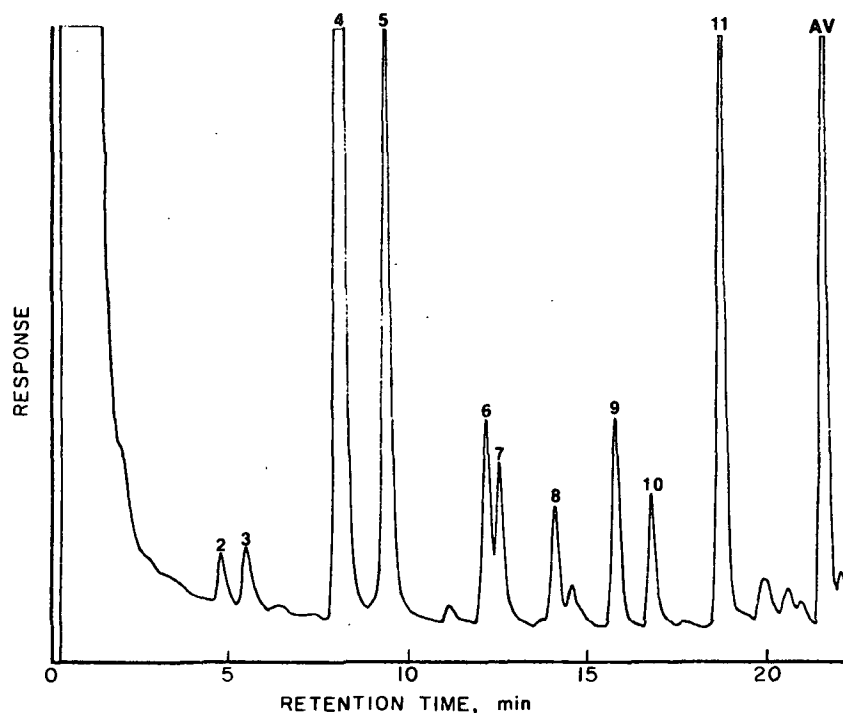


Figure 25. Sample GLC chromatogram of the acidic products of AV in oxygen (150 psig) and sodium bicarbonate (1.25N) at 80°C (initial pH = 8.9).

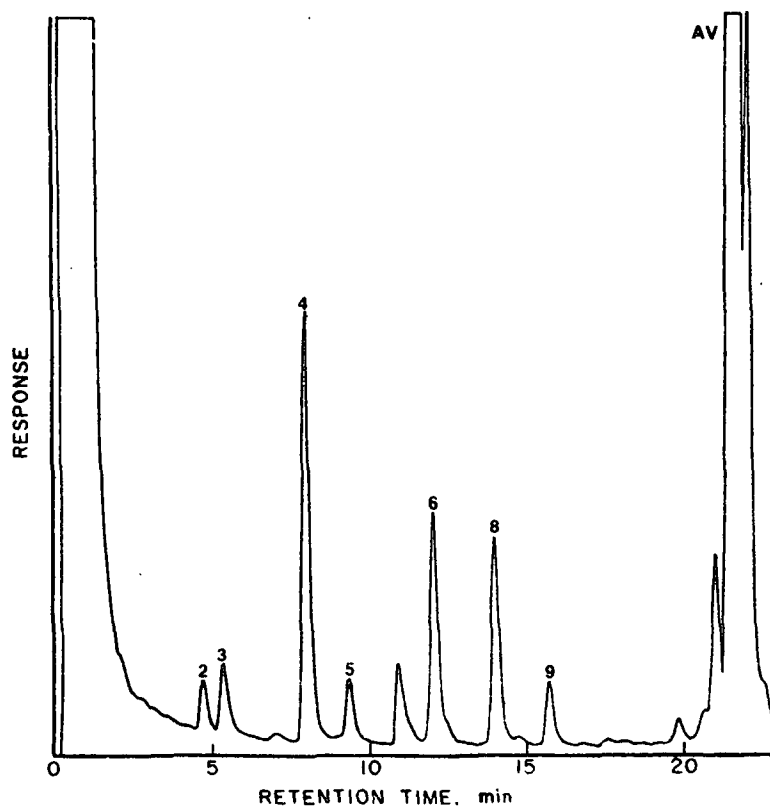


Figure 26. Sample GLC chromatogram of the acidic products of AV in oxygen (150 psig) and borax/NaOH buffer at 80°C (initial pH = 10.8).

<sup>a</sup>Decamethyl tetrasilane.

detected in AV-NaHCO<sub>3</sub>-O<sub>2</sub>. The amounts of the acidic products produced in each reaction were comparable (Table V), except for the high yield of oxalic acid (53%) and malonic acid (17%) in the reaction of AV-NaHCO<sub>3</sub>-O<sub>2</sub>, and the high yields of oxalic acid (19%) and succinic acid (12%) in the reaction of AV-borax/NaOH-O<sub>2</sub>. The errors encountered in the acidic product analyses have standard deviations in the range of 10-30%. However, these data still provide useful ground for comparing the acidic product formation in different oxygen-alkali systems.

TABLE V

ACIDIC PRODUCT DISTRIBUTION AFTER 24-HOUR REACTION OF AV IN DIFFERENT OXYGEN-ALKALI SYSTEMS. YIELDS ARE GIVEN IN mM AND MOLE PERCENTAGES BASED ON CONSUMED AV ARE GIVEN IN PARENTHESES<sup>a</sup>

Product	AV-NaOH-O <sub>2</sub> ,		AV-Na <sub>2</sub> CO <sub>3</sub> -O <sub>2</sub> ,		AV-NaHCO <sub>3</sub> -O <sub>2</sub> ,		AV-Borax/ HCl-O <sub>2</sub> ,	
	mM	%	mM	%	mM	%	mM	%
1. Hydroxyisobutyric acid	0.2	(2)						
2. Lactic acid	0.2	(2)	0.3	(2.5)	0.5	(3)	0.3	(3)
3. Glycolic acid	0.5	(5)	0.3	(2.5)	0.5	(3)	0.4	(4)
4. Oxalic acid	0.1	(1)	0.2	(1.5)	9.3	(53)	2.1	(19)
5. Malonic acid	0.3	(3)	0.7	(6)	3.0	(17)	0.4	(4)
6. Succinic acid	0.7	(7)	0.9	(7)	0.8	(5)	1.3	(12)
7. Maleic acid			0.1	(1)	0.7	(4)		
8. Hydroxymalonic acid	0.5	(5)	0.3	(2.5)	0.5	(3)	0.7	(6)
9. Malic acid	0.2	(2)	0.3	(2.5)	0.8	(5)	0.3	(3)
Consumed AV	10.1		12.3		17.5		11.0	

<sup>a</sup>For a given acidic product, the standard deviation for duplicated silylation samples was generally in the range of + 10-30%. Response factors used in semi-quantitative yield calculations are given in Appendix I.

The exact reaction routes were not pursued. Several possible pathways of generating acidic products are depicted in Fig. 27. These could account for some of the products found in our reaction solutions. Generally, the quinones formed from demethoxylations and side-chain eliminations of lignin compounds are unstable under oxygen-alkali conditions and give rise to acidic reaction products through ring fragmentations (30-36,41,77,78).



Table VI shows that the total acids (including acetic acid), based on the carbon balance, account for ca. 20-40 percent of consumed AV during the reactions. Kratzl, et al. (39) found that several of the carboxylic acids initially formed in the reaction of hydroquinone under oxygen-alkali conditions gradually disappear from the solution, forming carbon dioxide and carbon monoxide. High temperatures and high pH favor these types of reactions. Some of the small products, such as oxalic acid and glycolic acid, might be lost during the sample workup stage. Consequently, the actual amounts of acids produced in our reaction might be higher, especially at the higher pH reaction conditions. Nevertheless, our results indicate that during the oxidation of AV, the different alkaline solutions did change the reaction patterns somewhat.

#### BLACK PRECIPITATE

During the reactions at lower pH (AV-NaHCO<sub>3</sub>-O<sub>2</sub>, AV-borax/HCl-O<sub>2</sub>; init. pH = 8.9), the color of the reaction solutions became deep brown as the reaction proceeded. As the reaction sample was acidified, a black precipitate settled out. The amount of black precipitate was also proportional to the reaction time. By the end of 24-hours, the black precipitate accounted for ca. 15 percent by weight of consumed AV. These observations were in contrast with those made at higher pH's where no precipitate was observed.

The results of solubility tests of the black precipitate (Table VII) suggests that it is an organic material containing phenolic groups.

The IR spectrum (Fig. 28) of the black precipitate shows both broad hydroxyl (3200-3600 cm<sup>-1</sup>) and carbonyl (1650 cm<sup>-1</sup>) peaks. Figure 29 shows the UV spectra of the samples prior to and after the AV-NaHCO<sub>3</sub>-O<sub>2</sub> oxidation reaction (ca. 50% AV reacted). Both spectra have maxima at 230 and 276 nm and a minimum at 248 nm. The



TABLE VI

CARBON BALANCE OF ACIDIC PRODUCTS AFTER 24-HOUR REACTION OF AV IN  
DIFFERENT OXYGEN-ALKALI SYSTEMS. YIELDS ARE GIVEN IN mM AND  
TOTAL CARBONS ARE GIVEN IN PARENTHESES

Product	AV-NaOH-O <sub>2</sub> , mM (C)		AV-Na <sub>2</sub> CO <sub>3</sub> -O <sub>2</sub> , mM (C)		AV-NaHCO <sub>3</sub> -O <sub>2</sub> , mM (C)		AV-Borax/NaOH-O <sub>2</sub> , mM (C) <sup>a</sup>	
Hydroxyisobutyric acid	0.2	(0.8)						
Lactic acid	0.2	(0.6)	0.3	(0.9)	0.5	(1.5)	0.3	(0.9)
Glycolic acid	0.5	(1.0)	0.3	(0.6)	0.5	(1.0)	0.4	(0.8)
Oxalic acid	0.1	(0.2)	0.2	(0.4)	9.3	(18.6)	2.1	(4.2)
Malonic acid	0.3	(0.9)	0.7	(2.1)	3.0	(9.0)	0.4	(1.2)
Succinic acid	0.7	(2.8)	0.9	(3.6)	0.8	(3.2)	1.3	(5.2)
Maleic acid			0.1	(0.4)	0.7	(2.8)		
Hydroxymalonic acid	0.5	(1.5)	0.3	(0.9)	0.5	(1.5)	0.7	(2.1)
Malic acid	0.2	(0.8)	0.3	(1.2)	0.8	(3.2)	0.3	(1.2)
Acetic acid	9	(18.0)	6	(12.0)	9	(18.0)	6	(12.0)
Total acids		(26.6)		(22.1)		(58.8)		(27.6)
Consumed AV	10.1	(90.9)	12.3	(110.7)	17.5	(157.5)	11.0	(99.0)
% $\frac{\text{Total acids}}{\text{Consumed AV}}$		29%		20%		37%		28%
MeOH	6.5	(6.5)	6.9	(6.9)	9.2	(9.2)	6.5	(6.5)
Total acids + MeOH		(33.1)		(29.0)		(68.0)		(34.1)
% $\frac{\text{Acids + MeOH}}{\text{Consumed AV}}$		36%		26%		43%		34%

<sup>a</sup>Total carbon = concentration x number of carbons in each individual molecule.

main difference between the two spectra is a relatively shallow trough between 230 and 280 nm in the reaction sample (bottom). Pew (60) has found that a significant decrease in the size of this trough is an indication of polymerization products existing in a sample.

TABLE VII  
SOLUBILITY TEST OF BLACK PRECIPITATE

Solvent	Solubility	Solvent	Solubility
Water	Insoluble	DMF	Soluble
1N NaOH	Soluble	Ether	Insoluble
1N NaHCO <sub>3</sub>	Slightly soluble	Acetone	Insoluble
1N H <sub>2</sub> SO <sub>4</sub>	Insoluble	Chloroform	Insoluble
DMSO	Soluble	Carbon Tetrachloride	Insoluble
THF	Soluble		
Pyridine	Soluble		

Tables VIII and IX show the mass spectral data of the black precipitate, generated by using a direct insertion probe technique. The presence of high molecular weight fragments suggested that the black precipitate contains polymerization products (M.W. of AV = 166). The fact that the mass spectra differ depending on what acid was used to acidify the black precipitate means that the precipitate somehow incorporates some of the acid (96). This is readily apparent from the m/e 48(SO), 64(SO<sub>2</sub>), 80 (SO<sub>3</sub>), and 98 (H<sub>2</sub>SO<sub>4</sub>) signals observed (Table VIII) when H<sub>2</sub>SO<sub>4</sub> was used as the precipitating agent. Also the elemental analyses show the presence of sulfur (when H<sub>2</sub>SO<sub>4</sub> was used) and chlorine (when HCl was used) in the black precipitate.

Phenolic lignin compounds with saturated side-chains in the para-position can undergo oxidative dimerization via C-C coupling (28,30). However, only traces of

C-C coupling products can be detected from the models having alpha-carbonyl or alpha-carbinol groups in the para-position, such as AV (30). The tendency of quinones to undergo condensation reactions in oxygen-alkali is known (39). Very likely, the black precipitate observed here was due to condensation products formed in the solution. A black precipitate was only observed by us in the reactions done at low pH. This probably means condensation products were (1), not formed at the high pH or (2), if formed, degraded to small products at higher pH.

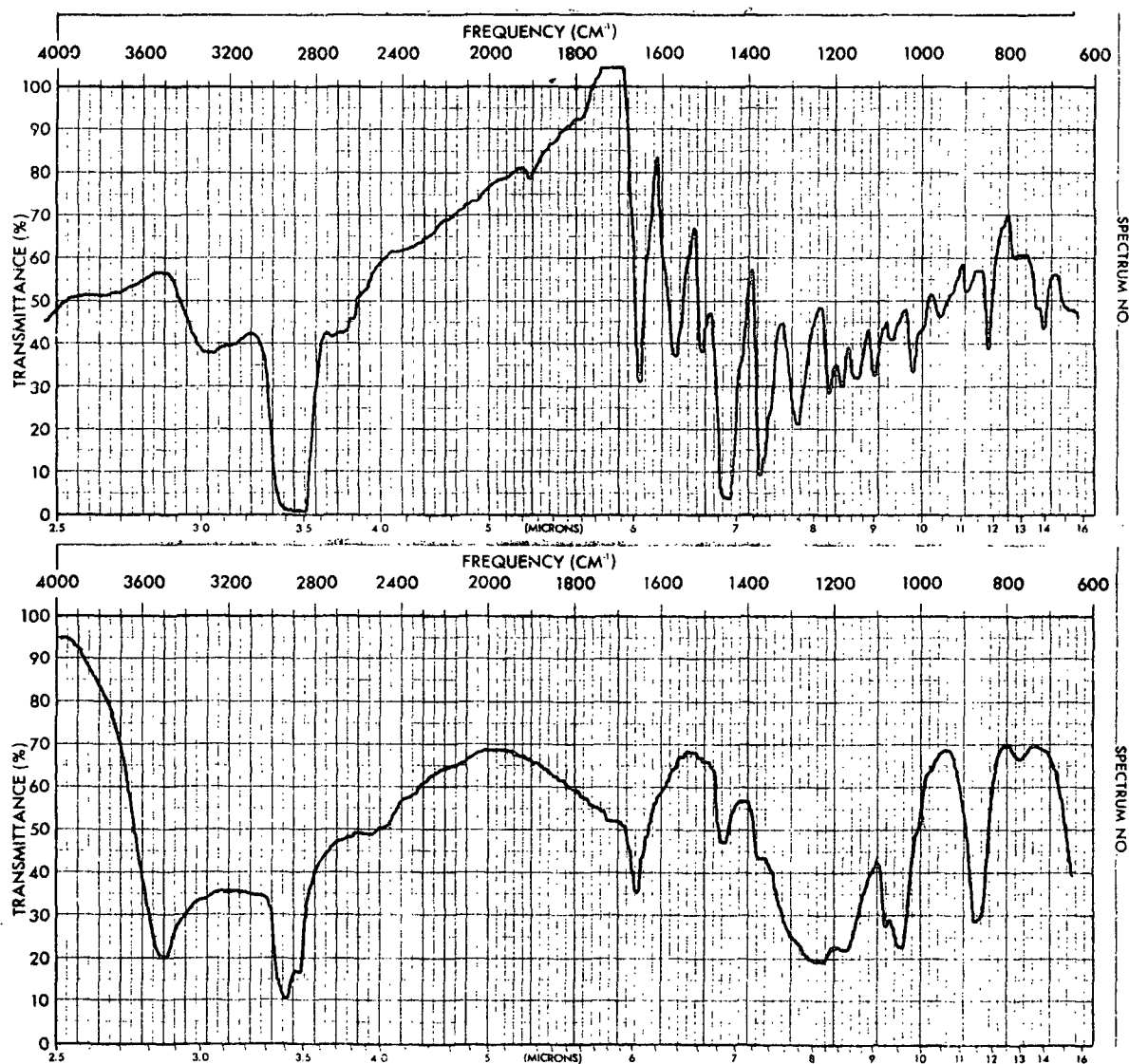


Figure 28. IR spectra of AV (top), and black precipitate (bottom) in mineral oil.

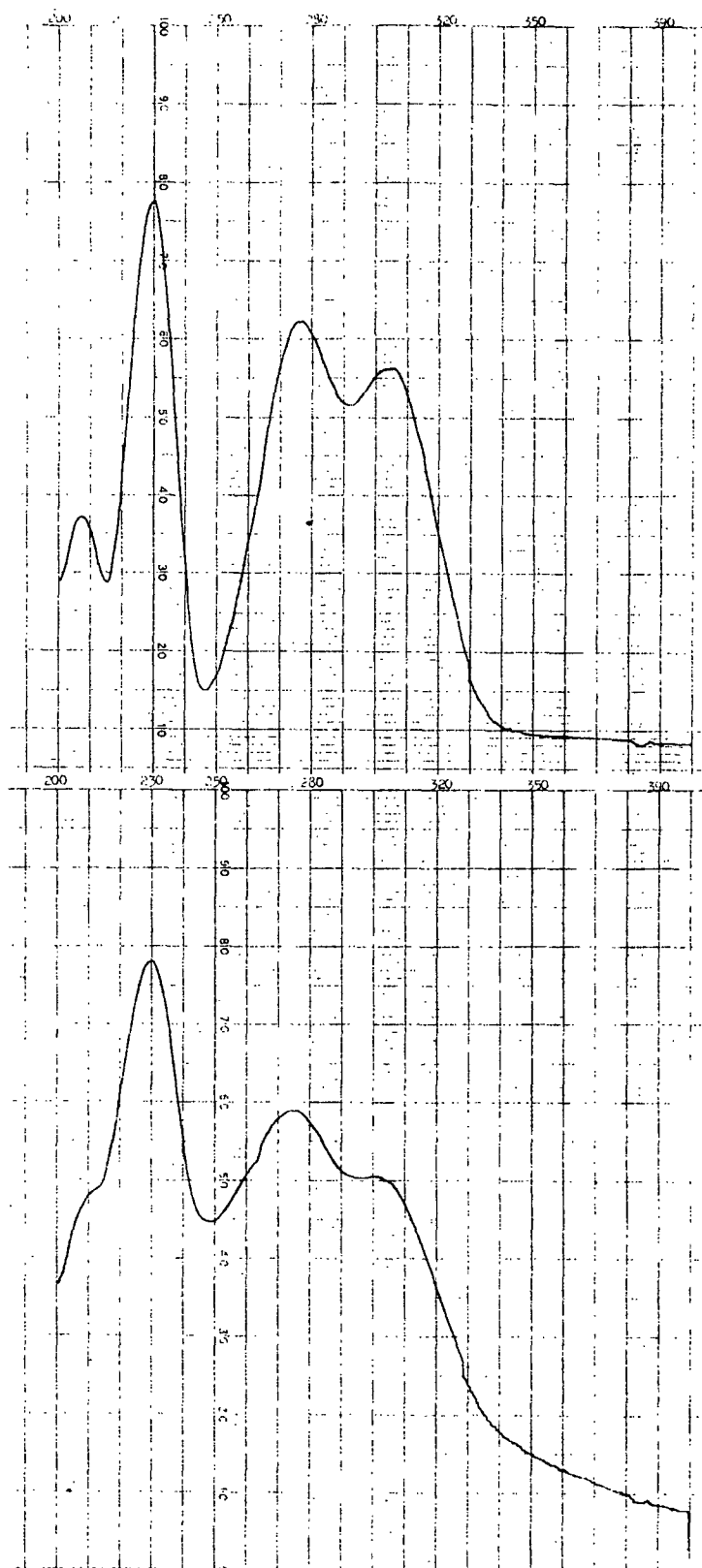


Figure 29. UV spectra of samples prior to (top) and after (bottom) AV-NaHCO<sub>3</sub>-O<sub>2</sub> oxidation reaction.

TABLE VIII  
MASS SPECTRAL DATA FOR BLACK PRECIPITATE<sup>a</sup>

Mass	Abund.	Mass	Abund.	Mass	Abund.	Mass	Abund.
40	2.6	67	2.9	98	51.0	163	3.1
41	8.2	69	3.8	99	6.6	165	3.6
42	3.0	70	1.6	100	5.6		
43	10.9	71	2.9	101	5.5	176	2.2
44	12.2	73	14.6	102	2.7	177	3.1
45	13.8	74	3.8	103	9.6	178	4.0
46	2.7	75	9.6			179	2.2
47	2.1			104	3.3		
		76	4.9	105	2.6	189	7.9
48	64.8	77	4.1	115	3.6	190	4.4
49	2.1	80	100.0	117	1.4	191	35.3
50	5.9	81	74.7			192	7.9
51	4.9	82	9.4	119	4.5	193	6.3
52	1.4	83	7.3	121	1.2	194	1.4
55	6.4	84	1.6	125	1.6	200	2.2
56	2.2	85	2.2	127	1.4	201	1.9
57	5.1	87	3.4	129	1.6		
58	1.4	88	4.8			202	8.5
59	10.3	89	11.8	132	1.9	203	7.4
60	5.7			133	59.5	204	3.3
61	5.2	90	2.5	134	9.8	205	14.9
		91	43.0	135	5.7	206	49.5
62	2.5	92	22.6	136	1.4	207	73.9
63	5.1	93	2.3			208	14.8
64	60.1	95	5.2	147	1.9	209	7.7
65	25.2	96	18.9	149	1.9	210	1.4
66	4.5	97	4.9	151	1.8	213	53.4

<CONT>

Mass	Abund.
214	7.1
215	6.6
249	2.2
251	1.6
265	2.2
267	2.6
281	19.8
282	6.3
283	3.8
287	27.5
288	5.7
289	4.2
355	1.5
361	12.6
362	4.1
363	3.0
435	3.0
436	1.2

>PAUSE

435 \ 74  
361 \ 74  
287 \ 74  
213 \ 74  
207 \ 74  
133 \ 74  
  
98 \ 18  
80 \ 16  
64 \ 16  
48 \ 16

<sup>a</sup>H<sub>2</sub>SO<sub>4</sub> was used to acidify the solution.

TABLE IX  
MASS SPECTRAL DATA FOR BLACK PRECIPITATE<sup>a</sup>

M/Z	Rel. Abund.	M/Z	Rel. Abund.	M/Z	Rel. Abund.	M/Z	Rel. Abund.
39	2.1	88	1.9	133	3.3	181	1.4
41	10.8	89	1.5	134	1.7	182	0.9
42	2.4	91	9.4	135	5.6	183	0.9
43	15.5	92	3.4	136	8.7	185	1.6
44	24.5	93	10.5	137	7.4	189	1.4
45	61.8	94	5.3	138	2.2	190	0.9
50	2.1	95	17.2	139	2.5	191	2.0
51	4.1	96	5.8	140	1.2	192	1.6
52	3.9	97	13.6	141	1.7	193	1.4
53	4.5	98	4.8	142	0.7	194	0.8
54	1.4	99	4.8	143	2.1	195	0.9
55	18.2	100	2.2	144	0.7	196	0.8
56	5.6	101	1.8	145	1.6	197	0.9
57	20.1	102	0.8	147	3.5	199	0.9
58	1.9	103	1.2	148	1.4	201	0.8
59	2.8	104	2.4	149	37.3	203	1.3
60	6.0	105	8.7	150	5.1	204	0.8
61	26.5	106	2.3	151	78.4	205	1.4
62	100.0	107	6.1	152	8.7	206	0.9
63	2.9	108	8.3	153	2.4	207	1.2
64	2.4	109	10.7	154	1.1	208	0.9
65	6.0	110	3.9	155	2.2	209	1.1
66	2.0	111	9.4	156	0.8	210	1.3
67	11.4	112	4.3	157	1.3	217	0.9
68	8.3	113	5.1	159	2.2	218	0.7
69	56.5	114	0.9	160	0.7	219	0.7
70	10.7	115	2.6	161	2.1	221	1.0
71	28.9	116	1.2	162	1.3	222	0.8
72	2.8	117	1.6	163	2.7	223	0.9
73	10.0	118	1.4	164	1.2	228	1.0
74	1.8	119	4.5	165	2.6	231	0.9
75	2.4	120	2.2	166	34.1	236	0.7
76	2.4	121	9.2	167	11.3	239	0.7
77	8.8	122	4.7	168	2.2	243	1.1
78	1.8	123	27.3	169	1.4	251	1.9
79	9.7	124	4.9	170	0.8	256	0.8
80	4.3	125	4.2	171	1.3	259	0.8
81	35.9	126	1.9	173	1.4	279	4.0
82	9.2	127	2.4	175	2.2	280	0.9
83	16.9	128	1.4	176	1.3	341	0.9
84	7.5	129	4.9	177	3.0	354	0.9
85	12.9	130	0.9	178	1.2	446	0.8
86	1.5	131	1.9	179	1.7		
87	2.5	132	1.9	180	1.0		

>PAUSE

<sup>a</sup>HCl was used to acidify the solution.

# MECHANISM

This section proposes a mechanism for the reaction of AV with oxygen in alkaline solutions. It is based on the previously proposed mechanisms of other researchers (28-32,34,36-39,41,43,50,51,72) with similar model compounds and on our results.

The oxidation of phenolic lignins can be represented by the free radical mechanism proposed by Kratzl, et al. (28-30) (Fig. 1). A typical free radical chain reaction includes initiation, propagation, and termination stages (27,51,73,74), as shown in Fig. 30.

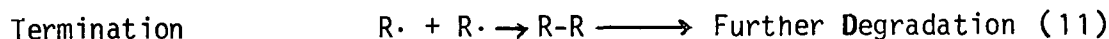
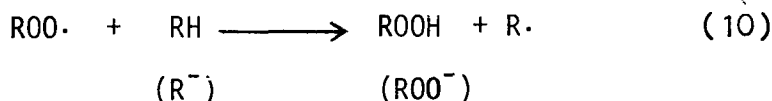
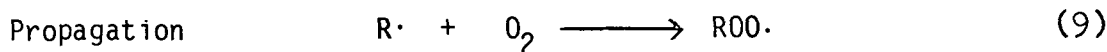
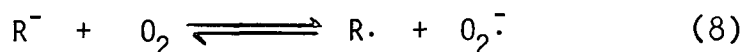
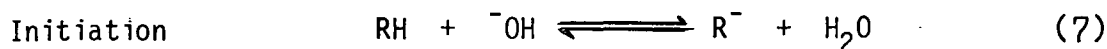


Figure 30. A free radical chain reaction in the oxidation of phenolic compounds (27,51,73,74).

During the initiation stage, (see Fig. 30) the phenolic substrates are first ionized [Eq. (7)], after which oxygen abstracts an electron to form resonance stabilized phenoxy radicals [Eq. (8)]. The existence of phenoxy radicals has been verified by electron spin resonance (ESR) during the oxidation of phenolic lignin compounds in alkaline solutions (28,30,32). It is very likely that the phenoxy radical of AV is also formed in the AV-oxygen-alkali systems. The electron transfer from a phenolate anion (high electron density) to oxygen, forming a phenoxy radical,

is expected to be slow and rate-determining (29,30,37). According to Kratzl, et al., AV has a relatively high critical oxidation potential (COP) value of 430 mV because of the strong deactivating influence of the p-positioned carbonyl group (28-30). The high pKa value of AV is consistent with the rather low reactivity of AV toward oxidation when compared with creosol (COP value = 185 mV) (28).

In the propagation stage, the phenoxy radicals ( $R\cdot$ ) can react with oxygen to form peroxy radicals ( $ROO\cdot$ ) [Eq. (9)]. The peroxy radicals can then further react with AV (RH) or phenolic anions ( $R^-$ ) to form cyclohexadienone hydroperoxides ( $ROOH$ ) and additional phenoxy radicals of AV ( $R\cdot$ ) [Eq. (10)].

Although peroxy radicals and cyclohexadienone hydroperoxides are difficult to isolate because of their instability, they have been recognized as "key intermediates" by most researchers in this area (30,31,34,43,72).

In the termination stage, nonradical species are formed (76). Cross-linking products can be formed via coupling of two phenoxy radicals (28,30,37,39,72) [Eq. (11)]. Degradation products can be formed via side-chain eliminations or demethoxylations (28-30,34,36,39) [Eqs. (12),(13)].

Hydrogen peroxide, which was observed on our AV degradation, could promote ionic destruction of the model compound. Thus, the reaction products could be formed by either radical or ionic pathways.

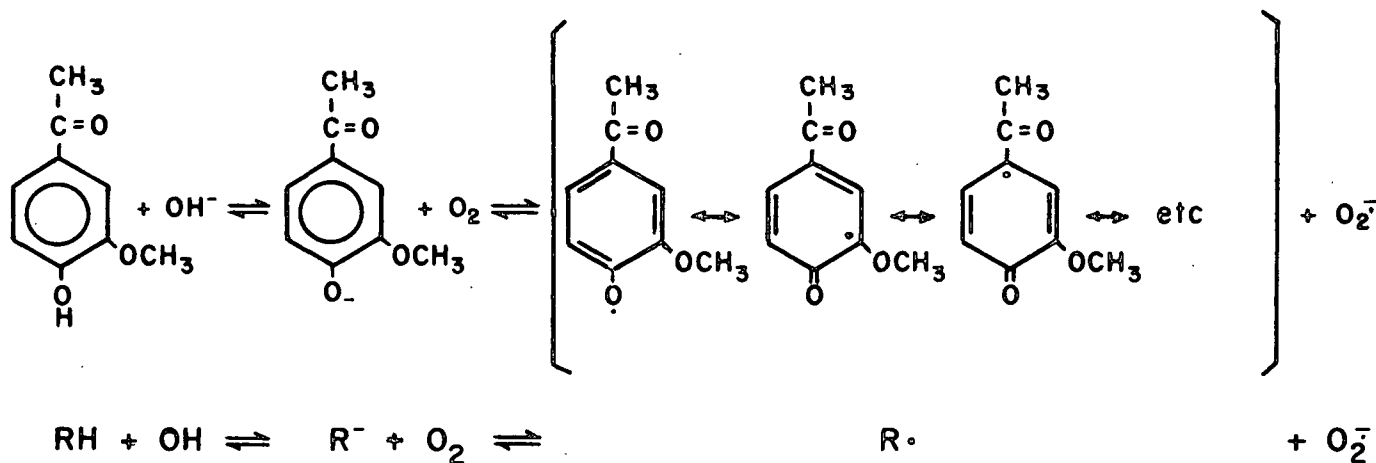
#### EFFECT OF pH

The ionization step will increase the electron density of a phenol and may thereby promote reactions with electron deficient oxidants attacking the molecule at positions of greatest electron density. The importance of the ionization step toward the entire reaction scheme is still not known.



Our results show that AV had the same reaction rate as long as the pH was kept above 7.5 (pKa of AV) during the entire reaction period, regardless of the initial pH of the solutions. Once the pH of the solution dropped below 7.5, the reaction slowed down (Fig. 19). These results imply that the ionization step is a very important stage.

Keeping the pH of the solution above the pKa of AV maintains a high phenolate anion concentration in the solution, and facilitates the electron transfer to the oxidant, which is believed to be the rate-determining step. Although further pH increase did not affect the reaction rate, the pH of the solution still plays an important role in the latter reaction stages by affecting reaction routes and product distributions as shown in the previous Product Formation section.



#### CARBONATE RADICAL ANION

To account for the faster initial rate (Table I) in oxygen-sodium carbonate/bicarbonate systems than in the other oxygen-alkali systems, we hypothesized that carbonate radical anions might be generated and that these aid the electron transfer rate-determining step.

Several species can be involved during the electron transfer rate-determining step, such as hydroperoxyl radical, hydroxyl radical, and carbonate radical anion

(Fig. 31). The hydroperoxyl radical has a pKa value of 4.8 (90) and must exist as a superoxide radical anion ( $O_2^{\cdot-}$ ) in all our reaction systems. Superoxide radical anions are known to react readily ( $k = 1.5 \times 10^7 M^{-1} \text{ sec}^{-1}$ ) in aqueous solution to form hydrogen peroxide (91).

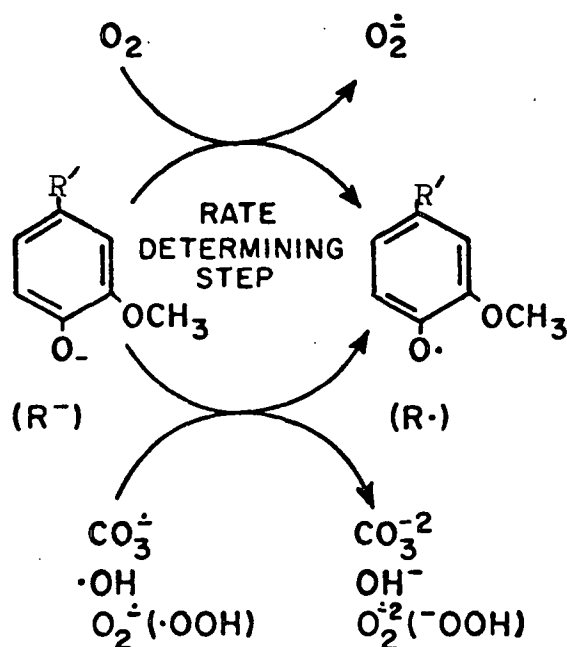
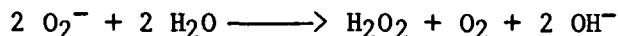
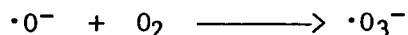


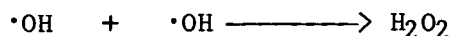
Figure 31. Species involved in the electron transfer rate-determining step during oxygen-alkali oxidation of phenolic compounds.

Hydroxyl radical ( $\cdot OH$ ) is a very strong oxidant (92). The results from AV-NaOH- $O_2$ -DMSO and AV-borax/HCl- $O_2$  (Fig. 21, Table I) indicate that hydroxyl radicals were involved in the electron transfer steps. The pKa of the hydroxyl radical is 11.9 (92). In electron transfer reactions,  $\cdot O^-$  and  $\cdot OH$  may behave differently. However, when DMSO was added to the reactions of AV-NaOH- $O_2$  (initial pH = 12.8) and AV-borax/HCl- $O_2$ , initial pH = 8.9) as a scavenging reagent, we observed that the two reactions had the same magnitude of rate reduction (Fig. 21). This implies that  $\cdot OH$  and  $\cdot O^-$  reacted similarly with phenolate anion over the pH range 8-13.

The addition of the  $\cdot\text{O}^-$  ion radical to oxygen has been studied in some detail (91,93). The rate constant of the reaction is very high ( $2.5 \times 10^9 \text{ M}^{-1} \text{ sec}^{-1}$ ) (93)



and the half-life of the ozonide ion ( $\cdot\text{O}_3^-$ ) in alkaline solutions is only a few milliseconds. There is no evidence that the hydroxyl radical reacts with oxygen (92). However, the reaction of recombination of hydroxyl radicals to give hydrogen peroxide is very common (92).



Hoffman, et al. have studied the reactivity of hydroxyl radical and carbonate radical anion toward phenolic compounds in aqueous solution (94). They reported that the carbonate radical anion exhibits a lower reactivity and a greater degree of selectivity toward phenolic compounds in comparison to the hydroxyl radical (94).

Acetovanillone had a faster reaction rate in the  $\text{NaHCO}_3\text{-O}_2$  than  $\text{Na}_2\text{CO}_3\text{-O}_2$  (Fig. 20). If carbonate radical anions were generated in the oxygen-carbonate/bicarbonate systems,  $\text{HCO}_3^\cdot$  (conjugate acid of carbonate radical anion) would be the dominant species in the bicarbonate solution [(pKa of  $\text{HCO}_3^\cdot = 9.6$  (94,95)]. Because  $\text{HCO}_3^\cdot$  lacks a negative charge, it will be more reactive toward phenolic anion than  $\text{CO}_3^{\cdot-}$  (97).

Why do carbonate radical anion and its conjugate acid seem to play more important roles during the rate-determining electron transfer step than the other species? The probable reasons are that  $\text{HCO}_3^\cdot/\text{CO}_3^{\cdot-}$  are more stable in the aqueous solution (having more resonance structures), more selective toward phenolic anions during the oxygen-alkali reaction, and can be regenerated during the propagation stage (Fig. 32) (85,94,96,97).

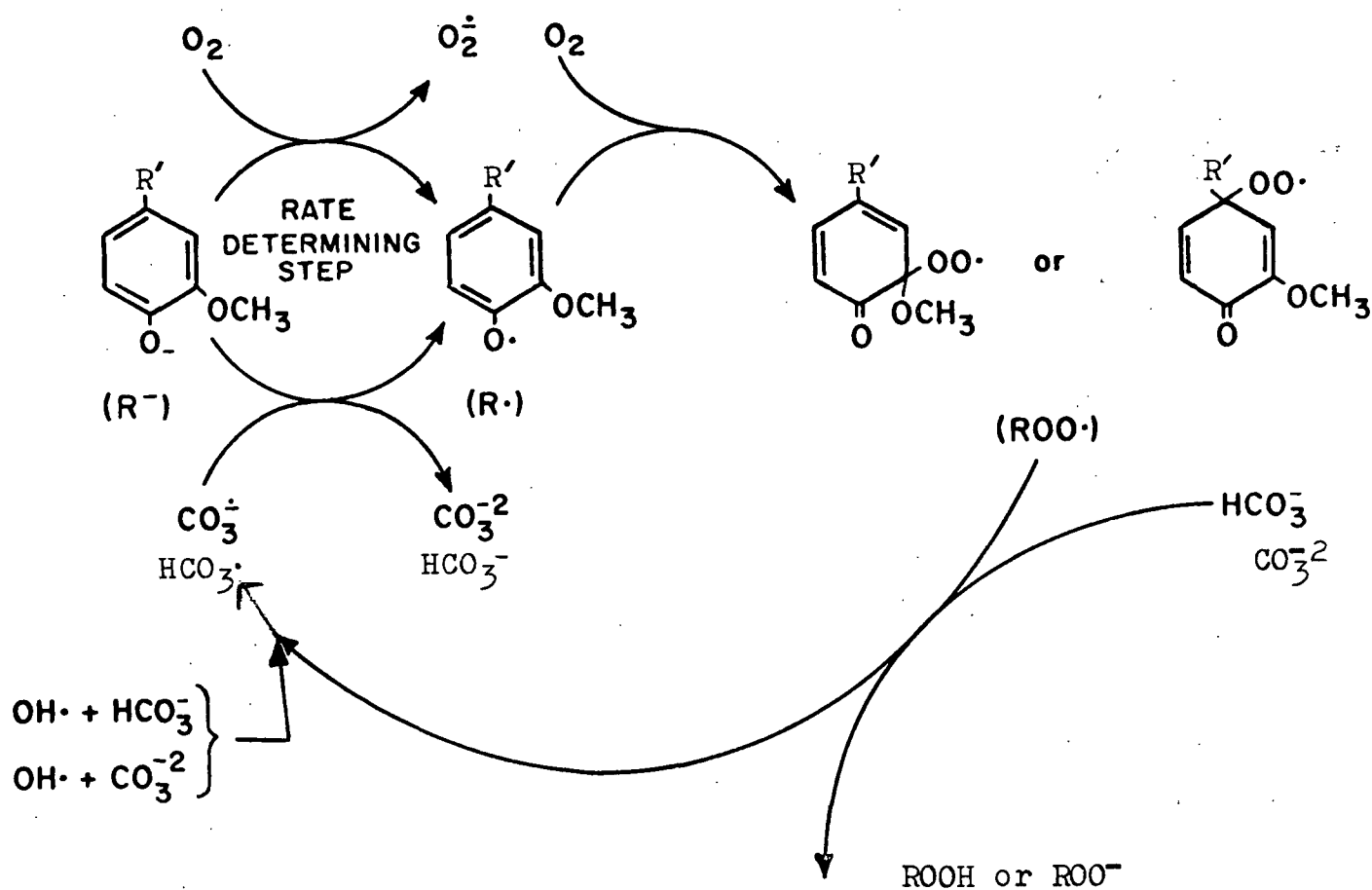


Figure 32. Generation of  $HCO_3^-/CO_3^{\cdot-}$  during the oxygen-alkali oxidation of phenolic compounds.

## CONCLUSIONS

Kinetic analysis of the reaction of AV with oxygen at 80°C in different alkaline media (carbonate, borate, sodium hydroxide) shows a first-order dependence of the rate on AV concentration. The results imply that in the noncarbonate buffered systems, the ionization step is very important. Keeping the pH of the solution above the pKa of AV (7.5) maintains a maximum concentration of phenolate anions in solution, which in turn, facilitates the rate-determining transfer of an electron to oxygen.

The reactions of AV in carbonate/bicarbonate buffers show a faster reaction rate than in oxygen-sodium hydroxide and other oxygen buffer systems (borate, phosphate). This behavior might be attributed to the generation of a carbonate radical anion ( $\text{CO}_3^{\cdot-}$ ) and its conjugate acid ( $\text{HCO}_3^\bullet$ ) in the oxygen-sodium carbonate/bicarbonate systems by the action of hydroxyl radicals. In support of this contention was the observation that the addition of small quantities of DMSO (molar ratio of DMSO to AV was 2) (a known hydroxyl radical quencher) inhibited the degradation of AV in the bicarbonate solution to a greater extent than it did in borax and sodium hydroxide solutions. This is also the first direct indication of the participation of hydroxyl radical in oxygen-alkali reaction systems.

Although further pH increases above the pKa of AV do not affect the reaction rate, the pH of the solution still plays an important role in the products forming stage. Data show that the higher pH favors side-chain elimination and demethoxylation, forming acetic acid and methanol. At the same pH level, decreasing the ionic strength had little effect on acetic acid production but increased methanol production. A condensation product is only observed at lower pH system, which implies that lower pH favors polymerization. Based on the product distributions, the different alkaline solutions do influence the reaction patterns.

## EXPERIMENTAL

### GENERAL ANALYTICAL PROCEDURES

Melting points were determined on a Thomas Hoover capillary melting point apparatus. The melting points were corrected against calibration based upon known compounds.

The quantitative visible spectroscopies and UV analyses were done with a Perkin-Elmer Model 576 ST Spectrophotometer.

The quantitative gas-liquid chromatography (GLC) was done on a Varian Aerograph 1200 gas chromatograph equipped with a hydrogen flame ionization detector. The output was recorded via a Honeywell Electronic 16 recorder equipped with a MOD 227 disc chart integrator and a Perkin-Elmer Sigma 10 Chromatography Data Station. Purified nitrogen (Matheson Gas Products) was used as the carrier gas. The other operating conditions employed for the various analyses are given in Appendix I.

Mass spectral analyses were conducted on a Hewlett-Packard 5985 GC/MS System interfaced with a jet separator to a Hewlett-Packard 5840A gas chromatograph. Helium (prepurified, Matheson Gas Products) was used as the carrier gas. Chromatographic conditions and mass spectrometer control settings are given in Appendix IV. When the direct insertion probe technique was employed (for the black precipitate), the temperature was raised from 40°C to 240°C at 10°/min.

Nuclear magnetic resonance (PMR and  $^{13}\text{C}$ -NMR) spectra were taken with a FX-100 pulse Fourier transform nuclear magnetic resonance spectrometer equipped with a Texas Instruments 980B computer.

The infrared spectroscopy was conducted on a Perkin-Elmer model 700 recording spectrophotometer.

## SOLUTIONS AND REAGENTS

### WATER

Triply-distilled (3-D) water was used in preparing reaction solutions, and in cleaning reactors and labware. This was done in an effort to minimize trace metal ion contamination.

### OXYGEN AND NITROGEN

Oxygen was obtained from Airco, Inc., New York, NY and had a minimum guaranteed purity of 99.5%. Nitrogen was obtained from Matheson Gas Products, Joliet, IL.

### ULTRAPURE CHEMICALS

Ultrapure grade chemicals - sodium hydroxide, sodium carbonate, sodium bicarbonate, sodium tetraborate and potassium dihydrogen phosphate - were purchased from Alfa Division, Ventron Corp., Danvers, MA.

### TITANIUM SULFATE REAGENT (56)

Titanium sulfate (10 g,  $\text{TiSO}_4 \cdot \text{H}_2\text{SO}_4 \cdot 8\text{H}_2\text{O}$ , Fisher Scientific Co.) was dissolved in concentrated sulfuric acid (10 mL) and diluted to 100 mL with 3-D water. After standing for one day, the solution was filtered and stored in a glass bottle.

### SODIUM THIOSULFATE SOLUTION

Sodium thiosulfate solution (0.01N) was prepared by consecutive dilution of a sodium thiosulfate standard solution obtained from Anachemia Chemicals, Ltd., Champlain, NY. The concentration was checked by titration against potassium iodate as a primary standard (80).

MODEL COMPOUND

ACETOVANILLONE (AV)

AV was purchased from Aldrich Chemical Company, Inc. (Milwaukee, Wisconsin). Due to the yellow-brown color of the unpurified material, AV was purified as follows: AV was boiled ca. 5 minutes in ether (20 mL/g). The solution had a yellow color. Decoloring carbon was added and the solution was heated to its boiling point with stirring. The hot solution was filtered by gravity through a fluted filter paper. The filtrate was allowed to stand undisturbed until it had cooled down to room temperature. The flask was then placed in a refrigerator overnight. The crystals were collected by suction filtration and dried in a desiccator for one day. The product had a melting point of 113.5-114.5°C. Literature (81): 115.0°C. Analysis by GLC and NMR showed no detectable impurities.

GAS-LIQUID CHROMATOGRAPHY INTERNAL STANDARDS

ACETOSYRINGONE (AS; 3,5-DIMETHOXY-4-HYDROXYACETOPHENONE)

Purified AS was obtained from the collection of Dr. N. S. Thompson; m.p. 122-123°C [lit. 122-123°C (81)]. The compounds were stored in a desiccator under vacuum.

ETHANOL

Reagent grade ethanol (95%) was used as an internal standard in the methanol analysis.



## BUTYRIC ACID

Butyric acid was purchased from Aldrich Chemical Company, Inc. (Milwaukee, Wisconsin). It showed a single peak when injected into a G. C. Butyric acid was used as an internal standard in the acetic acid analysis.

## REACTION PROCEDURE

### REACTION SYSTEM

The basic reaction system was patterned after a design conceived by McCloskey (58). Details of the reactor construction are illustrated in Fig. 33.

#### Reaction Vessel

The brass container was a one-liter Parr bomb cylinder (236HClO, Parr Instrument Co., Moline, Illinois). The insert was a completely Teflon-lined container which minimized the possibility of surface catalysis. The brass cover, bolted to the pot by means of flange fittings, was lined with Teflon underneath. The contact between the Teflon cover lining and the insert provided an effective seal.

The reactor cover contained three ports. The port leading to the sample line, oxygen tank, and the thermocouple connected through the reactor lid were the same as those described by Millard (82).

#### Magnetic Stirrer

An air-driven turbine Mag-Jet (Matheson Scientific, Inc., Elk Grove Village, Illinois) was clamped to the bottom of the reactor. A 1.5 inch cylinder magnet was used to drive the stirring bar effectively inside the reactor.

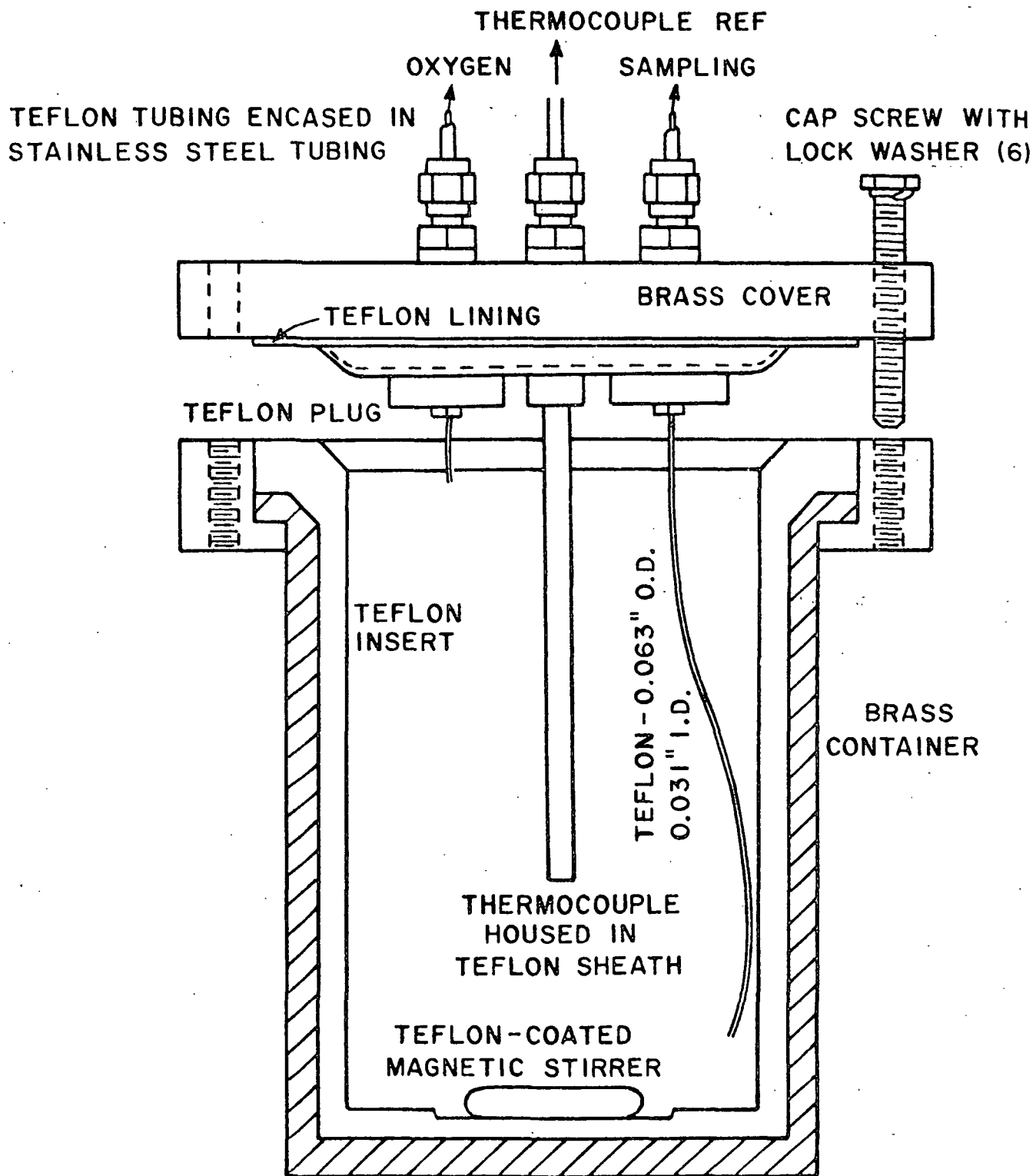


Figure 33. Reactor and cover.

### Oil Bath and Temperature Apparatus

The reactor-stirrer assembly was raised and lowered into an insulated oil bath manually. The bath was heated by a Chromalox I 1000-watt immersion heater equipped with a preset thermostat (80°C) to insure temperature reproducibility. As a safety precaution, the heater was plugged into an Oven-Temp Guard (Instruments for Research and Industry, Cheltenham, Pennsylvania) set at 125°C.

Reaction solution temperature was monitored by a thermocouple (Omega Engineering Inc., Stamford, Connecticut). The output was recorded on a Cole-Parmer Model 261 recorder. As sensed by the thermocouple, the reactor temperature was controlled to  $\pm 0.5^{\circ}\text{C}$ .

### Sampling System

The reaction solution was sampled under the internal oxygen pressure to force the liquid sample out through Teflon lines (0.063-inch OD x 0.031-inch ID. Chromatronix, Inc.) and a pressure tight inert valve (Chromatronix, Inc.) at various reaction times. Roughly 25 mL was collected at each sampling time.

### CONDITIONING OF REACTOR AND LABWARE

The reaction vessel and all glassware associated with preparation of reaction solutions and peroxide studies were washed using the procedure described as follows (59):

1. Alconox soak overnight
2. Acetone rinse, distilled water rinse
3. 35% nitric acid (v/v) soak
4. Distilled water rinse
5. 3-D water rinse

The reactor and glassware were then allowed to air dry before use.

## PREPARATION OF REACTION SOLUTIONS AND LOADING THE REACTOR

Triply distilled water (ca. 500 mL) was boiled for 10 minutes and allowed to cool in a nitrogen atmosphere inside a glove bag. Also placed in the glove bag were the Teflon-lined reactor, preweighed or premeasured ultrapure chemicals, and the preweighed model compound AV. After cooling, the alkaline solution was prepared, then transferred to the reactor, and the model compound was added to the reactor. The reactor was removed from the nitrogen atmosphere and the cover was immediately bolted into place. The solution was back-flushed through the sample line with nitrogen (3 min). The sample and oxygen lines were then connected (with valves closed), the reactor was lowered into the oil bath, the air-driven magnetic stirrer was started, and the bath turned on.

## REACTION SAMPLING

After the thermocouple output indicated that the reactor and its contents had reached the desired temperature (80°C), the reactor was pressurized with oxygen (150 psig). Immediately after that, the sample line was purged with reaction solution, and a time zero sample was taken. The sample (ca. 25 mL) was collected in a bottle and sealed with Parafilm. From this volume, 10 mL was taken for peroxide analysis, and 4-8 mL for starting material, methanol, acetic acid, and acidic products analyses. Prior to each sampling, the sample line was purged twice due to the dead volume between the reactor and the sample valve.

## ANALYSIS OF REACTION SOLUTION

### Starting Material Analysis

The reaction solution (ca. 1.0 mL) was transferred into a tared 4-mL vial and weighed. Internal standard solution (AS in dilute alkaline solution, ca. 1.0 mL) was added and weighed again. The solution was then poured into a test tube (25 x

150 mm) which contained 15 mL saturated sodium chloride aqueous solution, and neutralized by purging with gaseous carbon dioxide via a gas dispersion tube (ca. 3 min). The dual-tint pH paper was used to insure the pH of the solution was below 7 after the neutralization. The neutralized sample was then transferred to a 60 mL separatory funnel and extracted with carbon tetrachloride (2 x 5 mL). The carbon tetrachloride layer was dried over anhydrous sodium sulfate, decanted, concentrated in vacuo to a volume of 2 mL in a pear-shaped flask, then transferred via a disposable pipette to a threaded 3.5 mL vial, and evaporated to dryness. Traces of residual water were removed by vacuum evaporation with 1,2-dichloroethane (2 x). The sample was dissolved in anhydrous ether (0.4 mL). N,O-bis-(trimethylsilyl)-trifluoroacetamide (BSTFA, 0.2 mL; Pierce Chemical Co.) was then added to this solution, shaken vigorously by hand for 30 seconds, and shaken mechanically for at least another 3 hours. Each sample was analyzed in triplicate by GLC (Appendix I, Condition A).

#### Methanol Analysis

Each sample mass was determined gravimetrically and ethanol internal standard was added volumetrically (ca. 1 mL). The samples were then analyzed directly by GLC in triplicate (Appendix I, Condition B). The method of analysis was based on the technique reported by Sims (83).

#### Acetic Acid Analysis

Internal standard solution (butyric acid) was added gravimetrically to an accurately weighed sample of reaction solution (ca. 1.0 g). The mixture was analyzed directly, in triplicate, by GLC (Appendix I, Condition C).

#### Acidic Products Analysis

The final reaction sample (24-hour reaction time; ca. 5 mL) was deionized through an Amberlite IR-120 ( $H^+$ ) column (5 mL) and eluted with distilled water (3 x

5 mL). The pH of the deionized sample was determined to be ca. 2-3 by dual-tint pH paper, and was immediately made alkaline by addition of  $\text{NH}_4\text{OH}$ . The sample was then concentrated in vacuo ( $< 40^\circ\text{C}$ ) to ca. 1 mL in a pear-shaped flask and transferred to a threaded vial (3.5 mL). The sample was evaporated in vacuo to dryness and vacuum evaporated (2 x) with 1,2-dichloroethane to remove the last traces of water.

Each sample vial was fitted with a septum. Chloroform (0.4 mL) was added to the vial. The mixture was then derivatized with BSTFA + 1% TMCS (0.4 mL, Pierce Chemical Co.) and mechanically shaken for 12 hours. The silylated samples were analyzed by GLC (Appendix I, Condition D), or GLC-MS (Appendix IV).

#### Hydrogen Peroxide Analysis

The hydrogen peroxide analysis was conducted using a colorimetric method involving a yellow complex between hydrogen peroxide and titanium (IV) (52,53,56). The initial absorbance of each sample was taken as a measure of hydrogen peroxide. A straight line calibration curve was constructed by analyzing dilute hydrogen peroxide solutions by both the titanium sulfate method and a standard iodide-thiosulfate titration (Fig. 34) (85). The regression line for  $\text{H}_2\text{O}_2$  concentration less than  $10^{-3}\text{M}$  was

$$\text{H}_2\text{O}_2, \text{ mM} = 2.87 \times \text{absorbance}$$

After the peroxide sample was taken from the reactor, it was immediately analyzed. Colorimetric peroxide analyses were carried out by the following procedure: (1), the peroxide samples were prepared by adding reaction sample (5 mL) to two volumetric flasks (10 mL) each containing 2.0 mL of 10.5N  $\text{H}_2\text{SO}_4$ , (2), to one of the flasks was added titanium sulfate solution (8 drops) while the other served as a blank, (3), the two flasks were filled to mark with 3-D water, (4), the absorbance measurements were made on a spectrophotometer which had been set at 408.0 nm. The reference for the absorbance readings was distilled water. The difference between

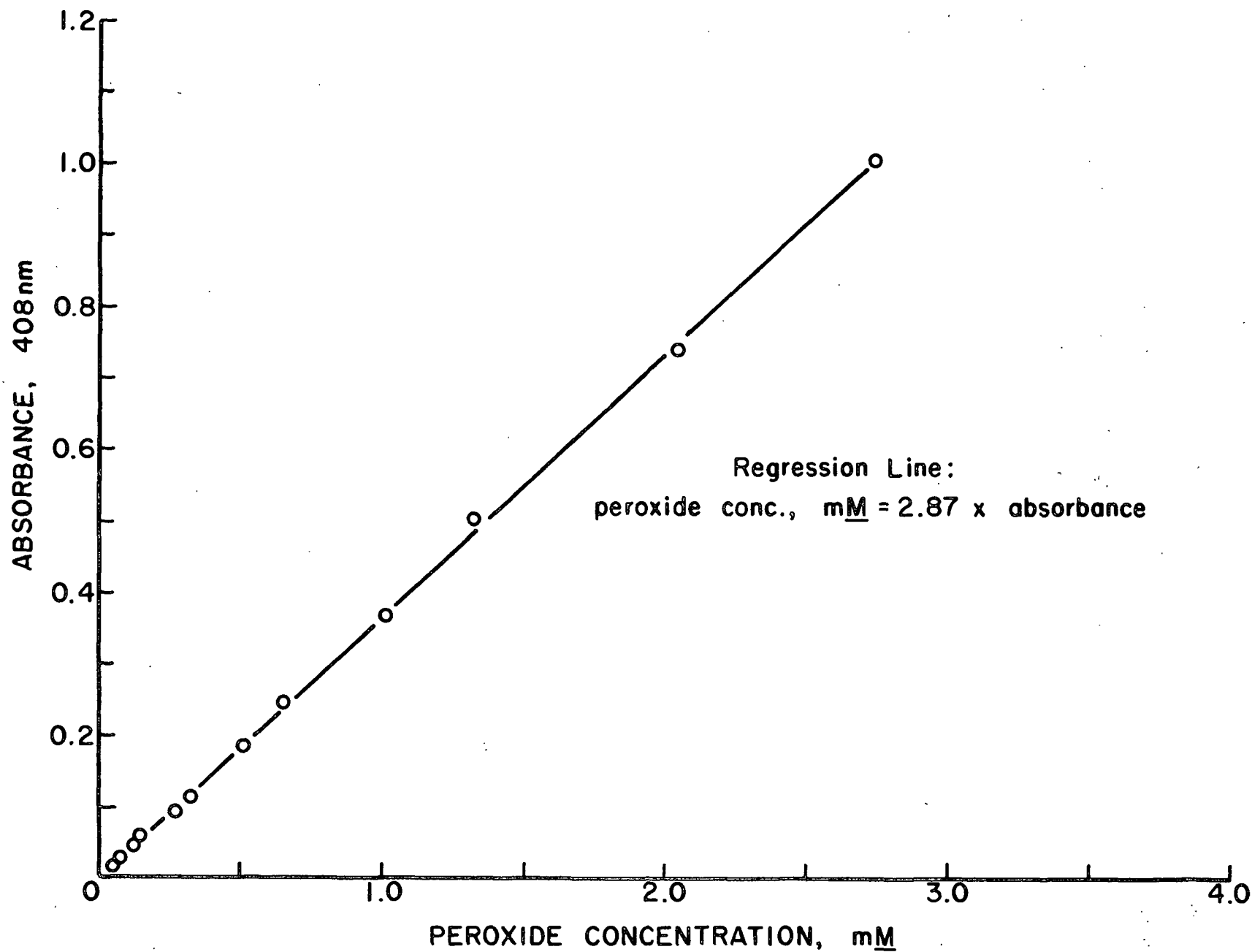


Figure 34. Absorbance at 408 nm vs. peroxide concentration as determined by the standard iodometric titration technique.

the readings of the samples with and without titanium sulfate was taken as the immediate absorbance. This procedure was designed to account for any absorbance in the blank sample due to the presence of chromophoric products of AV.

#### Black Precipitate

Reaction solutions (5 mL) from certain runs were acidified with concentrated mineral acid in a test tube. The solution became turbid and black precipitate settled down gradually. After centrifuging, the top clear solution was decanted and the bottom layer was transferred to a 4-mL vial. Freeze-dried overnight, the black precipitate had a tarry appearance.

#### UV Sample Preparation (84)

The samples used to provide the data illustrated in Fig. 29 were prepared as follows: the same volume (ca. 30 mL) of AV and reaction solution (ca. 50% AV reacted) were placed in 100-mL pear-shaped flasks. The samples were concentrated in vacuo to remove water, then dissolved in absolute ethanol. Aliquots of the resultant solutions were diluted with absolute ethanol to yield samples with a concentration of ca. 0.1 mg of AV monomer per millimeter of solution. UV spectra of the resultant samples were then obtained by scanning from 200 to 390 nm.



#### ACKNOWLEDGMENTS

The author gratefully acknowledges the assistance, guidance, and support provided by the members of his thesis advisory committee: Drs. D. R. Dimmel, T. J. McDonough, and N. S. Thompson, chairman.

The author would also like to thank other faculty and staff members for their contributions to this thesis research; especially Dr. W. F. W. Lonsky; and Messrs. H. M. Corbett, L. G. Borchardt, J. P. Rademacher, and J. C. Teed.

Financial support from the member companies of The Institute of Paper Chemistry is gratefully acknowledged.

The author wishes to thank faculty, staff, fellow students, recent alumni, and their families for their friendship, especially Bill Platt and Kim Melius.

I also wish to thank my father for his support, my wife, Chin-I, for her understanding and encouragement, and to our son, Frederick, who is a welcomed distraction.

LITERATURE CITED

1. Kleinert, T. N., Tappi 59(9):122(1976).
2. Harris, G. C., U.S. pat. 2,673,148(1954).
3. Noreus, S. E. O. and Samuelson, O., U.S. pat. 3,769,152(1970).
4. Samuelson, O. and Sjoberg, L-A., Svensk Papperstid. 75:583(1972).
5. Abrahamsson, K. and Samuelson, O., Svensk Papperstid. 75:869(1972).
6. Minor, J. L. and Sanyer, N., Tappi 57(5):123(1974).
7. Landucci, L. L. and Sanyer, N., Tappi 57(10):97(1974).
8. Minor, J. L. and Sanyer, N., Tappi 58(3):116(1975).
9. Sarkanen, K. V. and Johanson, L. N. Use of oxygen in pulping. Paper presented at the 1975 AIChE Conference, Boston, Mass. Sept. 1975.
10. Markham, L. D. Transactions of the technical section of CPPA, 4(4):TR110(1978).
11. Fujii, J. S. and Hannah, M. A., Tappi 61(8):37(1978).
12. Chang, H-m. and Kleppe, P. J., Tappi 56(1):97(1973).
13. Chang, H-m., Gratzl, J. S., McKean, W. T., Reeves, R. H., and Stockmann, V. E., Tappi 59(8):72(1976).
14. Pulp Paper Intern. 15(9):58(1973).
15. Broden, A. and Samuelson, O. Paperi Puu 55(9):607(1975).
16. Jamieson, A. G., Samuelson, O., and Smedman, L. A., Tappi 58(2):68(1975).
17. Cox, L. A. and Worster, H. E., Tappi 54(11):1890(1971).
18. Nikitin, V. M. and Akim, G. L., Trudy LTA 75:144(1956).
19. Nikitin, V. M. and Akim, G. L., Bumazh. Prom. 35:5(1960).
20. Robert, A., Rerolle, P., Viallet, A., and Martin-Borret, C., ATIP Bull. 18(4):151(1964).
21. Robert, A., Rerolle, P., Viallet, A., and Martin-Borret, C., ATIP Bull. 18(4):166(1964).
22. Chang, H-m., Pulp Paper 63(3):87(1980).
23. Rapson, H. W., Tappi 62(6):14(1979).
24. Manouchehri, M. and Samuelson, O., Svensk Papperstid. 78:211(1975).

25. Akim, G. L., Paperi Puu 55:389(1973).
26. Manouchehri, M. and Samuelson, O., Norsk Skogind. 33:219(1979).
27. Norin, T., Svensk Papperstid. 74:767(1971).
28. Kratzl, K., Gratzl, J. S., and Claus, P., Adv. in Chem. Series 59:157(1966).
29. Kratzl, K., Schafer, W., Claus, P., Gratzl, J. S., and Schilling, P., Monatsh. Chem. 98:891(1967).
30. Kratzl, K., Claus, P., Lonsky, W., and Gratzl, J. S., Wood Sci. and Tech. 8:35(1974).
31. Fricko, P., Martin, H-E., and Kratzl, K., Monatsh. Chem. 111:1025(1980).
32. Eckert, R. C., Chang, H-m., and Tucker, W. P., Tappi 56(6):134(1973).
33. Aoyagi, T., Hosaya, S., and Nakano, J., J. Japan Wood Res. Soc. 25:783(1979).
34. Gierer, J. and Imsgard, F., Svensk Papperstid. 80:510(1977)
35. Young, R. and Giere, J., J. Appl. Polymer Symp. 28:1213(1976).
36. Renard, J. J., Mackie, D. M. and Bolker, H. I., Paperi Puu 57:786(1975).
37. Landucci, L. L., Transactions of the technical section of CPPA 4(1):25(1978).
38. Fieser, L. F., J. Am. Chem. Soc. 52:5204(1930).
39. Martin, H-E., Fricko, P., and Kratzl, K. Oxygen oxidation of lignins, paper presented at EKMAN Days of Conference, Stockholm, Sweden, June 1981.
40. Dakin, H. D., Am. Chem. J. 42:477(1909).
41. Bailery, C. W. and Dence, C. W., Tappi 52:491(1969).
42. Aoyagi, T., Hosaya, S., and Nakano, J., J. Japan Wood Res. Soc. 26:27(1980).
43. Gratzl, J. S., Chang, H-m., and McKean, W. T. The degradation of lignin and carbohydrates in oxygen-alkali delignification processes, paper presented at the 4th Canadian Wood Chem. Symposium, Chateau Frontenac, Quebec, July 1973.
44. Sarkanen, K. V. and Schuerch, C., Anal. Chem. 27:1245(1955).
45. Aoyagi, T., Hosaya, S., and Nakano, J., J. Japan Wood Res. Soc. 23(3):156(1977).
46. Kratzl, K., Claus, P. K., Hruschka, A., and Vierhapper, F. W., Cellulose Chem. Technol. 12:445(1978).
47. Thompson, N. S., Crozier, T. E., and Johnson, D. C., Tappi 62(9):107(1979).

48. Sogo, M. and Hata, K., Japan Tappi 27:171(1973).
49. Karan, J. The oxidation of lignin by gaseous oxygen in aqueous media. Doctor's Dissertation. Seattle, Wash., University of Washington, 1976.
50. Renard, J. J., Mackie, D. M., Jones, H. G., Bolker, H. I., and Clayton D. W., Transactions of the technical section of CPPA 1(1):1(1975).
51. Freiberg, J. D. The interaction between acetovanillone and methyl- $\alpha$ -D-glucopyranoside in an oxygen-alkali system. Doctor's Dissertation. Appleton, Wisconsin, The Institute of Paper Chemistry, 1980.
52. Pobiner, H., Anal. Chem. 33:1423(1961).
53. Weaver, J. W., Schroeder, L. R., and Thompson, N. S., Carbohyd. Res. 48:C5(1976).
54. Volk, B. Applied statistics for engineers, 2nd ed. New York, McGraw-Hill Book Co. 1969.
55. Frost, A. A. and Pearson, R. G. Kinetics and Mechanism, 2nd ed. New York, John Wiley & Sons, 1961.
56. Sinkey, J. D. The function of magnesium compounds in an oxygen-alkali-carbohydrate system. Doctor's Dissertation. Appleton, Wisconsin, The Institute of Paper Chemistry, 1973.
57. Sims, E. W., J. Chromat. Sci. 14:65(1976).
58. McCloskey, J. T. The degradation of methyl- $\alpha$ -D-glucopyranoside by oxygen in alkaline solution. Doctor's Dissertation. Appleton, Wisconsin, The Institute of Paper Chemistry, 1971.
59. Hearne, D. O. The effect of the aglycon and hydroxyl orientation on alkali-oxygen degradation of methyl glycosides. Doctor's Dissertation. Appleton, Wisconsin, The Institute of Paper Chemistry, 1979.
60. Pew, J. C., J. Org. Chem. 28:1048(1963).
61. Lai, Y. Z. and Sarkanen, K. V., in "Lignin" (Sarkanen, K. V. and Ludwig, C. H., eds.), New York, Wiley-Interscience, 1971, p. 228.
62. Borrow, G., General Chemistry, Belmont, CA, Wadsworth Publishing Co. 1972.
63. Weeks, J. L. and Rabini, J., J. Phys. Chem. 70(7):2100(1966).
64. Hayon, E. and McGrarvey, J. J., J. Phys. Chem. 71(5):1492(1967).
65. Behar, D., Czapsk, G., and Duchovny, I., J. Phys. Chem. 74(10):2208(1970).
66. Adams, G. E., Boag, J. W., and Michael, B. D., Trans. Faraday Soc. 61:492(1965).

67. Adams, G. E., Boag, J. W., and Michael, B. D., Trans. Faraday Soc. 61:1417(1965).
68. Adams, G. E., Boag, J. W., and Michael, B. D., Trans. Faraday Soc. 61:1674(1965).
69. Veltwisch, D., Janata, E., and Asmus, K.-D., J.C.S. Perkin II: 146(1980).
70. Dixon, W. T., Norman, R. O. C., and Buley, A. J., J. Chem. Soc. 3625(1964).
71. Norman, R. O. C. and Gilbert, B. C., Adv. Phys. Org. Chem. (5):53(1967).
72. San Clemente, M. R., Sarkanen, K. V., and Sundin, S. E., Svensk Papperstid. 84:R1(1981).
73. Frank, C. E., Chem. Rev. 46:155(1950).
74. Ericsson, B., Lindgren, B. O., and Theander, O., Svensk Papperstid. 74:757(1971).
75. Fisher, J. H., Hawkins, W. L., and Hibbert, H., J. Am. Chem. Soc. 63:3031(1941).
76. Hawkins, E. G. E., Organic Peroxides. Princeton, New Jersey, D. Van Nostrand Co. Inc., 1961.
77. Kempf, A. W. and Dence, C. W., Tappi 58(6):104(1975).
78. Corbett, J. F. and Fooks, A. G., J. Chem. Soc. C:1909(1967).
79. Gellerstedt, G., Hardell, H.-L., and Lindfors, E.-L., Acta Chem. Scand. B34:669(1980).
80. Skoog, D. A. and West, D. M. Fundamentals of analytical chemistry. 2nd ed., New York, Holt, Rinehart, and Winston, 1969.
81. Handbook of Chemistry and Physics, 60th ed., R. C. Weast, Ed. in chief, Boca Raton, Florida, CRC Press, Inc., 1980: C-100,101.
82. Millard, E. C. The degradation of selected 1,5-anhydroalditols by molecular oxygen in alkaline media. Doctor's Dissertation. Appleton, Wisconsin, The Institute of Paper Chemistry, 1976.
83. Sims, E. W., J. Chromat. Sci. 14:65(1976).
84. Balousek, P. J. The effects of ozone upon a lignin-related model compound containing a beta-aryl ether linkage. Doctor's Dissertation. Appleton, Wisconsin, The Institute of Paper Chemistry, 1979.
85. Thompson, N. S., personal communication.
86. Singh, A., Photochem. and Photobiology 28:429(1978).

87. Barb, W. G., Baxendale, J. H., George, P., and Hargrave, K. R., Trans. Faraday Soc. 47:462(1951).
88. Stanff, J., Sander, U., and Jaeschke, W. Chemiluminescence and Bioluminescence. New York, Plenum Press, 1973: 131-141.
89. Brooks, R. D. and Thompson, N. S., Tappi 49(8):362(1966).
90. Rabani, J. and Nielsen, S. O., J. Phys. Chem. 73:3736(1969).
91. Czapski, G. and Dorfman, L. M., J. Phys. Chem. 68:1169(1964).
92. Draganic, I. G. and Draganic, Z. D. The radiation chemistry of water. New York, Academic Press, 1971.
93. Adams, G. E., Boag, J. W., and Michael, B. D., Nature 205:898(1965).
94. Chen, S-N., Hoffman, M. Z., and Parsons, G. H., J. Phys. Chem. 79:1911(1975).
95. Chen, S-N., Cope, V. W., and Hoffman, M. Z., J. Phys. Chem. 77:1111(1973).
96. Dimmel, D. R., personnel communication.
97. McDonough, T. J., personal communication.

# APPENDIX I

## GAS-LIQUID CHROMATOGRAPHY

Quantitative and semiquantitative GLC was accomplished through the use of an appropriate internal standard. Molar response factors were calculated according to Eq. (16).

$$F_X = (A_X/A_I)(M_I/M_X) = (A_r)(M_I/M_X) \quad (16)$$

where  $F_X$  = response factor for compound X relative to the internal standard

$A_X$  = the GC peak area of compound X

$A_I$  = the GC peak area of internal standard

$M_I$  = the mole of internal standard

$M_X$  = the mole of compound X

Response factors were determined experimentally by preparing a series of solution with varied molar ratios and subjecting the solutions to the appropriate workup procedure (Experimental section). Each solution was analyzed by GLC in triplicate, and response factors were calculated as an average of the values obtained. Semi-quantitative GLC analysis involved either calculation of response factors from a single solution containing the compounds of interest, or estimation of response factors on a molecular weight basis.

Table X lists the various GLC conditions used in this work and Table XI gives retention times and response factors of compounds associated with work.

The concentration of a compound X in the reaction samples was calculated through the use of Eq. (17).

$$X = (A_r)(IS)(D) 10^3/(W)(F_X) \quad (17)$$

where X = concentration of compound X, moles/liter

IS = mole of internal standard, moles

D = density of reaction mixture, g/mL

W = weight of sample, g

TABLE X

GAS-LIQUID CHROMATOGRAPHIC CONDITIONS

Conditions	A	B	C	D
Instrument	Varian 1200	Varian 1200	Varian 1200	HP 5840A
Column type	OV-17 <sup>a</sup>	Carbowax 20M <sup>b</sup>	AT-1000 <sup>c</sup>	OV-17 <sup>d</sup>
Derivative	Trimethyl-silylated	Underivatized	Underivatized	Trimethyl-silylated
Column temp., °C	150 —> 210 @4°/min	70	150	60 —> 235 @5°/min
Inject temp., °C	250	150	200	275
Detector Temp., °C	250	265	200	275
Carrier gas	N <sub>2</sub>	N <sub>2</sub>	N <sub>2</sub>	He
Carrier gas flow rate, mL/min	40	35	25	30

<sup>a</sup>Stainless steel column (5 ft x 0.125 inch) packed with 5% OV-17 on 80/90 mesh Anakrom ABS.

<sup>b</sup>Stainless steel column (4 ft x 0.125 inch) rigged for off-column injection and packed with 5% Carbowax 20M on 80/100 mesh Chromosorb 101.

<sup>c</sup>Stainless steel column (6 ft x 0.125 inch) rigged for off-column injection and packed with 10% AT-1000 on 80/100 mesh Chromosorb W-AW.

<sup>d</sup>Glass column (6 ft x 0.250 inch) rigged for off-column injection and packed with 3% OV-17 on 80/100 mesh Gas Chrom Q.



TABLE XI  
RETENTION TIMES ( $T_r$ ) AND RESPONSE FACTORS ( $F_x$ )

Conditions	Compound	Tr, min	$F_x$
A	Acetovanillone	7.1	$0.99 \pm 0.015^a$
	Acetosyringone	11.1	1.00 <sup>a</sup>
B	Methanol	2.3	$0.71 \pm 0.01^b$
	Ethanol	5.4	1.00 <sup>b</sup>
C	Acetic acid	3.7	$0.41 \pm 0.04^c$
	Butyric acid	7.6	1.00 <sup>c</sup>
D	2-Hydroxyisobutyric acid	4.1	0.9 <sup>e</sup>
	Lactic acid	4.8	0.8 <sup>e</sup>
	Glycolic acid	5.5	0.44 <sup>d</sup>
	Oxalic acid	8.1	0.54 <sup>d</sup>
	Malonic acid	9.4	0.68 <sup>d</sup>
	Succinic acid	12.0	0.74 <sup>d</sup>
	Maleic acid	12.4	0.76 <sup>d</sup>
	Hydroxymalonic acid	14.1	1.06 <sup>e</sup>
	Malic acid	15.8	0.80 <sup>d</sup>
	Acetovanillone	21.6	1.00

<sup>a</sup>Calculated relative to acetosyringone at the specified conditions.

<sup>b</sup>Calculated relative to ethanol at the specified conditions.

<sup>c</sup>Calculated relative to butyric acid at the specified conditions.

<sup>d</sup>Calculated from a single sample relative to acetovanillone.

<sup>e</sup>Estimated response factor on a molecular weight basis relative to acetovanillone.

APPENDIX II

EXPERIMENTAL DATA<sup>a</sup>

TABLE XII

REACTION OF ACETOVANILLONE (AV) IN 1.25N NaOH at 80°C AND 150 psig O<sub>2</sub>

Time, hours	AV x 10 <sup>3</sup> M	Time, hours	AV x 10 <sup>3</sup> M
AV-NaOH-O <sub>2</sub> -2		AV-NaOH-O <sub>2</sub> -3	
0.0	33.2	0.0	33.9
0.05	33.4	0.08	33.2
0.2	33.1	0.25	33.4
0.5	33.2	0.5	33.6
1.0	33.4	1.0	33.2
2.5	32.1	2.0	32.8
5.5	31.2	4.0	32.2
10.5	29.2	9.0	29.8
18.5	24.8	18.5	25.1
24.0	23.5	25.0	23.8
AV-NaOH-O <sub>2</sub> -4		AV-NaOH-O <sub>2</sub> -5	
0.0	11.2	0.0	100.2
0.08	11.2	0.08	101.3
0.3	11.15	0.3	100.1
0.83	11.1	0.8	98.8
1.5	11.0	1.5	98.0
3.0	10.7	3.0	93.8
6.0	10.15	6.0	88.0
10.0	9.6	10.0	83.5
18.5	8.4	18.5	72.0
24.0	7.4	24.0	62.5
AV-NaOH-O <sub>2</sub> -6(DMSO)			
0.0	33.7		
0.08	33.1		
4.0	32.6		
8.5	30.5		
20.0	26.2		
24.0	24.8		

<sup>a</sup>The designation of any one reaction is intended as a reference to the original data appearing in IPC Lab Notebook 3389.

APPENDIX II (Continued)

TABLE XIII

REACTION OF ACETOVANILLONE (AV) IN  $\text{Na}_2\text{CO}_3$  at  $80^\circ\text{C}$  AND 150 psig  $\text{O}_2$

Time, hours	AV x $10^3\text{M}$	Time, hours	AV x $10^3\text{M}$
<u>AV-<math>\text{Na}_2\text{CO}_3\text{-O}_2\text{-1}</math>(I = 1.875)</u>		<u>AV-<math>\text{Na}_2\text{CO}_3\text{-O}_2\text{-2}</math></u>	
0.0	34.2	0.0	33.2
0.05	33.3	0.05	32.9
0.3	32.5	0.25	32.8
2.0	32.0	0.75	31.8
2.5	31.4	1.5	32.4
4.5	29.2	3.0	30.6
7.0	28.7	7.0	28.1
10.5	26.9	13.0	26.2
20.0	23.6	17.0	25.0
24.0	21.3	24.0	21.6
<u>AV-<math>\text{Na}_2\text{CO}_3\text{-O}_2\text{-3}</math></u>		<u>AV-<math>\text{Na}_2\text{CO}_3\text{-O}_2\text{-4}</math></u>	
0.0	11.3	0.0	100.2
0.08	11.1	0.08	100.5
0.5	11.2	0.5	101.1
1.5	11.1	1.5	98.2
3.0	10.8	3.0	92.0
5.0	10.6	6.0	82.6
11.5	9.6	10.5	79.6
19.5	8.5	18.5	68.0
24.0	7.2	24.0	59.0
<u>AV-<math>\text{Na}_2\text{CO}_3\text{-O}_2\text{-5}</math>(I = 1.25)</u>			
0.0	33.6		
2.5	32.3		
6.5	29.1		
18.5	24.0		
24.0	21.2		

APPENDIX II (Continued)

TABLE XIV

REACTION OF ACETOVANILLONE (AV) IN 1.25N  $\text{NaHCO}_3$  at 80°C AND 150 psig  $\text{O}_2$

Time, hours	AV x $10^3\text{M}$	Time, hours	AV x $10^3\text{M}$
<u>AV-NaHCO<sub>3</sub>-O<sub>2</sub>-2</u>		<u>AV-NaHCO<sub>3</sub>-O<sub>2</sub>-3</u>	
0.0	33.0	0.0	33.3
0.05	32.6	0.05	33.0
0.3	32.9	0.5	33.1
0.8	32.0	1.3	32.0
1.3	31.4	2.5	30.9
3.0	29.6	5.5	29.1
5.5	28.2	8.5	25.7
9.5	25.0	17.0	20.4
18.5	19.5	21.0	17.4
24.0	16.0	24.0	16.2
<u>AV-NaHCO<sub>3</sub>-O<sub>2</sub>-4</u>		<u>AV-NaHCO<sub>3</sub>-O<sub>2</sub>-5</u>	
0.0	11.2	0.0	99.4
0.08	11.2	0.16	100.2
0.5	10.9	1.0	95.0
1.0	10.5	2.0	93.0
2.0	10.4	4.0	88.0
4.5	9.9	7.0	77.5
9.5	9.3	11.0	65.5
18.0	8.3	19.0	48.0
24.0	7.1	24.0	35.0
<u>AV-NaHCO<sub>3</sub>-O<sub>2</sub> (DMSO)</u>			
0.0	33.6		
0.08	33.0		
3.0	31.8		
9.0	28.0		
20.0	21.7		
24.0	19.0		

APPENDIX II (Continued)

TABLE XV

REACTION OF AV IN DIFFERENT ALKALINE MEDIA AT 80°C AND 150 psig O<sub>2</sub>

Time, hours	AV x 10 <sup>3</sup> M	Time, hours	AV x 10 <sup>3</sup> M
<u>AV-0.025M Borax/0.1M HCl-O<sub>2</sub>-1</u>		<u>AV-0.025M Borax/0.1M NaOH-O<sub>2</sub>-1</u>	
0.0	33.2	0.0	34.0
0.17	33.6	0.17	33.5
0.5	33.0	1.0	33.4
1.0	33.3	3.0	33.2
3.5	32.8	6.0	31.7
7.0	30.9	12.5	28.2
11.5	28.6	19.5	25.1
19.0	25.2	24.0	22.5
24.0	22.8		
<u>AV-0.025M Borax/0.1M NaOH-O<sub>2</sub>-2</u>		<u>AV-0.025M Borax/0.1M NaOH-O<sub>2</sub>-3</u>	
0.0	11.1	0.0	101.2
0.05	11.2	0.05	100.4
0.42	11.15	0.5	99.4
1.5	11.0	1.5	96.0
3.0	10.9	4.0	89.3
6.0	10.1	6.5	87.2
13.0	9.7	9.5	78.3
24.0	7.5		
<u>AV-0.1M KH<sub>2</sub>PO<sub>4</sub>/0.1M NaOH-O<sub>2</sub>-1</u>		<u>AV-0.05M Na<sub>2</sub>HPO<sub>4</sub>/0.1M NaOH-O<sub>2</sub>-1</u>	
0.0	33.4	0.0	33.8
0.07	33.6	0.05	33.5
1.0	33.5	0.5	33.5
2.5	33.0	2.0	33.3
6.0	31.4	4.0	32.9
10.0	30.0	7.5	30.8
18.5	27.0	14.0	28.0
24.0	26.0	20.5	25.5
		24.0	22.7
<u>AV-0.025M Borax/0.1M HCl-O<sub>2</sub>-2</u>		<u>AV-0.025M Borax/0.1M HCl-O<sub>2</sub> (DMSO)</u>	
0.0	33.3	0.0	33.6
4.5	32.9	2.0	33.5
12.0	31.1	8.5	30.8
20.5	30.3	17.0	26.7
24.0	29.6	24.0	24.5

APPENDIX II (Continued)

TABLE XVI

METHANOL AND ACETIC ACID PRODUCTION FROM AV BY THE END OF 24-HOUR REACTION PERIOD  
DURING THE OXIDATION IN DIFFERENT ALKALINE MEDIA AT 80°C, 150 psig O<sub>2</sub>

Reaction	Initial pH	MeOH, mM	MeOH, % <sup>a</sup>	CH <sub>3</sub> COOH, mM	CH <sub>3</sub> COOH, % <sup>a</sup>
AV-NaOH-O <sub>2</sub>	12.8	6.5	65	9	90
AV-Na <sub>2</sub> CO <sub>3</sub> -O <sub>2</sub>	10.8	6.9	56	6	50
AV-NaHCO <sub>3</sub> -O <sub>2</sub>	8.9	9.2	53	9	50
AV-Borax/NaOH-O <sub>2</sub>	10.8	6.5	59	6	55
AV-Borax/HCl-O <sub>2</sub>	8.9	5.6	51	5.5	50
AV-Na <sub>2</sub> HPO <sub>4</sub> /NaOH-O <sub>2</sub>	11.0	5.8	53	5.5	50
AV-KH <sub>2</sub> PO <sub>4</sub> /NaOH-O <sub>2</sub>	8.0	3.6	48	4	50

<sup>a</sup>% of theoretical for consumed AV.

# APPENDIX III

## DATA ANALYSIS BY MULTIPLE REGRESSION ANALYSIS PROGRAM

A multiple regression analysis program (MRP-in IPC Library) was performed by a computer in order to determine the significant differences between sets of disappearance curves of AV. The following Eq. (18) was employed.

$$\log Y = b_0 + b_1X_1 + b_2X_2 + b_{11}X_1^2 + b_{12}X_1X_2 + b_{112}X_1^2X_2 \quad (18)$$

where  $Y$  = concentration of AV, mM

$X_1$  = reaction time, hours

$X_2$  = independent variable assigned either a 0 or a 1 in value

(e.g.,  $X_2 = 0$  for AV-NaOH-O<sub>2</sub>;  $X_2 = 1$  for AV-NaOH-O<sub>2</sub>-DMSO)

$X_1X_2$  and  $X_1^2X_2$  = interaction terms between  $X_1$  and  $X_2$

$b_0, b_1, b_2, b_{11}, b_{12}, b_{112}$  = regression coefficients

Figures 35 and 36 are two examples of the output from the MRP program. A difference between sets of AV disappearance curves was considered significant if either  $t_{12}$  ( $T_5$ ; slope) or  $t_{112}$  ( $T_6$ ; curvature) exceeded the 95% confidence level value of a student's  $t$  distribution. In the case of Fig. 35, the two duplicate reactions (AV-NaOH-O<sub>2</sub>-2; AV-NaOH-O<sub>2</sub>-3) are statistically not distinguishable because of both  $T_5$  (0.361) and  $T_6$  (0.416) are smaller than  $t_{0.975,DF=14}$  (2.145). On the other hand, the difference between the reactions with and without DMSO shown in Fig. 36 (AV-NaHCO<sub>3</sub>-O<sub>2</sub>-2,3; AV-NaHCO<sub>3</sub>-O<sub>2</sub>-DMSO) is significant because  $T_5$  (3.639) is greater than  $t_{0.975,DF=20}$  (2.086). The results are listed in Table XVII.

THE DEFINITION OF VARIABLES AVAILABLE FOR ANALYSIS

```

X( 1) = LOG(INPUT 1 +      0.0  )
X( 2) = INPUT( 2) +      0.0
X( 3) = INPUT( 3) +      0.0
X( 4) = X( 2) * X( 2) PLUS    0.0
X( 5) = X( 3) * X( 2) PLUS    0.0
X( 6) = X( 4) * X( 3) PLUS    0.0

```

$$\text{Log } Y = b_0 + b_1X_1 + b_2X_2 + b_{11}X_1^2 + b_{12}X_1X_2 + b_{112}X_1^2X_2$$

X(1)            X(2)    X(3)    X(4)            X(5)            X(6)

THE SIMPLE CORRELATION MATRIX

	2	3	4	5	6	1
2	1.00	-0.02	0.97	0.62	0.63	-1.00
3	-0.02	1.00	-0.01	0.46	0.36	0.05
4	0.97	-0.01	1.00	0.61	0.66	-0.97
5	0.62	0.46	0.61	1.00	0.97	-0.60
6	0.63	0.36	0.66	0.97	1.00	-0.62
1	-1.00	0.05	-0.97	-0.60	-0.62	1.00

THE AVERAGES AND VARIANCES FOR THE VARIABLES

```

2  0.61040000D 01  0.13416851D 04
3  0.50000000D 00  0.50000000D 01
4  0.10434307D 03  0.70001692D 06
5  0.29665000D 01  0.84456645D 03
6  0.51028445D 02  0.40366708D 06

```

I	B(I)	SE(I)	T	R(X) -
2	-0.133834D-01	0.197172D-02	6.787690	0.967774
3	0.870906D-02	0.822571D-02	1.058761	0.503151
4	-0.748331D-04	0.866388D-04	0.863737	0.968010
5	-0.104834D-02	0.290600D-02	0.360752	0.976432
6	0.528493D-04	0.127169D-03	0.415584	0.974251

```

CONSTANT= 0.350926D 01  TSS= 0.304114D 00  SSW= 0.235326D-02
F=      359.05  DFI= 5  DF2= 14  RSQ= 0.99

```

Figure 35. Output of computer program MRP from reactions  
AV-NaOH-O<sub>2</sub>-2 and AV-NaOH-O<sub>2</sub>-3.



THE DEFINITION OF VARIABLES AVAILABLE FOR ANALYSIS

```

X( 1) = LOG(INPUT 1 +      0.0  )
X( 2) = INPUT( 2) +      0.0
X( 3) = INPUT( 3) +      0.0
X( 4) = X( 2) * X( 2) PLUS      0.0
X( 5) = X( 3) * X( 2) PLUS      0.0
X( 6) = X( 4) * X( 3) PLUS      0.0

```

$$\text{Log } Y = b_0 + b_1X_1 + b_2X_2 + b_{11}X_1^2 + b_{12}X_1X_2 + b_{112}X_1^2X_2$$

X(1)            X(2)    X(3)    X(4)            X(5)            X(6)

THE SIMPLE CORRELATION MATRIX

	2	3	4	5	6	1
2	1.00	0.10	0.97	0.46	0.48	-0.98
3	0.10	1.00	0.11	0.65	0.57	0.03
4	0.97	0.11	1.00	0.47	0.50	-0.96
5	0.46	0.65	0.47	1.00	0.98	-0.30
6	0.48	0.57	0.50	0.98	1.00	-0.33
1	-0.98	0.03	-0.96	-0.30	-0.33	1.00

THE AVERAGES AND VARIANCES FOR THE VARIABLES

```

2  0.76684615D 01  0.20039335D 04
3  0.23076923D 00  0.46153846D 01
4  0.13587967D 03  0.10923832D 07
5  0.21569231D 01  0.94504615D 03
6  0.41000246D 02  0.45471148D 06

```

I	B(I)	SE(I)	T	R(X) -
2	-0.270291D-01	0.150446D-02	17.966027	0.958990
3	0.117070D-01	0.101165D-01	1.157224	0.606211
4	-0.119068D-03	0.650739D-04	1.829736	0.959789
5	0.110448D-01	0.303554D-02	3.638508	0.978640
6	-0.182018D-03	0.128151D-03	1.420337	0.975091

```

CONSTANT= 0.349576D 01  TSS= 0.156409D 01  SSW= 0.372016D-02
F= 1677.75  DFI= 5  DF2= 2C  RSQ= 1.00

```

Figure 36. Output of computer program MRP from reactions AV-NaHCO<sub>3</sub>-O<sub>2</sub>-2,3 and AV-NaHCO<sub>3</sub>-O<sub>2</sub>-DMSO.

TABLE XVII

## SIGNIFICANT DIFFERENCES BETWEEN SETS OF AV RESULTS

Reactions in Data Set	Variable	Curve Fit, RSQ	Degree of Freedom, DF2	Student's t from Regression T <sub>5</sub>	Student's t from Regression T <sub>6</sub>	t at 95% Confident Interval	Conclusion (Difference Significant?)
AV-NaOH-O <sub>2</sub> -2 AV-NaOH-O <sub>2</sub> -3	Duplicated Reactions	0.99	14	0.361	0.416	2.145	No
AV-Na <sub>2</sub> CO <sub>3</sub> -O <sub>2</sub> -1 AV-Na <sub>2</sub> CO <sub>3</sub> -O <sub>2</sub> -2	Duplicated Reactions	0.99	14	0.797	0.607	2.145	No
AV-NaHCO <sub>3</sub> -O <sub>2</sub> -2 AV-NaHCO <sub>3</sub> -O <sub>2</sub> -2	Duplicated Reactions	1.00	14	0.237	0.081	2.145	No
AV-Borax/HCl-O <sub>2</sub> AV-Borax/NaOH-O <sub>3</sub>	Different Initial pH	1.00	11	0.106	0.286	2.201	No
AV-NaOH-O <sub>2</sub> -2,3 AV-Na <sub>2</sub> HPO <sub>4</sub> /NaOH-O <sub>2</sub>	Different pH	0.99	23	1.427	1.675	2.069	No
AV-NaOH-O <sub>2</sub> -2,3 AV-Na <sub>2</sub> CO <sub>3</sub> -O <sub>2</sub> 1,2	NaOH <u>vs.</u> Na <sub>2</sub> CO <sub>3</sub>	0.99	34	2.507	1.560	2.032	Yes
AV-Na <sub>2</sub> CO <sub>3</sub> -O <sub>2</sub> -1,2 AV-NaHCO <sub>3</sub> -O <sub>2</sub> -2,3	Na <sub>2</sub> CO <sub>3</sub> <u>vs.</u> NaHCO <sub>3</sub>	0.99	34	2.703	2.178	2.032	Yes
AV-NaOH-O <sub>2</sub> -2,3 AV-NaOH-O <sub>2</sub> -DMSO	No DMSO <u>vs.</u> DMSO added	0.99	20	2.663	1.782	2.086	Yes
AV-NaHCO <sub>3</sub> -O <sub>2</sub> -2,3 AV-NaHCO <sub>3</sub> -O <sub>2</sub> -DMSO	No DMSO <u>vs.</u> DMSO added	1.00	20	3.639	1.420	2.086	Yes
AV-NaOH/KCl-O <sub>2</sub> -1 AV-NaOH/KCl-O <sub>2</sub> -2	Different Ionic Strength	0.99	11	0.334	0.168	2.201	No

#### APPENDIX IV

##### GAS CHROMATOGRAPHIC-MASS SPECTRAL ANALYSIS

A Hewlett-Packard 5840A gas chromatograph interfaced with a Hewlett-Packard 5985 GC/MS System was used in this study. Chromatographic separations were performed on a 3% OV-17 on 80/100 mesh Gas Chrom Q column (6 ft x 0.250 inch, glass) under the following conditions:

Carrier gas: helium, 30 mL/min

Injector temperature: 275°C

Column temperature: 60°C to 235°C at 5°/min

Detector temperature: 275°C

The operating conditions for the mass spectrometer are listed below:

Jet separator temperature: 250°C

GC transfer line probe: 250°C

Actual source temperature: 200°C

Analyzer manifold: 200°C

EM voltage: 1600 V

Ionizing voltage: 70 eV

Vacuum:  $3 \times 10^{-6}$  torr

Mass scan range: 33-700

The mass spectral data for trimethylsilylated acidic products are presented in Tables XX-XXVIII. Spectra are uncorrected for background.

TABLE XX

MASS SPECTRAL DATA FOR HYDROXYISOBUTYRIC ACID (TMS DERIVATIVE)

Mass	Abund.	Mass	Abund.	Mass	Abund.
39	1.7	77	8.1	170	1.2
41	4.2	81	1.5		
42	2.1	83	5.7	205	11.7
43	10.9	85	4.6	206	2.4
44	13.5	87	1.9	207	1.3
45	25.2				
46	1.9	93	1.5	233	5.1
47	10.0	95	8.3	>PAUSE	
		96	1.6		
48	1.7	101	2.7		
55	1.6	103	2.3		
56	1.5				
57	2.8	105	2.3		
58	5.0	115	2.9		
59	6.6	116	1.7		
60	1.2	117	1.9		
61	4.0				
		120	2.5		
66	6.1	131	95.8		
69	3.2				
70	2.3	132	9.7		
72	5.1	133	8.7		
73	100.0	143	2.4		
74	11.7				
75	51.1	147	48.9		
		148	5.9		
76	5.1	149	4.9		

TABLE XXI

MASS SPECTRAL DATA FOR LACTIC ACID (TMS DERIVATIVE)

Mass	Abund.	Mass	Abund.	Mass	Abund.
40	2.4	74	7.4	132	1.1
42	1.3	75	66.9	133	5.7
43	6.0				
44	7.6	76	5.3	146	1.7
45	13.9	77	4.6	147	100.0
46	1.6	83	2.8	148	16.9
47	6.1	85	2.4	149	9.7
		87	2.8	150	1.1
48	1.1	88	5.0		
51	1.0	89	1.8	190	11.6
52	2.2			191	8.2
53	1.0	93	4.1	192	2.4
55	2.1	94	1.1	193	1.0
57	1.5	95	2.1		
58	3.3	101	2.2	219	7.3
59	9.3	102	1.7	220	1.1
60	1.6	103	2.7	221	1.5
61	3.6			>PAUSE	
		105	1.3		
63	1.4	115	1.3		
65	1.3	116	2.6		
66	8.0	117	59.5		
69	1.3				
70	1.0	118	5.8		
71	1.2	119	3.2		
72	4.6	120	1.1		
73	68.5	131	4.6		

TABLE XXII

MASS SPECTRAL DATA FOR GLYCOLIC ACID (TMS DERIVATIVE)

Mass	Abund.	Mass	Abund.	Mass	Abund.
40	1.1	76	1.2	148	12.8
42	2.3	77	2.9	149	8.3
43	11.9	81	3.8		
44	6.1	87	1.8	161	3.9
45	24.4	88	2.4	162	0.9
46	1.3	89	1.9		
47	4.9			177	10.2
		95	1.4	178	1.4
51	1.9	100	1.0	179	0.9
52	2.1	101	0.9		
53	0.9	102	0.8	190	1.0
55	2.3	103	4.9		
56	2.4			205	11.6
57	3.1	105	1.2	206	2.2
58	8.1	113	0.8	207	1.5
59	11.2	115	1.3	>PAUSE	
60	2.0	116	0.9		
61	1.9	117	3.4		
65	1.0	131	3.7		
66	27.0				
70	1.3	132	0.8		
71	1.2	133	11.6		
72	5.8	134	1.2		
73	100.0				
74	12.1	146	0.8		
75	16.2	147	95.8		

TABLE XXIII

MASS SPECTRAL DATA FOR OXALIC ACID (TMS DERIVATIVE)

Mass	Abund.	Mass	Abund.	Mass	Abund.	Mass	Abund.
39	0.2	74	9.1	131	4.7	219	7.2
41	0.8	75	11.0			220	1.0
42	2.5			132	0.8	221	0.6
43	12.4	76	0.5	133	5.2	>PAUSE	
44	4.5	77	0.4	134	0.8		
45	26.7	83	0.2	135	0.4		
46	2.3	85	0.3	144	2.7		
47	2.8	86	0.4	145	0.3		
		87	1.3				
51	0.5	88	0.3	146	1.8		
52	1.8	89	0.8	147	74.7		
53	1.0			148	15.9		
54	0.5	93	0.4	149	6.2		
55	2.0	100	0.6	150	1.0		
56	1.1	101	0.8	158	0.5		
57	2.2	102	2.4				
58	8.5	103	1.9	175	2.0		
59	10.7			176	0.3		
60	1.6	104	0.4				
61	1.6	105	0.8	188	3.2		
		113	0.3	189	0.6		
65	0.2	115	1.6	190	9.0		
66	6.0	116	0.6	191	1.2		
70	1.2	117	2.7	192	0.8		
71	1.3						
72	8.2	118	0.3	202	1.3		
73	100.0	119	0.3				

TABLE XXIV  
MASS SPECTRAL DATA FOR MALONIC ACID (TMS DERIVATIVE)

Mass	Abund.	Mass	Abund.	Mass	Abund.	Mass	Abund.
39	0.2	72	5.3	117	1.4	189	0.6
41	0.8	73	49.5			190	0.2
42	1.5	74	6.9	118	0.3	191	0.2
43	6.2	75	27.5	119	0.4		
44	2.2			130	1.9	202	1.0
45	15.4	76	2.2	131	3.4	204	0.3
46	0.9	77	1.4				
47	7.2	83	0.2	132	0.6	217	0.7
		85	0.3	133	5.0	218	0.3
48	0.3	86	0.4	134	0.7		
49	0.3	87	1.2	135	0.4	233	11.3
52	0.3	88	0.8	143	1.8	234	2.1
53	0.5	89	0.5	144	0.3	235	1.1
54	0.2			145	0.2		
55	1.1	91	0.2			248	1.9
56	0.6	93	0.3	147	100.0	249	0.4
57	1.3	99	3.9	148	16.9	250	0.2
58	2.7	100	0.7	149	10.1	>PAUSE	
59	5.2	101	1.9	150	1.0		
60	1.5	102	0.7	151	0.2		
61	3.4	103	0.8	158	0.3		
62	0.3	104	0.2	173	0.3		
66	6.2	105	0.6				
69	1.6	109	1.2	174	1.5		
70	0.7	115	1.3	175	0.2		
71	1.0	116	0.9				

TABLE XXV  
MASS SPECTRAL DATA FOR SUCCINIC ACID (TMS DERIVATIVE)

Mass	Abund	Mass	Abund	Mass	Abund	Mass	Abund
39	0.3	71	0.9	128	0.5	245	0.4
40	0.5	72	3.8	129	7.1	247	18.6
41	0.3	73	62.8	130	1.6	248	2.8
42	0.8	74	8.0	131	2.1	249	1.8
43	4.4	75	32.8				
44	3.0			132	0.6	262	1.6
45	17.9	76	3.0	133	4.4		
46	0.9	77	2.0	134	0.6	299	0.5
47	7.8	82	0.4	135	0.5	>PAUSE	
		83	0.4	143	0.7		
51	0.4	85	0.9	145	0.7		
51	0.4	86	1.2				
53	1.0	87	0.6	147	100.0		
54	0.5	88	0.4	148	13.1		
55	16.9	89	0.8	149	8.5		
56	6.8			150	0.8		
57	3.2	99	0.6	157	0.3		
58	3.8	101	0.9				
59	4.4	103	0.7	172	3.7		
60	1.4			173	1.9		
61	5.1	105	0.4				
		113	0.9	174	0.6		
62	0.5	115	1.0				
63	0.4	116	3.2	203	0.4		
66	0.4	117	1.3				
67	0.4			218	1.2		
70	0.8	119	0.4				

TABLE XXVI

MASS SPECTRAL DATA FOR MALEIC ACID (TMS DERIVATIVE)

Mass	Abund.	Mass	Abund.	Mass	Abund.	Mass	Abund.
40	0.4	71	0.7	111	0.3	157	1.0
42	0.6	72	2.5	113	0.9	159	0.4
43	3.3	73	45.4	115	5.6		
44	2.5	74	5.8	117	1.1	170	2.7
45	10.6	75	18.0			171	0.8
46	0.6			119	0.4	172	0.3
47	3.7	76	1.6	126	2.3	173	0.3
		77	1.0	127	0.5		
51	0.3	82	0.7	128	0.4	215	1.5
52	0.4	83	3.9	129	0.4		
53	1.3	84	1.9	131	1.4	216	0.4
54	0.8	85	1.2			217	0.4
55	1.4	86	0.3	132	0.5		
56	0.4	87	0.6	133	4.5	242	1.3
57	0.9	88	0.3	134	0.6	243	0.3
58	1.9	89	0.5	135	0.6		
59	3.6			142	0.4	245	28.5
60	0.8	93	0.9	143	4.0	246	4.6
61	1.8	95	0.4	144	0.3	247	3.0
		97	0.3	145	0.4	248	0.4
63	0.3	98	0.9				
65	0.3	99	0.7	147	100.0	299	0.6
66	2.8	101	0.3	148	12.0	>PAUSE	
67	0.9	102	0.3	149	8.3		
68	1.1	103	0.8	150	0.7		
69	1.1			155	0.7		
70	0.6	105	0.5	156	0.3		

TABLE XXVII

MASS SPECTRAL DATA FOR HYDROXYMALONIC ACID (TMS DERIVATIVE)

Mass	Abund.	Mass	Abund.	Mass	Abund.	Mass	Abund.
40	0.5	76	2.1	134	2.5	233	0.5
42	0.5	77	1.5	135	1.4		
43	3.8	83	0.7	145	0.5	245	1.3
44	4.5	85	0.6				
45	14.5	87	0.8	147	86.9	292	38.5
46	1.2	89	0.8	148	11.6	293	35.0
47	3.9			149	7.3	294	10.6
		93	1.6	150	0.6	295	4.2
53	0.5	95	1.1			296	0.7
55	1.3	99	0.9	161	1.0	299	0.4
57	1.0	101	1.0	163	0.9		
58	1.5	102	21.2			305	0.5
59	5.3	103	4.0	177	1.0		
60	0.6					321	14.8
61	1.4	104	1.5	189	0.5	322	4.5
		105	0.9	190	1.0	323	1.8
65	0.5	115	1.6	191	1.2	>PAUSE	
66	1.4	116	0.6	192	0.5		
67	0.5	117	2.2				
69	1.7			204	0.5		
70	0.8	119	1.3	205	1.2		
71	1.0	129	0.5	207	1.0		
72	4.0	130	4.8				
73	100.0	131	5.6	219	1.4		
74	11.4			221	8.8		
75	21.9	132	1.4	222	2.6		
		133	13.8	223	1.0		

TABLE XXVIII

MASS SPECTRAL DATA FOR MALIC ACID (TMS DERIVATIVE)

Mass	Abund.	Mass	Abund.	Mass	Abund.	Mass	Abund.
40	0.3	75	18.7	131	3.2	189	7.8
42	0.4					190	9.1
43	2.2	76	1.4	132	0.7	191	6.0
44	2.9	77	0.8	133	10.2	192	1.7
45	9.3	82	0.3	134	1.8	193	0.5
46	0.9	84	0.3	135	1.0		
47	2.2	85	0.6	143	1.7	203	1.1
		87	0.5	144	0.3	204	0.5
53	0.5	89	0.4	145	0.4	205	0.5
54	0.3					207	0.6
55	7.8	93	0.7	147	66.3		
56	0.5	95	0.4	148	9.7	217	4.8
57	0.8	99	0.7	149	6.7	218	0.9
58	1.2	100	0.4	150	1.0	219	1.0
59	5.4	101	8.1	151	0.6	221	1.7
60	0.5	102	1.1	157	0.3	222	0.4
61	1.8	103	1.3	159	0.3		
						233	27.6
63	0.4	105	0.4	163	0.3	234	7.5
66	0.5	115	1.2	171	2.6	235	2.9
68	0.3	116	1.0	172	0.5	236	0.4
69	0.3	117	5.3	173	0.5		
70	0.6					245	20.3
71	1.0	118	0.6	175	5.8	246	3.5
72	5.0	119	1.3	176	1.2	247	3.0
73	100.0	129	1.3	177	1.6	248	0.4
74	10.2	130	0.3	178	0.4		

<CONT>

Mass	Abund.	Mass	Abund.
259	0.3	350	0.8
260	0.5	>PAUSE	
263	2.2		
264	0.6		
265	4.2		
266	1.0		
267	0.6		
291	0.3		
292	0.4		
293	0.3		
305	2.1		
306	3.3		
307	7.2		
308	2.0		
309	1.0		
319	2.8		
320	0.9		
321	0.6		
335	10.8		
336	3.7		
337	1.8		
338	0.5		



APPENDIX V

TABLE XXIX

TRACE METALS IN REACTION SOLUTIONS<sup>a</sup>

Metal	Concentration in NaOH Solution, ppm	Concentration in Na <sub>2</sub> CO <sub>3</sub> Solution, ppm	Concentration in NaHCO <sub>3</sub> Solution, ppm
Cadmium	<0.40	<0.40	<0.40
Cobalt	<1.8	<1.8	<1.8
Chromium	<0.32	<0.32	<0.32
Copper	<0.64	<0.64	<0.64
Iron	<1.8	<1.8	<1.8
Magnesium	<0.10	0.85	0.62
Manganese	<0.26	<0.26	<0.26
Nickle	<2.4	<2.4	<2.4
Zinc	<0.32	<0.32	<0.32

<sup>a</sup>Metal ion analyses were conducted by the Analytical Department at The Institute of Paper Chemistry using the atomic absorption techniques.